Statistical Analysis of Electromagnetic Fields Modulated by Depolarizers through Complex ABCD Optical Systems

Ning Ma

Submitted for the degree of Doctor of Philosophy

Heriot-Watt University

Institute of Photonics and Quantum Sciences

School of Engineering and Physical Sciences

December 2015

ABSTRACT

A polarization-dependent modulation device, the rough-surfaced retardation plate is proposed as a depolarizer in this thesis. It realizes the decorrelation to the incident field like the traditional diffuser, and scrambles the polarization state simultaneously like a depolarizer. For various surface-roughness plate models, the comprehensive and rigorous analysis of its modulation behaviour is achieved. On the basis of the 2×2 beam coherence-polarization matrix, the statistical properties of the modulated field are examined to reveal the dependence on the surface structure of the rough-surfaced retardation plate. Within the framework of the Complex ABCD matrix theory for general optical propagation systems under the paraxial approximation, the propagated polarization speckle on observation plane over a distance is studied. The analytical expression of its beam coherence-polarization matrix illustrating the change of degree of coherence and polarization on propagation is obtained too. It is approved that the depolarizer provides a flexible and simple method to generate the randomly de-correlated and depolarized speckle with spatially varying polarization states. In addition, the dynamic properties of polarization speckle are analysed to reveal the shape and the motion features of the polarization speckles on the observation plane. At last, a depolarizer consisting of random polarizer cells is introduced to generate polarization speckle as an attempt for a potential method different from the common phase modulation screens.

ACKNOWLEGEMENT

The works presented in this thesis were done at the Institute of Photonics and Quantum Sciences (IPaQS), School of Engineering and Physical Sciences (EPS), Heriot-Watt University, from 2010 to 2015. It is neither possible nor appropriate to pay tribute here to the many people whose friendly help and encouragement always accompanied me through these years. I sincerely apologize if I unintentionally have omitted anyone.

First of all, I would like to express my sincere gratitude to my supervisor, Dr. Wei Wang, for originally attracting me in this fascinating area by his introduction and offering me the valuable opportunity to further my study. His advice, support, help, encouragement, patience, kindness and guidance both to my research and to my life is strongly impressed on my memory. Although it is obvious, but worth mentioning, that this thesis would never have been accomplished without his supervision.

My sincere gratitude goes also to Professor Hanson, Steen Grüner, who invited me to DTU Fotonik for a short-term visit in 2012 where I compiled the very important part of work for this thesis. He taught me so much concealed inside the complex ABCD theory and spread his infectious enthusiasm for speckle phenomena. He is also a very important co-author in most of my scientific papers, and provides many insights into mathematical and theoretical conclusions through interesting and helpful discussions. It is with equal pleasure that I acknowledge Professor Mitsuo Takeda whose work pervaded my later thinking. I have got much benefit from his patient review and helpful comments on my works. He is so kindly to present our papers in conferences. I must not forget to thank Professor Tim K. Lee, and Dr. Michael Linde Jakobsen for collaborating in the research work.

I am very grateful to my internal examiner Dr. Xu Wang and external examiner Professor Giancarlo Pedirini for proofreading the manuscript. I have got much benefit from their invaluable and insightful suggestions during the qualifier examination that help me to improve and bring this thesis to completion.

I will never forget all the colleagues in the Institute of Photonics and Quantum Sciences (IPaQS), our Friday coffee & donuts, highland hiking, and those intriguing discussions. Special thanks to my teammate, Dr. Juan Zhao, for much help and support.

I am grateful to all of the staff of the EPS Postgraduate Research Office, especially, Genna Nothard and Mrs Alex Campbell for their support. I also sincerely thank all staff of International Student Services Office of the Heriot-Watt University for their help. Special thanks to Mr. Peter Reinbold for his patience and help in minimizing the difficulties in life I encountered in UK.

I acknowledge the Heriot-Watt University for generously granting me a scholarship to support my study. Without this financial support this thesis would not have been possible.

In addition, I wish to express my gratitude to Professor Jungang Miao from Beihang University who inspired and guided me to the academic research.

At last, but definitely not least, I wish to thank my parents Mr. Yueping Ma and Mrs. Changlong Deng for their endless support and unconditional love. I am also deeply indebted to my beloved girlfriend Qian Xie, who has heroically endured through my long term research and encouraged me in times of desperation.

DEDICATION

I dedicate this work to my father Mr. Yueping Ma and my mother Mrs. Changlong Deng for bringing me into this world and raising me up to who I am.

To my dear girlfriend Qian Xie, for her love, understanding, patience and faith in me.

ACADEMIC REGISTRY
Research Thesis Submission

Name*:*	Ning Ma		
School/PGI:	EPS / IPAQS		
Version: *(i.e. First, Resubmission, Final)*	FINAL	Degree Sought (Award and Subject area)	PhD Physics

Declaration

In accordance with the appropriate regulations I hereby submit my thesis and I declare that:

1) the thesis embodies the results of my own work and has been composed by myself
2) where appropriate, I have made acknowledgement of the work of others and have made reference to work carried out in collaboration with other persons
3) the thesis is the correct version of the thesis for submission and is the same version as any electronic versions submitted*.
4) my thesis for the award referred to, deposited in the Heriot-Watt University Library, should be made available for loan or photocopying and be available via the Institutional Repository, subject to such conditions as the Librarian may require
5) I understand that as a student of the University I am required to abide by the Regulations of the University and to conform to its discipline.

* *Please note that it is the responsibility of the candidate to ensure that the correct version of the thesis is submitted.*

Signature of Candidate*:*		Date:	

Submission

Submitted By *(name in capitals):*	NING MA
Signature of Individual Submitting:	
Date Submitted:	

For Completion in the Student Service Centre (SSC)

Received in the SSC by *(name in capitals):*			
Method of Submission *(Handed in to SSC; posted through internal/external mail):*			
E-thesis Submitted *(mandatory for final theses)*			
Signature:		Date:	

LIST OF PUBLICATIONS BY THE CANDIDIATE

[1] **N. Ma** and W. Wang, “Statistical analysis based on complex representation of real-valued two-dimensional signal derived from modified Hilbert transform,” in *2013 6th International Congress on Image and Signal Processing (CISP)*, 2013, vol. 03, pp. 1179–1183.

[2] W. Wang, S. Zhang, and **N. Ma**, “Correlation properties of the vector signal representation for speckle pattern,” *Appl. Opt.*, vol. 53, no. 10, pp. B147–B152, 2014.

[3] W. Wang, S. Zhang, **N. Ma**, S. G. Hanson, and M. Takeda, “Riesz transforms in statistical signal processing and their applications to speckle metrology: a review,” in *Proc. SPIE: The International Conference on Photonics and Optical Engineering*, 2015, vol. 9449, p. 944904.

[4] **N. Ma**, S. G. Hanson, T. K. Lee, M. Takeda, and W. Wang, “Coherence and polarization of polarization speckle generated by depolarizers and their changes through complex ABCD matrix,” in *Proc. SPIE: SPECKLE 2015: VI International Conference on Speckle Metrology*, 2015, vol. 9660, p. 96601D.

[5] **N. Ma**, S. G. Hanson, M. Takeda, and W. Wang, “Coherence and polarization of polarization speckle generated by a rough-surfaced retardation plate depolarizer,” *J. Opt. Soc. Am. A*, vol. 32, no. 12, pp. 2346–2352, Nov. 2015.

CONTENTS

LIST OF FIGURES

LIST OF ACRONYMS

AP	aperture
BCPM	beam coherence-polarization matrix
BS	non-polarizing beam splitter
DoC	degree of coherence
DoP	Degree of polarization
FT	Fourier transform
FFT	Fast Fourier transform
FDS	fully developed speckle
GG	ground glass
LC	Liquid Crystal
LDV	laser Doppler velocimeter
LTV	Laser time-of-flight velocimeter
PDF	probability distribution function
TLIC	time-lagged intensity covariance
MCF	mutual coherence function
OPD	optical path difference
PDS	partially developed speckle
RPA	random polarizer array
rms	Root mean square
RPM	Random phase modulation
RPS	Random phase screen
SOP	State of polarization
SLM	spatial light modulator

LIST OF SYMBOLS

C	time-lagged intensity covariance
d	thickness of screen
$\mathbf{E}$	Field vector
E_x, E_y	orthogonal components of the field
f	focal length
G	Green‘s transform kernel
I	intensity
I_o	on optical-axis intensity
j	Imaginary unit
J	Mutual intensity function
$\mathbf{J}$	Polarization matrix
k	Wave number
l	Size of polarizer cell in random depolarizer consisting of random polarizer array
$\mathbf{M} = \begin{pmatrix} A & B \\ C & D \end{pmatrix}$	ABCD matrix
n_x, n_y	refractive indices
P	degree of polarization
$p(\bullet)$	probability distribution function
r_s	$1/e$ amplitude radius of Gaussian beam source
r_d	Lateral correlation length of plate thickness

r_η	average speckle size on the observation plane
r_w	size of illuminated spot region on the observation plane
$\mathbf{T}$	Jones matrix
$\mathbf{v}_s$	moving speed of speckle translation
$\mathbf{W}$	beam coherence-polarization matrix, ,
z	Propagation distance
$z_R = kr_s^2/2$	Rayleigh range
φ	Effective phase delay
γ	polarization angle of polarizer cell in RCPA
Γ	Scalar mutual coherence function
δ	Dirac delta function
η	degree of coherence
θ	polarization angle
λ	Wave length
σ_d^2	Covariance of plate thickness
τ	time lag
τ_c	temporal correlation length of dynamic speckle
τ_d	peak shift of the temporal correlation of dynamic speckle
φ_x, φ_y	phase modulations to horizontal and vertical field components
$\langle \cdots \rangle$	Ensemble average
$\wedge(\bullet)$	unit triangle function
$Sinc(\bullet)$	cardinal sine function
tr	Trace of matrix

det	Determinant of matrix
$\mathrm{Re}[\bullet]$	Real part of complex number
$\mathrm{Im}[\bullet]$	imaginary part of complex number
$\bullet^{*}$	Complex conjugate
$\bullet^{\dagger}$	Hermitian conjugate
$*$	convolution

Chapter 1

Introduction

The speckle pattern, one of the most important concepts in optics, describes the phenomena of fine-scale, high-contrast granular light intensity distribution generated by the interference of coherent optical field within the scattering spot [1, 2]. As Denis Gabor once said [3] “the novelty in holography is speckle noise”, it plays a significant role in the statistical theoretical optics research and profoundly affects relevant applications. To generate the speckle pattern, a kind of optical device named as diffusers with fine structure is introduced to scatter the coherent incident light and provide phase retardance or amplitude fluctuation with a random spatial distribution on the wave front. The randomly modulated field will diffract and then superpose after propagation to generate a remarkable intensity variation named as speckle on the observation plane. Take a transmitting rough plate for example, its random thickness fluctuation will cause optical path difference (OPD) for wave components passing through different locations on the plate. A good understanding of the modulation device’s structure is quite important for the speckle research work, because the shape of speckle patterns is highly dependent on the surface structure of the diffuser where the field is reflected from or transmits through. In the past decades, most of the researchers’ attentions were dedicated to the interaction between the incident source and the diffuser with structured rough surface causing decorrelation, and the statistical properties of the resultant speckle pattern after propagation in some specialized systems. On the basis of related conclusions, the optical researchers might

be able to extract the information of the modulation device and propagation system contained in the speckle image, and thus, non-contact metrology including the measurement of the surface roughness [4, 5], the displacement, the strain and the movement [6] becomes feasible. Moreover, the researchers could employ random spatial modulation device with specialized surface structure to generate speckle with prescribed statistical properties.

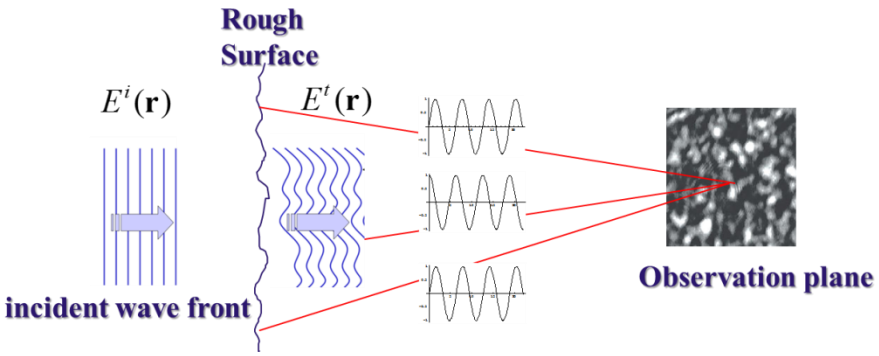

Figure 1.1. Intensity speckle generated by rough plate

However, most of the traditional speckle pattern analyses were achieved in the frame work of the coherence theory formulated for scalar optical field description, and made it extremely difficult to capture the polarization state of the field, though the field is vector in essence[7]. Associated with this scalar optical field description, the light modulation effect under consideration was usually assumed to be polarization–independent, and thus the scattering field originating from the device was considered to possess wave front fluctuation without the change of polarization state. Since the polarization is an intrinsic property of the electromagnetic field, the simplification of the traditional research method in disregard of the polarization feature gives rise to substantial uncertainties in speckle characterization and loses useful information.

Recent research works, both theoretical and experimental, indicate that the polarization state of speckle displays much more complicated behaviour than a constant one as people assumed before. The polarization of a special kind of random field could change on propagation even in free space system, and the spatial distribution of the polarization state will vary and could be non-uniform on the cross

section of a beam [8-18]. Similar phenomena are also detected while electromagnetic beams propagate through the turbulent atmosphere, Gaussian cavity and other optical systems [19-23]. To investigate the statistical properties of speckle including spatial polarization variations, the premise is the generation of the corresponding decorrelated and depolarized field with known statistical properties. It becomes crucial to propose and improve the modulation method which does not only realize the decorrelation to the incident field like the traditional diffuser, but also scrambles the polarization state of the uniformly polarized incident beam like a the depolarizer. It is also important to reveal the quantitative relationship between the structural features of the device and the statistical properties of the propagated speckle patterns with the demonstration of the vector nature of the electromagnetic field.

1.1 Motivation and literature review

Aiming to help the reader better understand the background, the motivation and the methodology of this project, I will review the related literature concisely first. In an effort to make the main text as accessible as possible, some notations will also be specified.

1.1.1 The statistical analysis of speckle patterns, from scalar to vector

The speckle pattern is a physical phenomenon often regarded as random twinkling particles in beam spots. The interest in this topic has a long history that could trace back to great names including Newton, Exner, and Rayleigh [1]. But it was only with the advent of the ideal coherent light source laser in 1960s when the related research work got a real boost. After the development for nearly a half century, it spans across a significant wide variety of disciplines including physics, medical science, biology, astronomy, and remote sensing with an emphasis on the optics. The burgeoning appearance of the concept “speckle patterns” in optical journals was recognized from 1970s, and a history retrospect to this emerging technique was provided by Hariharan [24] in 1972. Some mathematical simplicities and physical assumptions are settled down to keep a balance between the validity and feasibility of the analysis. This speckle phenomenon embodied the *coherence* of superposed fields. The concept

coherence was originally conceived in connection with the interference visibility in Young's slit experiment [25] and was defined to quantify how well correlated the waves were. Adequate introduction to the subject of modern coherence theory for a fundamental treatment of optical field is provided by D. Gabor (chapter 4 of [26]), E. Wolf (chapter 10 of [27]) and it was further discussed in details by M. J. Beran and G. B. Parrent [28], J. W. Goodman[29], and K. Blomstedt[30]. Thus the so-called spatial-temporal mutual coherence function (MCF) [31, 32] is regarded as the second-order characteristic quantity and basic entity to demonstrate the speckle statistically. For a typical monochromatic optical field with wave length λ at point $\mathbf{r}$, its complex amplitude is denoted as $E(\mathbf{r},t)$. If the optical fields and sources of interest are assumed to be wide-sense stationary, the corresponding mutual coherence function for two space-time points $(\mathbf{r}_1,t)$ and $(\mathbf{r}_2,t+\tau)$ depending on the time-difference τ and is given by

$$W\left(\mathbf{r}_1,\mathbf{r}_2,t,t+\tau\right)=\left\langle E^*\left(\mathbf{r}_1,t\right)E\left(\mathbf{r}_2,t+\tau\right)\right\rangle=\left\langle E^*\left(\mathbf{r}_1,0\right)E\left(\mathbf{r}_2,\tau\right)\right\rangle, \tag{1.1}$$

where asterisk $\bullet^*$ means complex conjugate, and angular brackets $\langle\cdots\rangle$ denote ensemble average. To distinguish the scalar quantities from vectors/matrices, they will be expressed in Italics and bold respectively in the following discussion. Furthermore, while a large number of independent wave components contribute to the resultant field at any point in the observation plane, it will approximately obey the Gaussian random process because of the Central-limit Theorem (page 362 of [33]). Hence, higher-order correlation functions could be expressed in terms of this second-order mutual coherence function of Eq. (1.1)[34-37]. On the issue of the scalar speckle statistics, a series of articles and books covered different aspects. Different extents of modulation were considered, like the fully developed speckles [38] and partially developed speckle [39]. Both the first and second-order statistical properties were studied [40-43]. Dynamic speckle in Gaussian statistics generated by moving diffuser were observed and approved [44]. Various kinds of sources, especially the Gaussian beam were examined in the speckle generation [45-47]. Researchers also devoted their time to analysing the propagation of speckle in different systems, for

example, in the image systems with lenses [48, 49], and in 3D free space [50]. Then the research extended to the general system [51, 52]. Based on the study of speckle dynamics associated with its relationship to structure and motion of diffuser, some early attempts of non-contact speckle metrology were proposed [53]. Equipments and methods [5, 54-60] including the laser-time-of-flight velocimeter and the laser Doppler technique were presented and applied to probe the surface roughness, object deformation [61], rotation angle [62] and the in-plane displacement/velocity [63] which might be caused by the stain, torque and temperature. The foundation laid in the early stage for the later development could be found in several notable publications of J. W. Goodman [40, 64, 65], J. C. Dainty [1, 37, 43, 66], T. Asakura [67-69] G. Parry [70], Francon [71] and T. Yoshimura [72]. For the research conducted on this subject in recent years, the readers can refer to references [2, 34] and [73].

Most of the scalar analysis ignored the polarization state and implicitly asserted that a bundle of rays had the same and would maintain their polarization state during propagation. It is applicable under most common conditions where the source is specialized uniformly and the diffusers or scattering objects are isotropic. However, the scalar field description might be improper while the modulation devices embodying significant polarization direction selectivity introduced by various reasons like the different refraction indices by birefringence [74]. Whereas the polarization and coherence spatial variations are observed during propagation and on beam cross section in recent researches[8-14, 75], the polarization speckle with coherence and polarization spatial variation needs to be re-examined in a new vectorial formalism of modern optical theory.

In recent years, more and more attention was paid to the analysis of the vectorial speckle description to illustrate the polarization variation during propagation and on beam cross sections. The pioneering study has been conducted by Gori who developed the theorem in terms of the 2x2 beam coherence-polarization matrix [76-78] (also named as mutual intensity matrix), and examined coherence and polarization properties of the field generated by an incoherent unpolarised source

covered with a specific polarizing filter[79]. For the optical field vector $\mathbf{E}(\mathbf{r}) = \{E_x(\mathbf{r}), E_y(\mathbf{r})\}$ at point specified by position vector $\mathbf{r}$ on the plane perpendicular to the propagating axis z, $E_x(\mathbf{r})$ and $E_y(\mathbf{r})$ are the components polarized vertically and horizontally. The 2×2 beam coherence-polarization matrix in respect to this vectorial field expression is defined as

$$\begin{aligned}\mathbf{W}(\mathbf{r}_1,\mathbf{r}_2,\tau) &= \left\langle \mathbf{E}^{\dagger}(\mathbf{r}_1,t)\mathbf{E}(\mathbf{r}_2,t+\tau)\right\rangle \\ &= \begin{pmatrix} \left\langle E_x^*(\mathbf{r}_1,t)E_x(\mathbf{r}_2,t+\tau)\right\rangle & \left\langle E_x^*(\mathbf{r}_1,t)E_y(\mathbf{r}_2,t+\tau)\right\rangle \\ \left\langle E_y^*(\mathbf{r}_1,t)E_x(\mathbf{r}_2,t+\tau)\right\rangle & \left\langle E_y^*(\mathbf{r}_1,t)E_y(\mathbf{r}_2,t+\tau)\right\rangle \end{pmatrix},\end{aligned} \tag{1.2}$$

where the dagger $\bullet^{\dagger}$ depicts the Hermitian conjugate. While there is no time-lagged in discussion, the beam coherence-polarization matrix could be written as $\mathbf{W}(\mathbf{r}_1,\mathbf{r}_2)$ for simplicity. This matrix of 2-D vector fields implies the polarization and coherence information, and is especially appropriate for the analysis of monochromatic source in spatial-temporal domain. It is also easy to be converted into stocks parameters. On the basis of this matrix definition, three parameters illustrating the speckle features viz. the intensity I **,** degree of coherence (DoC) η and degree of polarization (DoP) P could be determined by:

$$I(\mathbf{r}) = tr\mathbf{W}(\mathbf{r},\mathbf{r}) \tag{1.3}$$

$$\eta(\mathbf{r}_1,\mathbf{r}_2) = \frac{tr\mathbf{W}(\mathbf{r}_1,\mathbf{r}_2)}{\sqrt{tr\mathbf{W}(\mathbf{r}_1,\mathbf{r}_1)\,tr\mathbf{W}(\mathbf{r}_2,\mathbf{r}_2)}} \tag{1.4}$$

$$P(\mathbf{r}) = \left\{1 - \frac{4\det\mathbf{W}(\mathbf{r},\mathbf{r})}{\left[tr\mathbf{W}(\mathbf{r},\mathbf{r})\right]^2}\right\}^{1/2} \tag{1.5}$$

where tr and $\det$ mean the trace and determinant of matrix, respectively.

E. Wolf extended this theorem to a cross-density matrix in the spatial-spectral domain for polychromatic source later. He also achieved the setup of a unified theory of coherence and polarization within this framework [34, 80-83], and these two concepts were no longer treated as independent.

At last, it has to be pointed out that, the beam coherence-polarization matrix approach for field expressed in a vector form is different from the RF/microwave "vectorial" method in Maxwell equations (chapter 3.2 of [84]). In statistical optics research, the concept "electromagnetic field" is usually cited to characterize the field expression in vector form with polarization indication, while the "optical field" usually means the scalar expression [82, 85, 86]. To put it simply, in the beam coherence-polarization matrix mentioned here, we will not consider the *coupling* between the various wave components, and the "cross talk" between them is ignored.

The simple matrix description for the statistical properties of electromagnetic fields indicates significant aspects of fields not covered by the scalar field expression, and now it is regarded as an applicable method in field coherence analyses implicating the polarization information. For example, it is applied to study the vectorial extension of Van Cittert-Zernike Theorem [79, 85, 87, 88] and other topic in theoretical physics [89]. It is also utilised in the research of anisotropic speckle diffusers [13, 14]. Among these pioneering works, the analysis on the ***polarization speckle*** [15], or named as ***electromagnetic beam*** [13] might be a representative one. The polarization speckle is a concept [15, 16] to distinguish the speckle arising from stochastic electromagnetic fields with random non-uniform polarization on beam cross section from the concept ***intensity speckles*** focusing on the intensity random distribution of speckle pattern. Some related metrology applications [17, 90, 91] have been developed based on this field with spatial polarization distribution.

1.1.2 Random depolarization and decorrelation device/system

The random phase/amplitude distortion introduced by modulation device is one of the determinative factors for the generation of speckle pattern. The interpretation of its performance will implicate the materialogy, chemistry, mechanics and physics. It is

obviously beyond the ability of the researchers to cover these broad subjects, therefore, some assumptions and simplifications are adopted in the statistical optics. Although the phase and amplitude modulation are always carried out together by the modulation device, most attention in the speckle analysis is paid to the random phase-screen (RPS) modulation model [92] providing a constant amplitude transmittance equal to unity and randomly varying phase retardance φ to incident electromagnetic beam.

To investigate the polarization and coherence properties of random electromagnetic fields implicating non-uniform spatial polarization distribution, and the polarization speckle arising from it, random modulation device/system has to be employed to introduce random phase difference between the two components of the electric field across the beam's cross section. By this, depolarization and decorrelation effects are realized simultaneously to generate this kind of random electromagnetic field with prescribe statistical properties, which is often required as a secondary source for experimental test and theoretical analysis in statistical optics [93-96]. For example, it could be applied in the research of coupling electromagnetic field into optical fibre [97], turbulent atmosphere [98, 99], quantum partially polarized state [96], and the effect of polarization speckle on the resolution of the optical system [100].

The liquid-crystal (LC) spatial light modulator (SLM) is a commonly used depolarizer to achieve randomly phase modulation to one of the field components in two mutually orthogonal polarization directions [13, 14, 101] (Figure 1.2), and to generate partially depolarized and partially coherent electromagnetic field. However, the other field component will not be distorted, and thus it is unable to realize whole field decorrelation. Another typical conceptual scheme is to insert two LC SLMs into the opposite arms of a Mach-Zehnder interferometer [86, 95, 102]. A polarized beam splitter (PBS) is used to split the beam into two wave components in mutually orthogonal polarization directions, and then, different random phase retardance could be introduced by the LC SLMs to them. A minor variant of this method is to insert moving phase diffusers e.g. ground glass plates to one [18, 103] or both [15, 104, 105] of optical arms instead of the expensive commercial LC SLMs controlled by

computer. The whole field correlation will be realizable for the two arms modulation method, but the cost is a more complicated and bulkier system. In addition, the modulation and propagation through multi-individual devices might introduce extra errors.

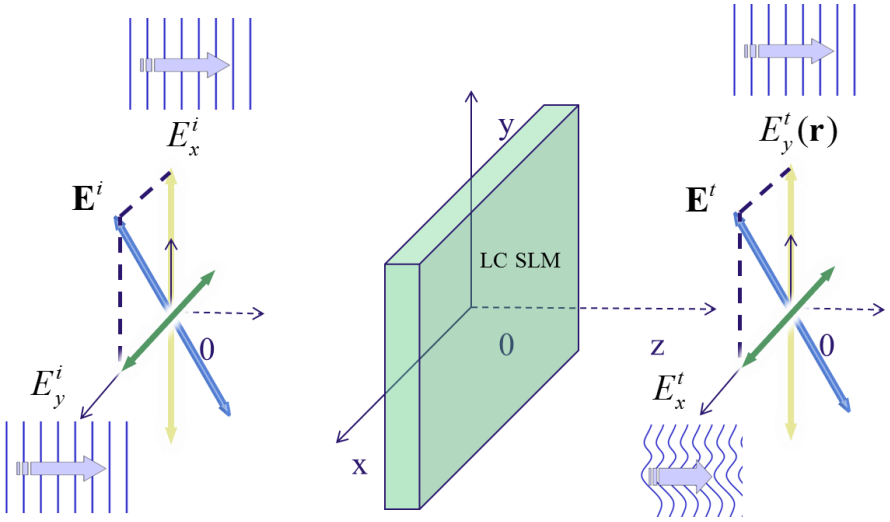

Figure 1.2. Illustration of the technique for generating the partially coherent and partially polarized field by LC SLM

To develop an efficient and simple method by a compact system to diffuse and depolarize field simultaneously is one of the main objectives of this thesis.

1.1.3 The speckle Propagation in complex ABCD matrix system with inherent apertures

When the modulated laser speckle propagates over an appreciable distance from the diffuser to the observation plane, it should be considered as a beam with diffraction instead of a bundle of perfect collimated rays. Since the Huygens-Fresnel principle [25, 106, 107] is the general method for wave propagation and diffraction analysis for arbitrary input source, it is obviously applicable to the examination of the speckle propagation problem of this thesis. However, analytical solution of the integral is usually impossible for all but the simplest diffraction geometries. Furthermore, if the

field propagates through a train of optical elements, it will lead to a heavy computational burden to calculate the propagation in a step-by-step way.

Although, the random modulation device introduce in the thesis could be introduced in applications with a much more general propagation system, and the propagation could be numerically computed by the Huygens-Fresnel principle. The discussion within this thesis will be confined to system under approximation as well as a near perpendicularly illumination on the surface of device.

For quadratic optical system under paraxial approximation, the generalized Huygens-Fresnel integral formulation could be calculated on the basis of the complex ABCD matrix theory [108, 109]. The relation between incident field **E**(**r**) and propagated field $\mathbf{E}^{o}(\mathbf{p})$ is given by

$$\mathbf{E}^{o}(\mathbf{p}) = \iint \mathbf{E}(\mathbf{r}) G(\mathbf{r},\mathbf{p})\, d\mathbf{r}, \tag{1.6}$$

while the Green's transform kernel $G(\mathbf{r},\mathbf{p})$ is defined as

$$G(\mathbf{r},\mathbf{p}) = -\frac{jk}{2\pi B}\exp\left\{-\frac{jk}{2B}\left(A|\mathbf{r}|^2 - 2\mathbf{r}\cdot\mathbf{p} + D|\mathbf{p}|^2\right)\right\}. \tag{1.7}$$

In the above equation, k is the wave number and j is the imaginary unit. *A*, *B* and *D* are the elements of the ABCD ray-transfer matrix [110-114] **M** for the whole propagation system. **M** is determined by the multiplication of all individual optical elements' matrices that must be arranged in inverse order in which the ray physically encounters the corresponding elements. This elegant formalism was developed from a kind of Linear Canonical Transforms [115, 116], the ABCD matrix formalism [110-113, 117, 118], and it provides a modular transformation describing the propagation system as the cascaded operations of its components. Various classical optical elements besides the lens, the free space and the dielectric interfaces are described by the 2×2 real-value ray-transfer matrices [84, 110, 117, 118]. Therefore, propagation

in many classical optical systems besides free space system, Fourier system, image system could be encompassed by Eq. (1.6).

In particular, Hanson and Yura [108] suggested the Gaussian shaped aperture with complex-value matrix in the complex ABCD matrix theory instead of a hard truncated aperture. This aperture is invoked for the sake of achieving the analytical integrals in equation (1.6) and therefore provides attractable results of the general transmission function for optical systems such as the free space system, image system, and Fourier system in both the Fresnel and the Fraunhofer diffractions.

This inherent aperture caters to the common Gaussian beam source in speckle investigations. For example, the irradiance on the beam cross section of commonly used He-Ne lasers is given by a Gaussian function. For an illuminating Gaussian beam source with a $1/e^2$ intensity radius r_s, the spot size r_s is omitted on purpose while calculating the global ABCD matrix, but a limited Gaussian aperture [108-121] will be added in as the first device in train to compensate, whose matrix $\mathbf{M}$ is given by

$$\mathbf{M} = \begin{pmatrix} 1 & 0 \\ -\dfrac{j}{z_R} & 1 \end{pmatrix} \tag{1.8}$$

The parameter z_R in equation (1.8) is Rayleigh range defined as

$$z_R = k r_s^{\,2}/2 \tag{1.9}$$

For a typical 633nm He-Ne laser which is often cited as example in discussions later, if the aperture radius r_s is 0.1mm, we have $z_R = 5$ m. In the following discussions, the system is simplified as circular symmetric, and the intermediary is assumed to be non-absorbing medium. The turbulent inhomogeneity of the transfer medium is not taken into account. There is no cross talk between the two orthogonally polarized

wave components during propagation, which is ensured by the definition of the propagation equation.

At last, for the integral results from complex ABCD theory, a succinct discussion about its specific scope of application will be provided. Generally speaking, the complex ABCD theory is based on general Fresnel diffraction formula due to its integral form with Green function, and sets restriction of applicable propagation distance. The calculation results are valid when the separation of the optical elements is large compared with the beam size [109], and this sets restriction of applicable propagation distance to meet the paraxial approximation. This formulation is accurate in the Fresnel zone and is adequate to describe the beam propagation problems arising in this thesis. The free space propagation system employed as an example was explained well by J. Goodman in Chapter 4 of [84] and E. Wolf in Chapter 8 of [25]. Usually, a view angle no more than 30 degree or 0.5 rad would be acceptable as described by Siegman, Anthony E [110]. Furthermore, as Goodman has pointed out, the Fresnel approximation could also provide a very high accuracy even when the observation point approaches the diffracting aperture. We could say, for most of the propagation range we considered, the ABCD theory is valid.

1.2 Objective and organization of the thesis

To provide a deep insight into the statistical properties of a stochastic electromagnetic field with random change of polarization and the polarization speckle arising from it, a rough-surfaced retardation plate is introduced as a depolarizer for generation of the specially modulated field with prescribed statistical properties. The statistical analyses of the modulated field next to the plate are carried out in a vectorial form on the basis of the 2×2 beam coherence-polarization matrix. Depending on the extent of the surface roughness, its modulation behaviour to electric field is discussed under three conditions: the common rough-surface model, the gentle rough-surface model and the extremely rough-surface model. Within the framework of the complex ABCD matrix theory including inherent Gaussian apertures, analytical results for the propagation of polarization speckle in general optical systems are derived under the

paraxial approximation. The evolution of the degree of coherence and polarization on propagation is also illustrated.

The investigation is not only vital for the promotion of the advanced modulation device for statistical analysis of vectorial electromagnetic, but also crucial for the development of metrology methods based on polarization speckle. This thesis will focus on the investigation to answer the following questions:

- Could the decorrelation and depolarization effects to the whole field be realized simultaneously by a compact system consisting of a single device?

- For the random field generated by a rough-surfaced retardation plate, how will the polarization state vary on propagation and with different locations on the cross section of the beam?

- How will the roughness and the birefringent refractive indices affect the statistical parameters of the resultant field including the degree of coherence and the degree of polarization?

- What is the quantitative relationship between the features of propagation system and the statistical properties of the propagated speckle on the observation plane?

- What are the new features of the shape and dynamic properties of the generated polarization speckle?

- Instead of the rough-surfaced retardation plate, is depolarizer consisting of random polarizer array able to generate polarization speckles? And what are the statistical properties of the generated speckle?

The presentation of this thesis is organised as follows:

Firstly in Chapter 2, the basic surface model of rough-surfaced retardation plate is briefly introduced. For rough-surfaced retardation plate generating fully developed polarization speckle, the statistical properties of the resultant field are investigated in the form of a 2×2 beam coherence-polarization matrix. Analytical description of the coherence and polarization propagation will be expressed in terms of the matrix elements. Then in Chapter 3, the subject is the analytic conclusion about the statistical properties of the random electromagnetic field and the arising partially developed polarization speckle in vector form. The concise derivation of the propagation of coherence and polarization for general system will be provided within the framework of complex ABCD matrix theory. As a general demonstration of vectorial Van Cittert-Zernike theorem, the topic about the incoherent partially polarized field generated by an extremely rough-surfaced retardation plate and its propagation will be discussed in Chapter 4. Chapter 5 addresses the dynamic statistical properties of polarization speckle generated by a moving rough-surfaced retardation plate in the form of 2×2 time-lagged beam coherence-polarization matrix. The sensitivities of spatial-temporal characteristics of the dynamic polarization speckle to the plate surface structures, motion characters and the features of propagation system are discussed and interpreted. In Chapter 6, a random polarizer array is proposed as an alternative design scheme of depolarizer to generate polarization speckle with non-uniformly distributed polarization states. Finally, the summary of the main conclusions along with an outlook for future research work is given in Chapter 7.

Chapter 2

Statistics of Fully Developed Polarization Speckle Generated by a Rough-surfaced Retardation Plate Depolarizer

The coherence and polarization of polarization speckle, arising from a stochastic electromagnetic field with random change of polarization, modulated by a depolarizer are examined on the basis of the beam coherence-polarization matrix. The depolarizer is a rough-surfaced retardation plate with a random function of position introducing random phase differences between the two orthogonal components of the electric vector, thus imposing simultaneous depolarization and decorrelation on incident field. Under the assumption of Gaussian statistics with zero mean, the surface model for the depolarizer of the rough-surfaced retardation plate is obtained. The propagation of the modulated fields through any quadratic optical system is examined within the framework of the complex ABCD-matrix theory to show how the degrees of coherence and the degree of polarization of the beam change on propagation, including propagation in free space.

2.1 Introduction

Statistical properties of laser speckle have long been a subject of great importance in a broad area of physical optics and have received much attention due to its wide applications [1, 2, 29, 73]. In the majority of studies on laser speckle phenomena, these random optical fields have been traditionally treated as scalar optical fields without polarization information. Recently, statistical properties of random electric vector fields, referred to as polarization speckle, have attracted new research interest because of their theoretical importance and experimental interest in biology and metrology [34, 122]. Although a number of different methods have been proposed to produce polarization speckle in experimental studies [16, 101, 123], it is not an easy task to prepare the random vector fields with prescribed statistical properties, and therefore, their applicability has been somewhat limited.

On the other hand, a depolarizer is an optical device used to scramble the polarization of incident light [124]. In some applications such as spectrometry, even slight polarization of light can be a serious nuisance to the examination of specimens with polarizing tendencies; therefore, a depolarizer has been used to produce a random polarized output. So far, all the commercially available depolarizers consist of two pieces of components optically contacted to form a compound plate with at least one piece of birefringent material. Any ray passing through the depolarizer effectively introduces a varying phase difference between the two components of the electric field across the beam's cross section due to the thickness variation of the birefringent plate. Yet, as we know, for an input beam with uniform polarization, the output polarization from all commercially available depolarizers will be pseudo-random with a spatially periodic variation across the beam's cross section. An ideal depolarizer would give rise to really random polarized light, whatever its input polarization. To overcome this difficulty of pseudo-randomness in the polarization state, a number of different methods have been proposed [125-128]. One of the most promising methods among them is the use of a plate made of a birefringent material with a rough surface [125, 126]. Although this device has been proposed as early as in the 1960s, its strong capability and great importance to scramble the polarization state of the input light and to generate random electric fields have not yet received due attention. Therefore,

a theoretical and mathematical analysis of the physical properties that can characterize this efficient and practical field modulation device has not yet, to our knowledge, been elaborated.

In this chapter, we present a model for this depolarizer consisting of a rough-surfaced retardation plate. Within the framework of the complex ABCD method, the statistical properties of polarization speckle generated by the depolarizer are discussed. Following this, we examine the evolution of random electric fields modulated by the depolarizer to show how the spatial coherence and the polarization of such a beam changes during propagation.

2.2 Preliminary and formulation of the problem

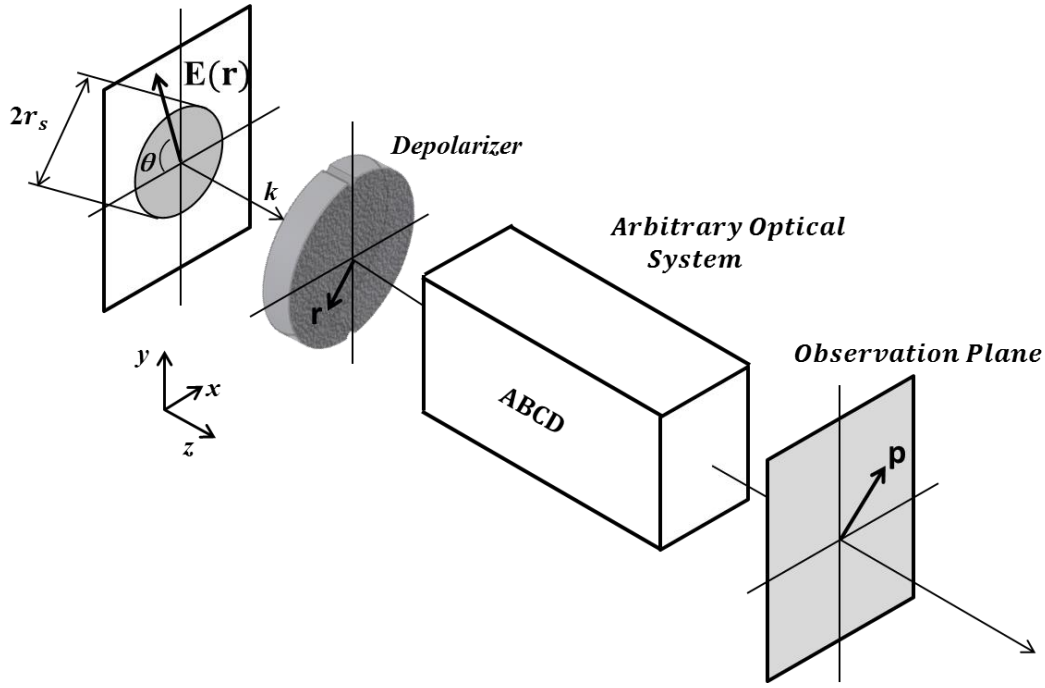

Figure 2.1 Schematic of the basic setup to examine the coherence and polarization properties of the electric field modulated by a rough-surfaced retardation plate traveling through a complex ABCD optical system

The concept of spatial coherence including spatial polarization effects for random vector electric fields has been studied extensively, where the two complex

components of the electric vector $\mathbf{E}(\mathbf{r}) = \{E_x(\mathbf{r}), E_y(\mathbf{r})\}$ obey circular symmetric Gaussian statistics. Before explaining the proposed surface models for the rough-surfaced retardation plate, we first briefly review the propagation of coherence and polarization in arbitrary optical system after the beam has passed a birefringent plate with known statistical properties.

Figure 2.1 shows the optical system that forms the basis of the chapter, where an incident beam with its width r_s and wave vector $\vec{k}$ is incident on the depolarizer with its statistical properties proposed in Section 2.3. The modulated light will pass through the optical ABCD system and arrive at the observation plane, where the statistical properties such as coherence and polarization have undergone changes. The second-order statistical properties of the stochastic vector electric fields are conveniently described by a 2×2 beam coherence-polarization matrix [31, 34]

$$\mathbf{W}(\mathbf{r}_1, \mathbf{r}_2) = \begin{pmatrix} \left\langle E_x^*(\mathbf{r}_1) E_x(\mathbf{r}_2) \right\rangle & \left\langle E_x^*(\mathbf{r}_1) E_y(\mathbf{r}_2) \right\rangle \\ \left\langle E_y^*(\mathbf{r}_1) E_x(\mathbf{r}_2) \right\rangle & \left\langle E_y^*(\mathbf{r}_1) E_y(\mathbf{r}_2) \right\rangle \end{pmatrix}, \tag{2.1}$$

where the asterisk * means complex conjugate, and angular brackets $\langle \cdots \rangle$ denote ensemble average. On the basis of the above beam coherence-polarization matrix, two parameters of primary interest, i.e., the degree of coherence η and degree of polarization P defined in Eq. (1.4) and (1.5) could be extracted from matrix elements of Eq. (2.1).

As the incident electric field passes through a depolarizer, the beam coherence-polarization matrix is changed accordingly. Let $\mathbf{W}^i(\mathbf{r_1}, \mathbf{r_2})$ be the beam coherence-polarization matrix of the incident beam and $\mathbf{T}(\mathbf{r})$ be the transmission matrix (also named as Jones matrix or ray-transfer matrix) of the depolarizer [118, 129]. Then the beam coherence-polarization matrix $\mathbf{W}^t(\mathbf{r}_1, \mathbf{r}_2)$ of the electric field just behind the depolarizer is given [31, 13]

$$\mathbf{W}^t\left(\mathbf{r}_1,\mathbf{r}_2\right)=\left\langle \mathbf{T}^\dagger\left(\mathbf{r}_1\right)\mathbf{W}^i\left(\mathbf{r}_1,\mathbf{r}_2\right)\mathbf{T}\left(\mathbf{r}_2\right)\right\rangle, \tag{2.2}$$

where the dagger † denotes the Hermitian conjugate and the superscript i or t represents incident or transmission fields before and after passing through the depolarizer, respectively. The beam coherence-polarization matrix in Eq. (2.2) is assumed to arise from transmission through the depolarizer with its surface described by the statistical properties. Under the paraxial approximation, the propagation of the beam coherence-polarization matrix through a complex ABCD optical system is given by

$$\mathbf{W}^o(\mathbf{p_1},\mathbf{p_2})=\iint \mathbf{W}^t(\mathbf{r_1},\mathbf{r_2})G^*(\mathbf{r_1},\mathbf{p_1})G(\mathbf{r_2},\mathbf{p_2})d\mathbf{r}_1 d\mathbf{r}_2. \tag{2.3}$$

where the superscript o indicates the fields at the observation plane, and the Green's function in the matrix formalism is

$$G\left(\mathbf{r},\mathbf{p}\right)=-\frac{jk}{2\pi B}\exp\left\{-\frac{jk}{2B}\left(A\left|\mathbf{r}\right|^2-2\mathbf{r}\cdot\mathbf{p}+D\left|\mathbf{p}\right|^2\right)\right\}. \tag{2.4}$$

In the equation above, j is the imaginary unit and the A, B and D are complex values that can be determined by multiplying the matrices for all the individual optical components in the optical train, i.e., lenses, free space propagation, and apertures [108, 110]. The benefit of the above expression in Eq. (2.4) is that it usually enables us to give an analytical result, covering a broad range of optical systems. In arriving at the above expression, we have tacitly assumed that the refractive indices in the input and output planes are identical but not necessarily unity.

2.3 Modulation behaviour of a rough-surfaced retardation plate to incident beam

The depolarizer analysed in this chapter employs a plate of birefringent material with a rough surface. From the principle of operation for a retardation plate, it resolves an

incident beam of polarized light into two orthogonal components; retards the phase of one component relative to the other; then recombines the components into a single beam with changed polarization state. The birefringence will depend on the plate thickness of the material as well as the wavelength of the incident light and the birefringence value. Thus, if the retardation plate has a surface roughness on the order of the polarization beat length $\lambda / \left| n_x - n_y \right|$ with λ being wavelength of light in vacuum and n_m $(m = x, y)$ being the corresponding refractive index for the birefringent material [130], a light beam coming from such a surface will contain rays with all states of polarization. For the sake of simplicity in the derivation, we will assume the statistics of the surface to be space and time independent, i.e., stationary and homogeneity in the micro-structure are invoked. Finally, we will also assume the intensity transmission coefficient for the retardation plate with a rough surface to be equal to unity. It should be noticed that the surface model, derived here, is addressed with respect to a transparent structure, while the model is equally applicable for the analysis of reflective structures.

Figure 2.2 Diagram of depolarizer: rough-surfaced retardation plate

Figure 2.2 shows the schematic diagram of such depolarizer: rough-surfaced retardation plate with a line connecting the notches indicating the optical axis of the birefringent material. Suppose now that the rough-surfaced retardation plate is aligned along the y axis with the incident field perpendicular to the depolarizer. For a “thin” device without taking internal reflection and scattering into account, the transmission matrix then becomes [129]

$$\mathbf{T}(\mathbf{r}) = \begin{pmatrix} e^{-j\varphi_x(\mathbf{r})} & 0 \\ 0 & e^{-j\varphi_y(\mathbf{r})} \end{pmatrix} = \begin{pmatrix} e^{-jd(\mathbf{r})k(n_x-1)} & 0 \\ 0 & e^{-jd(\mathbf{r})k(n_y-1)} \end{pmatrix}, \tag{2.5}$$

where $k = |\vec{k}|$ is the wave number of light in vacuum, $d(\mathbf{r})$ is the local thickness, and $\varphi_m(\mathbf{r}) = d(\mathbf{r})k(n_m - 1)$, $(m = x, y)$ is the effective phase delay for the x or y components of the electric fields introduced by an optical path passing through the retardation plate with surface thickness fluctuation and the remaining region of free space. Thus, the relative phase shift between the two orthogonal components $\Delta = k(n_y - n_x)d(\mathbf{r})$ proportional to the local thickness varies with the local position; therefore the rough-surfaced retardation plate forms an effective depolariser to introduce random polarization transformations.

To understand the performance of the rough-surfaced retardation plate as a depolarizer, we first derive the beam coherence-polarization matrix of the modulated fields just behind the depolarizer. After substitution of Eq. (2.5) into Eq. (2.2), we have

$$\begin{aligned} \mathbf{W}^t(\mathbf{r}_1, \mathbf{r}_2) &= \begin{pmatrix} \langle E_x^{t*}(\mathbf{r}_1)E_x^t(\mathbf{r}_2)\rangle & \langle E_x^{t*}(\mathbf{r}_1)E_y^t(\mathbf{r}_2)\rangle \\ \langle E_y^{t*}(\mathbf{r}_1)E_x^t(\mathbf{r}_2)\rangle & \langle E_y^{t*}(\mathbf{r}_1)E_y^t(\mathbf{r}_2)\rangle \end{pmatrix} \\ &= \begin{pmatrix} \mathbf{W}_{xx}^i(\mathbf{r}_1, \mathbf{r}_2)\langle e^{j\Delta\varphi_{xx}(\mathbf{r}_1,\mathbf{r}_2)}\rangle & \mathbf{W}_{xy}^i(\mathbf{r}_1, \mathbf{r}_2)\langle e^{j\Delta\varphi_{xy}(\mathbf{r}_1,\mathbf{r}_2)}\rangle \\ \mathbf{W}_{yx}^i(\mathbf{r}_1, \mathbf{r}_2)\langle e^{j\Delta\varphi_{yx}(\mathbf{r}_1,\mathbf{r}_2)}\rangle & \mathbf{W}_{yy}^i(\mathbf{r}_1, \mathbf{r}_2)\langle e^{j\Delta\varphi_{yy}(\mathbf{r}_1,\mathbf{r}_2)}\rangle \end{pmatrix}. \end{aligned} \tag{2.6}$$

When Eq. (2.6) was derived, we have made use of the fact that the coherence property of the incident field and the correlation property of the depolarizer are statistically independent and the ensemble average denoted by angular brackets has been taken over the rough-surfaced retardation plate.

We recognize every element in the beam coherence-polarization matrix in Eq. (8) as being closely related to the characteristic function of the random variable $\Delta\varphi_{lm}(\mathbf{r}_1, \mathbf{r}_2) = d(\mathbf{r}_1)k(n_l - 1) - d(\mathbf{r}_2)k(n_m - 1)$, $(l, m = x, y)$ [29]. In fact we can write,

$$\left\langle \exp\left\{ j\Delta\varphi_{lm} \right\} \right\rangle = \mathbf{M}_{\Delta\varphi_{lm}}(\omega)\,|_{\omega=1}, \tag{2.7}$$

where $\mathbf{M}_{\Delta\varphi_{lm}}(\omega)$ is the characteristic function of the random variable $\Delta\varphi_{lm}$ [29]. We now take advantage of the assumption that the probability distributions for the phase delays (or equivalently the random surface-thickness) are Gaussian and their statistics are isotropic. Further progress can be made in a similar way used to describe the Gaussian random-phase screen [2, 29]. The characteristic function of the phase difference is

$$\left\langle \exp\{ j\Delta\varphi_{lm} \} \right\rangle = \exp\left[j\left\langle \Delta\varphi_{lm}(\mathbf{r}_1, \mathbf{r}_2) \right\rangle - \frac{\sigma^2_{\Delta\varphi_{lm}}}{2} \right], \tag{2.8}$$

where $\sigma^2_{\Delta\varphi_{lm}}$ is the variance of the phase shift. On the basis of the relationship between the phase delay and the local depolarizer thickness, the average value of the relative phase shift can be evaluated as

$$\left\langle \Delta\varphi_{lm}(\mathbf{r}_1, \mathbf{r}_2) \right\rangle = \left\langle d(\mathbf{r}_1) \right\rangle k(n_l - 1) - \left\langle d(\mathbf{r}_2) \right\rangle k(n_m - 1) \tag{2.9}$$

Notice the fact that the average surface thickness $\langle d(\mathbf{r}) \rangle$ in the retardation place will make no contribution to the scrambling of the polarization state of the incident beam as a depolarizer and therefore can tacitly be assumed to be zero without loss of generality. Therefore, the variance of the relative phase shift is

$$\begin{aligned} \sigma^2_{\Delta\varphi_{lm}} &= \left\langle [\Delta\varphi_{lm}(\mathbf{r}_1, \mathbf{r}_2) - \left\langle \Delta\varphi_{lm}(\mathbf{r}_1, \mathbf{r}_2) \right\rangle]^2 \right\rangle \\ &= k^2 \left\{ (n_l - 1)^2 \left\langle d^2(\mathbf{r}_1) \right\rangle + (n_m - 1)^2 \left\langle d^2(\mathbf{r}_2) \right\rangle \right. \\ &\quad \left. -2(n_l - 1)(n_m - 1)\left\langle d(\mathbf{r}_1) d(\mathbf{r}_2) \right\rangle \right\}. \end{aligned} \tag{2.10}$$

Next, we make a convenient mathematical assumption about the form of the surface thickness correlation function, namely, let

$$\left\langle d(\mathbf{r}_1)d(\mathbf{r}_2)\right\rangle = {\sigma_d}^2 \exp\left\{-\frac{|\Delta\mathbf{r}|^2}{{r_d}^2}\right\}, \tag{2.11}$$

where $\Delta\mathbf{r} = \mathbf{r}_1 - \mathbf{r}_2$, r_d is the radius at which the normalized surface thickness correlation falls to $1/e$, and ${\sigma_d}^2$ is the variance of the local surface thickness. We then have

$$\begin{aligned}&\left\langle \exp\left\{ j\Delta\varphi_{xx}(\mathbf{r}_1,\mathbf{r}_2)\right\}\right\rangle \\ &= \exp\left[-k^2{\sigma_d}^2(n_x-1)^2\left\{1-\exp\left\{-\frac{|\Delta\mathbf{r}|^2}{{r_d}^2}\right\}\right\}\right],\end{aligned} \tag{2.12}$$

$$\begin{aligned}&\left\langle \exp\left\{ j\Delta\varphi_{yy}(\mathbf{r}_1,\mathbf{r}_2)\right\}\right\rangle \\ &= \exp\left[-k^2{\sigma_d}^2(n_y-1)^2\left\{1-\exp\left\{-\frac{|\Delta\mathbf{r}|^2}{{r_d}^2}\right\}\right\}\right],\end{aligned} \tag{2.13}$$

$$\begin{aligned}&\left\langle \exp\left\{ j\Delta\varphi_{xy}(\mathbf{r}_1,\mathbf{r}_2)\right\}\right\rangle = \left\langle \exp\left\{ j\Delta\varphi_{yx}(\mathbf{r}_1,\mathbf{r}_2)\right\}\right\rangle \\ &= \exp\left\{-\frac{k^2{\sigma_d}^2}{2}\left[(n_x-1)^2+(n_y-1)^2-2(n_x-1)(n_y-1)\exp\left\{-\frac{|\Delta\mathbf{r}|^2}{{r_d}^2}\right\}\right]\right\},\end{aligned} \tag{2.14}$$

Equations (2.12)-(2.14) provide us with the desired correlation properties for the depolarizer of the rough-surfaced retardation plate and can be considered as one of the prime results of this chapter to describe the correlation properties of the scattered electric field and the surface thickness fluctuations of the birefringent material without any restriction on the incident source. Notice that the correlation widths measured by the width of the curves at their half-maxima are different for every element in the beam coherence-polarization matrix, thus indicating different "average widths" of a polarization speckle along the x and y direction. It's the birefringence associated with the rough-surfaced retardation plate that introduces the anisotropy for the generated polarization speckle with difference average width.

Under the assumption of a large surface roughness with large phase variance, owing to the smaller lateral distance required to obtain a phase difference of 2π, we can make further progress. In this case, the second exponential term in Eq. (2.12)-(2.14) may be series expanded, and only the first two terms in the series are essential [131]. For $(n_l - 1)(n_m - 1)k^2{\sigma_d}^2 >> (2\pi)^2$, $(l, m = x, y)$, we directly have

$$\begin{aligned} &\left\langle \exp\{j\Delta\varphi_{lm}\}\right\rangle \\ &= \exp\left\{-\frac{k^2{\sigma_d}^2}{2}\left[(n_l - n_m)^2 + 2(n_l - 1)(n_m - 1)\frac{|\Delta\mathbf{r}|^2}{{r_d}^2}\right]\right\}. \end{aligned} \tag{2.15}$$

The approximation in Eq. (2.15) has resulted in the breaking down of the double exponential into a single exponential, thus facilitating further mathematical analysis in order to later arrive at an analytical solutions for the propagation of the beam coherence-polarization matrix through a complex ABCD optical system.

2.4 Changes in the degree of polarization and the degree of coherence on propagation

We now have the necessary tools to calculate the propagation of the beam coherence-polarization matrix through an optical system when the electric fields are modulated by the given depolarizer. For demonstration purpose only, and without loss of generality, we will perform our calculations only for an incident field that is a linearly polarized, spatially coherent Gaussian beam with the electric field, thus making an angle θ with the x axis.

According to the Eq. (2.1), the beam coherence-polarization matrix for the linearly polarized Gaussian beam just in front of the depolarizer is given by,

$$\mathbf{W}^i(\mathbf{r}_1, \mathbf{r}_2) = I_o \exp\left\{-\frac{|\mathbf{r}_1|^2 + |\mathbf{r}_2|^2}{{r_s}^2}\right\}\begin{pmatrix} \cos^2\theta & \cos\theta\sin\theta \\ \cos\theta\sin\theta & \sin^2\theta \end{pmatrix}, \tag{2.16}$$

where I_o is the on-axis intensity of the incident field. On substituting from Eq. (2.15) and Eq. (2.16) into Eq. (2.6), we obtain the expressions for each element in the beam coherence-polarization matrix of the initially linearly polarized beam just behind the depolarizer

$$\mathbf{W}_{xx}^{t} = I_o \cos^2\theta \exp\left\{-\frac{|\mathbf{r}_1|^2 + |\mathbf{r}_2|^2}{r_s^{\,2}}\right\} \exp\left\{-\frac{k^2 \sigma_d^{\,2} (n_x - 1)^2 |\Delta\mathbf{r}|^2}{r_d^{\,2}}\right\}, \tag{2.17}$$

$$\mathbf{W}_{yy}^{t} = I_o \sin^2\theta \exp\left\{-\frac{|\mathbf{r}_1|^2 + |\mathbf{r}_2|^2}{r_s^{\,2}}\right\} \exp\left\{-\frac{k^2 \sigma_d^{\,2} (n_y - 1)^2 |\Delta\mathbf{r}|^2}{r_d^{\,2}}\right\}, \tag{2.18}$$

$$\begin{aligned}\mathbf{W}_{xy}^{t} = \mathbf{W}_{yx}^{t} = I_o \sin\theta\cos\theta \exp\left\{-\frac{|\mathbf{r}_1|^2 + |\mathbf{r}_2|^2}{r_s^{\,2}}\right\} \\ \times \exp\left\{-k^2 \sigma_d^{\,2}\left[\frac{(n_x - n_y)^2}{2} + \frac{(n_x - 1)(n_y - 1)|\Delta\mathbf{r}|^2}{r_d^{\,2}}\right]\right\}.\end{aligned} \tag{2.19}$$

Our interest here is the static random spatial distribution of the state of polarization of the modulated electric fields. To describe the statistical property of such fields, we have replaced the conventional time average by spatial average for ensemble average in Eq.(2.1) [16, 132]. On substituting from Eqs. (2.17)-(2.19) into Eq.(1.5), we obtain the expression of the spatial degree of polarization for the modulated fields by the depolarizer. That is

$$P^t(\mathbf{r}) = \sqrt{1 - \sin^2 2\theta\left[1 - \exp\left\{-k^2 \sigma_d^{\,2} (n_x - n_y)^2\right\}\right]}, \tag{2.20}$$

which is a constant no matter where the observation point is chosen. As expected, a perfectly polarized coherent incident beam has become spatially partially polarized or depolarized after passing through the static depolarizer. To provide physical insight into these results, we consider three special cases, namely, $\theta = 0$, $\theta = \pi/4$ and

$\theta = \pi/2$. When $\theta = 0$ or $\theta = \pi/2$ where the polarization direction of the incident electric field vector is parallel or perpendicular to the optical axis of the rough-surfaced retardation plate, the spatial degree of polarization equals one, i.e., $P^t(\mathrm{r})|_{\theta=0,\pi/2} = 1$, thus indicating that the polarization state for the incident field will be maintained without depolarization effect. One the other hand, when $\theta = \pi/4$, the spatial degree of polarization attains its minimum value, i.e., $P^t(\mathrm{r})|_{\theta=\pi/4} = \exp\{-k^2\sigma_d^2(n_x - n_y)^2\}$ indicating the best performance for the depolarizer to scramble the incident polarization. This is a direct consequence of the fact that the depolarizer plate has strong polarization dependence, as already demonstrated. In a similar way, the degree of spatial coherence of the modulated electric fields behind the depolarizer is obtained by use of Eqs. (2.17)-(2.19) and Eq. (1.4) on the basis of the spatial average, thus giving

$$\eta^t(\mathbf{r_1}, \mathbf{r_2}) = \cos^2\theta \exp\left[-\frac{k^2{\sigma_d}^2(n_x - 1)^2|\Delta\mathbf{r}|^2}{{r_d}^2}\right] + \sin^2\theta \exp\left[-\frac{k^2{\sigma_d}^2(n_y - 1)^2|\Delta\mathbf{r}|^2}{{r_d}^2}\right], \tag{2.21}$$

indicating that spatially partial coherence has been achieved for the transmitted fields regardless of the incident polarization angle.

We next consider the propagation of the electric field just behind the depolarizer of a rough-surfaced retardation plate illustrated by a linearly polarized Gaussian beam. After substitution of Eqs. (2.17)-(2.19) into Eq. (2.3), the beam coherence-polarization matrix after passing the ABCD system can now be written as

$$\mathbf{W}^o(\mathbf{p_1},\mathbf{p_2})=I_o\cos\theta\sin\theta e^{-\frac{k^2\sigma_d^2(n_x-n_y)^2}{2}}$$
$$\begin{pmatrix} e^{\frac{k^2\sigma_d^2(n_x-n_y)^2}{2}}\cot\theta W_a^{ABCD}\left(\mathbf{p_1},\mathbf{p_2};\frac{r_d^{\,2}(k\sigma_d)^{-2}}{(n_x-1)^2}\right) & W_a^{ABCD}\left(\mathbf{p_1},\mathbf{p_2};\frac{r_d^{\,2}(k\sigma_d)^{-2}}{(n_x-1)(n_y-1)}\right) \\ W_a^{ABCD}\left(\mathbf{p_1},\mathbf{p_2};\frac{r_d^{\,2}(k\sigma_d)^{-2}}{(n_x-1)(n_y-1)}\right) & e^{\frac{k^2\sigma_d^2(n_x-n_y)^2}{2}}\tan\theta W_a^{ABCD}\left(\mathbf{p_1},\mathbf{p_2};\frac{r_d^{\,2}(k\sigma_d)^{-2}}{(n_y-1)^2}\right) \end{pmatrix}, \tag{2.22}$$

where $W_a^{ABCD}(\mathbf{p}_1,\mathbf{p}_2;\beta)$ is an integral function with a parameter β evaluated analytically as

$$\begin{aligned} W_a^{ABCD}(\mathbf{p}_1,\mathbf{p}_2;\beta) &= \int_{-\infty}^{\infty}\int \exp\left\{-\frac{|\mathbf{r}_1|^2+|\mathbf{r}_2|^2}{r_s^{\,2}}-\frac{|\Delta\mathbf{r}|^2}{\beta}\right\}G^*(\mathbf{r}_1,\mathbf{p}_1)G(\mathbf{r}_2,\mathbf{p}_2)\,d\mathbf{r}_1 d\mathbf{r}_2 \\ &= \frac{\beta}{4\,\mathrm{Im}\left[A^*B\right]/k+\beta|A|^2}\exp\left\{\frac{-|\mathbf{p}_1-\mathbf{p}_2|^2}{4\,\mathrm{Im}\left[A^*B\right]/k+\beta|A|^2}\right\} \\ &\exp\left\{\frac{-j\left(|\mathbf{p}_1|^2-|\mathbf{p}_2|^2\right)\left\{\mathrm{Im}\left[B^2\right]-2\,\mathrm{Im}\left[A^*B\right]\mathrm{Re}\left[D^*B\right]+\frac{k\beta}{2}\left(\mathrm{Re}\left[AB\right]-\mathrm{Re}\left[D^*B\right]|A|^2\right)\right\}}{\left(4\,\mathrm{Im}\left[A^*B\right]/k+\beta|A|^2\right)|B|^2}\right\} \\ &\exp\left\{\frac{-\left(|\mathbf{p}_1|^2+|\mathbf{p}_2|^2\right)\left\{-2\,\mathrm{Im}\left[B\right]^2+2\,\mathrm{Im}\left[A^*B\right]\mathrm{Im}\left[D^*B\right]+\frac{k\beta}{2}\left(|A|^2\,\mathrm{Im}\left[B^*D\right]-\mathrm{Im}\left[AB\right]\right)\right\}}{\left(4\,\mathrm{Im}\left[A^*B\right]/k+\beta|A|^2\right)|B|^2}\right\}. \end{aligned}$$

(2.23)

When Eq. (2.23) is evaluated, we have intentionally omitted the illuminating beam size r_s and possible radius of curvature, as they can conveniently be included as the first optical element, i.e., an aperture and a lens, when the total ABCD matrix is calculated, just remembering to properly compensate for the incident power in case it is held constant and is of importance for the parameters to be found [108]. Equations (2.22) and (2.23) provide the analytic results for the propagation of the beam coherence-polarization matrix through a complex ABCD optical system. Using these

results, along with the formulas in Eqs. (1.4) and (1.5), one can calculate the corresponding degree of spatial coherence and spatial degree of polarization of the stochastic electric fields in any observation plane $z > 0$ in the case where the depolarizer is illuminated by a linearly polarized Gaussian electromagnetic beam.

As an example, we will consider a typical case of free space propagation over a distance $z > 0$ with a preceding aperture of size r_s to compensate the spot size, as shown in Figure 2.1. The corresponding ABCD matrix can be written as

$$\mathbf{M} = \begin{pmatrix} 1 - jz / z_R & z \\ -j / z_R & 1 \end{pmatrix}, \tag{2.24}$$

where z_R is the Rayleigh range $z_R = kr_s^2/2$. By substituting these elements of the ABCD matrix into Eq. (2.23), one can study the changes in the degree of polarization and the degree of coherence for free space propagation. To present some numerical examples, we have taken the following parameters: $r_s = 1\text{mm}$, $r_d = 0.1\text{mm}$, $\lambda = 0.633\mu\text{m}$, $\sigma_d = 2.073\mu\text{m}$, $n_x = 1.486$ and $n_y = 1.658$ for the birefringent material: Calcite [133].

Figures 2.3(a)-(c) show the degree of polarization of the polarization speckle for free-space propagation, plotted against the normalized propagation distance z/z_R and normalized lateral distance measured in spot size p/r_s for some selected values of the polarization angle $\pi/6$, $\pi/4$ and $\pi/3$, respectively. As expected, the degree of polarization changes appreciably depending on the propagation distance z and on the polarization angle of incident beam. Instead of a uniform distribution for the modulated electric fields just behind the depolarizer, the spatial degree of polarization for the polarization speckle after propagation does not remain uniform. Such behaviour is in agreement with some early studies on the changes on polarizations of light on propagation [8, 13].

Figures 2.3(d)-(f) give the absolute values of the degree of coherence of the polarization speckle generated by the depolarizer at two positions $\Delta\mathbf{p} = \mathbf{p}_1 - \mathbf{p}_2$ located symmetrically with respect to the z axis along the normalized propagation distance. It can readily be seen that the degree of coherence takes a large value close to unity for two points located near the optical axis. These figures indicate how the degree of coherence evolves for the selected polarization angle of the incident beam. Here it's also interesting to notice that the different polarization angles for the incident beams have little effect on the coherence propagation.

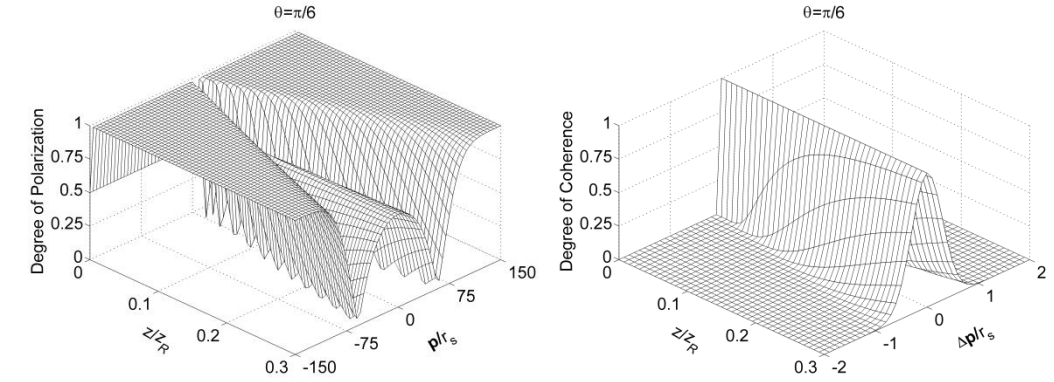

(a) (d)

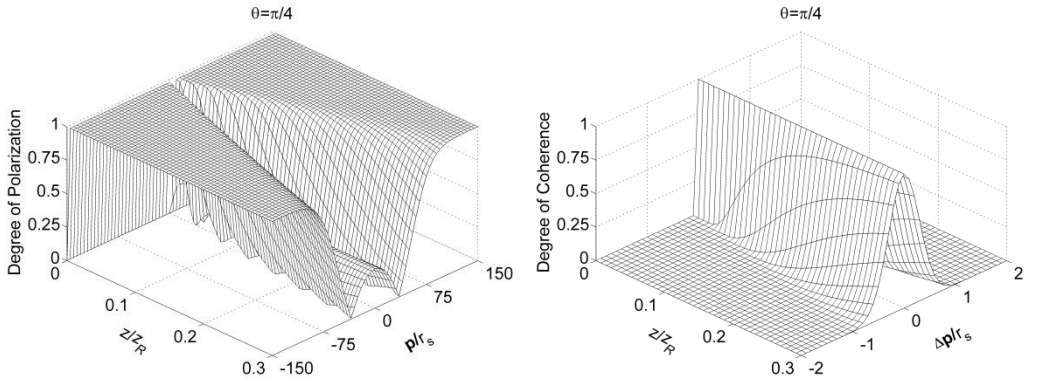

(b) (e)

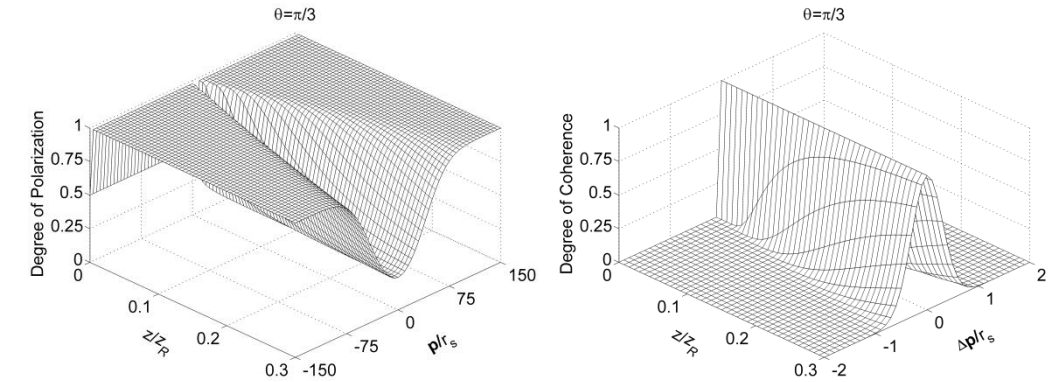

(c) (f)

Figure 2.3 Degree of polarization (left column) and coherence (right column) for free-space propagation. The angles of incidence of the polarized light are: $\pi/6$, $\pi/4$, and $\pi/3$.

2.5 Conclusion

In summary, we have examined the degree of coherence and degree of polarization of the polarization speckle generated by the depolarizer of rough-surfaced retardation plate. Under the Gaussian assumption, we have presented a model for the rough-surfaced retardation plate acting as a depolarizer and have established a close relationship between the correlation of the scattered electric fields and the surface thickness fluctuations for a polarization-sensitive surface of a birefringent material. Within the framework of the complex ABCD method, we have also studied the changes in the degree of polarization and the degree of coherence for the generated polarization speckle on propagation in free space. In particular, we have shown that the degree of polarization becomes nonuniform depending on the propagation distance and the polarization angle of the incident beam despite its uniform distribution across the source beam cross section. Further, a systematic analysis of the depolarization effect introduced by the rough-surfaced retardation plate is important because it will facilitate our understanding of the polarization speckle generation. Hence, this chapter can provide practical insight into a wide class of phenomena associated with the random polarization.

Chapter 3

Statistics of Partially Developed Polarization Speckle Generated by Gentle Rough-surfaced Retardation Plate Depolarizer

For a rough-surfaced retardation plate as a particular polarization-dependent phase modulation device, its performance is affected by its surface roughness structures. In the previous chapter, its decorrelation and depolarization effect have been investigated under an assumption of rough surface model with great covariance of thickness fluctuation, and then fully developed speckle is able to be generated by this plate. In this chapter, the analysis of the rough-surfaced retardation plate will continue but focuses on a gentle roughness model. While the thickness fluctuation is relatively small, the partially developed speckle will be generated. The statistics of partially developed polarization speckle with nonuniform spatial distribution of polarization state will be discussed in the form of matrix elements of beam coherence-polarization matrix. The propagation of the partially developed speckle will be traced within the framework of complex ABCD matrix theory under paraxial approximation to reveal the evolution of its degree of coherence and polarization on propagation. The differences of statistical features to the fully developed polarization speckle are also illustrated.

3.1 Introduction

The research work in the chapter is considered as the natural extension of the discussion in the last chapter for the rough-surfaced retardation plate, with a different extent of the surface roughness, and thus generated random vector electromagnetic field with different modulation depth. The rough-surfaced retardation plate's modulation behaviour to the field determined by its surface-roughness and birefringence, together with the variation tendency of the field's statistical properties on propagation will still be the major concerns. Unless otherwise specified, the notations of the last chapter will be cited directly.

In the previous chapter, the rough-surfaced retardation plate with a great roughness model implying $(n_l - 1)(n_m - 1)k^2\sigma_d{}^2 >> (2\pi)^2$ is applied to generate fully polarized speckle, and has been statistically studied in the vectorial form. Randomly distributed phase difference between the two orthogonal components of the electric field on the beam cross section is brought in by the random thickness variation of the birefringent plate, and thus, the depolarization and decorrelation effects are realized. These modulation effects imposed on incident beam show significant dependence on the statistical description of the plate's surface roughness. Since the variety of roughness models and resulted polarization speckles are far beyond what can be covered, a widely accepted Gaussian-Gaussian roughness model with great covariance of thickness fluctuation compared with wavelength was discussed first. Analytical conclusions about the statistical properties of the modulated field were derived under this assumption, and then promoted the statistical study of the propagated polarization speckle in optical systems.

To provide a more comprehensive understanding of the modulation performance of rough-surfaced retardation plate, the same kind of depolarizer with different extent of the surface roughness needs to be investigated too. In this chapter, a gentle rough surface model accompanied with resultant partially developed speckle will be

discussed in a vectorial context. By "gentle rough" surface, we mean a rough-surfaced retardation plate producing random phase fluctuations $(n_m - 1)k\sigma_d$, $(m = x, y)$ that are smaller than or comparable to 2π radians. For the investigation about its modulation behaviour and the propagation of the polarization and coherence properties in general optical systems, the research work will also be carried out in form of the 2×2 beam coherence-polarization matrix in company with complex ABCD theory.

3.2 Modulation behaviour of gentle rough-surfaced retardation plate to incident beam

The setup of the optical system that forms the basis for this chapter is the same as the diagram shown in Figure 2.1. For a rough-surfaced retardation plate employed as depolarizer, its optical axis will be aligned along the y axis. Therefore, its transmission matrix $\mathbf{T}$ is given by [129]

$$\mathbf{T}(\mathbf{r}) = \begin{pmatrix} e^{-j\varphi_x(\mathbf{r})} & 0 \\ 0 & e^{-j\varphi_y(\mathbf{r})} \end{pmatrix} = \begin{pmatrix} e^{-jd(\mathbf{r})k(n_x-1)} & 0 \\ 0 & e^{-jd(\mathbf{r})k(n_y-1)} \end{pmatrix}, \tag{3.1}$$

where n_m $(m = x, y)$ denotes the refractive indices of the birefringent material, $k = |\vec{k}|$ is the wave number of light in vacuum, and $\varphi_m(\mathbf{r}) = d(\mathbf{r})k(n_m - 1)$ is the effective phase delay for corresponding component of the electric fields proportional to the local thickness $d(\mathbf{r})$. The transmission matrix $\mathbf{T}$ governs the relationship $\mathbf{E}^t = \mathbf{E}^i\mathbf{T}$ between the incident field $\mathbf{E}^i$ just before the plate and the transmission field $\mathbf{E}^t$ after the plate. It is easy to find that the random polarization transformation will be introduced as a result of the phase shift $k(n_y - n_x)d(\mathbf{r})$ between the two orthogonal components of local field dominated by the random thickness variation of the plate. Employ the statistical independence between the correlation property of the plate surface roughness and the coherence state of the incident field, a 2×2 beam

coherence-polarization matrix for the modulated field at points $\mathbf{r}_1$ and $\mathbf{r}_2$ could be established

$$\begin{aligned}\mathbf{W}^t(\mathbf{r}_1,\mathbf{r}_2) &= \begin{pmatrix} \left\langle E^{t*}_x(\mathbf{r}_1)E^t{}_x(\mathbf{r}_2)\right\rangle & \left\langle E^{t*}_x(\mathbf{r}_1)E^t{}_y(\mathbf{r}_2)\right\rangle \\ \left\langle E^{t*}_y(\mathbf{r}_1)E^t{}_x(\mathbf{r}_2)\right\rangle & \left\langle E^{t*}_y(\mathbf{r}_1)E^t{}_y(\mathbf{r}_2)\right\rangle \end{pmatrix} \\ &= \begin{pmatrix} W^i_{xx}(\mathbf{r}_1,\mathbf{r}_2)\left\langle e^{j\Delta\varphi_{xx}(\mathbf{r}_1,\mathbf{r}_2)}\right\rangle & W^i_{xy}(\mathbf{r}_1,\mathbf{r}_2)\left\langle e^{j\Delta\varphi_{xy}(\mathbf{r}_1,\mathbf{r}_2)}\right\rangle \\ W^i_{yx}(\mathbf{r}_1,\mathbf{r}_2)\left\langle e^{j\Delta\varphi_{yx}(\mathbf{r}_1,\mathbf{r}_2)}\right\rangle & W^i_{yy}(\mathbf{r}_1,\mathbf{r}_2)\left\langle e^{j\Delta\varphi_{yy}(\mathbf{r}_1,\mathbf{r}_2)}\right\rangle \end{pmatrix}.\end{aligned} \tag{3.2}$$

To evaluate the characteristic functions $\left\langle \exp\{j\Delta\varphi_{lm}(\mathbf{r}_1,\mathbf{r}_2)\}\right\rangle$ of the corresponding random variables $\Delta\varphi_{lm}(\mathbf{r}_1,\mathbf{r}_2) = d(\mathbf{r}_1)k(n_l-1) - d(\mathbf{r}_2)k(n_m-1)$, $(l,m = x,y)$ in elements of the Eq. (3.2), an assumption about the statistics of the random surface thickness $d(\mathbf{r})$ has to be made. The most commonly adopted Gaussian-Gaussian model [29, 64, 134] is utilized again for further progress. Thus, the surface thickness fluctuation is a zero mean Gaussian distribution. At the same time, the lateral correlation of thickness is given by a Gaussian function of distance between points $\Delta\mathbf{r} = \mathbf{r}_1 - \mathbf{r}_2$:

$$\left\langle d(\mathbf{r}_1)d(\mathbf{r}_2)\right\rangle = {\sigma_d}^2 \exp\left\{-\frac{|\Delta\mathbf{r}|^2}{{r_d}^2}\right\}, \tag{3.3}$$

where r_d is the scale of the lateral correlation length and ${\sigma_d}^2$ depicts the covariance of surface roughness. Following similar steps in the last chapter, we arrive at an exact expression

$$\begin{aligned}&\left\langle \exp\{j\Delta\varphi_{lm}(\mathbf{r}_1,\mathbf{r}_2)\}\right\rangle \\ &= \exp\left\{-\frac{k^2{\sigma_d}^2}{2}\left[(n_l-n_m)^2 + 2(n_l-1)(n_m-1)\left(1-\exp\left\{-\frac{|\Delta\mathbf{r}|^2}{{r_d}^2}\right\}\right)\right]\right\}.\end{aligned} \tag{3.4}$$

This is general conclusion for Gaussian-Gaussian model with arbitrary extent of the surface roughness. While the assumption of large surface roughness implying $(n_l-1)(n_m-1)k^2{\sigma_d}^2 >> (2\pi)^2$ leads to a Gaussian approximation in Eq. (2.15) for rough-surfaced retardation plate discussed in Chapter 2, the classical method to handle the double exponential function in Eq. (3.4) for a gentle rough to smooth surface[135, 136] model producing small random phase fluctuations is expanding it into an infinite Taylor series for further discussion[131, 137]. The advantage is a good accuracy for any roughness models, if the number of the Taylor series terms included in numerical calculation is large enough. However, a long computation time will be required, and it is hard to conclude a result in close-term from this pure numerical approximation. To simplify the analysis and mathematical derivation of the field modulation, a modified approximation as a combination of a constant and a Gaussian function was proposed by B. Rose, H. Imam, S. G. Hanson, and H.T. Yura [137, 138] for the analysis of scalar speckle. With essential amendment and derivations, it is now extended to describe the vectory coherence properties of partially developed polarization speckle originated form the random electric field modulated by a gentle rough-surfaced retardation plate. By this way, for gentle rough-surfaced retardation plate discussed here, Eq. (3.4) is approximately rewritten as

$$\begin{aligned}&\left\langle \exp\left\{ j\Delta\varphi_{lm}(\mathbf{r}_1,\mathbf{r}_2)\right\}\right\rangle \\ &\approx \exp\left\{-\frac{k^2{\sigma_d}^2}{2}(n_l-n_m)^2\right\} \\ &\left[\exp\left\{-k^2{\sigma_d}^2(n_l-1)(n_m-1)\right\}+\left(1-\exp\left\{-k^2{\sigma_d}^2(n_l-1)(n_m-1)\right\}\right)\exp\left\{-\frac{|\Delta\mathbf{r}|^2 c_{lm}}{{r_d}^2}\right\}\right],\end{aligned} \tag{3.5}$$

where c_{lm} is a parameter given by

$$c_{lm}=\frac{k^2{\sigma_d}^2(n_l-1)(n_m-1)}{1-\exp\left\{-k^2{\sigma_d}^2(n_l-1)(n_m-1)\right\}}. \tag{3.6}$$

As a consequence, the double exponential in Eq. (3.4) is simplified into a combination of Gaussian function with a constant. As we will demonstrate in the following section, on the basis of this result, analytical expression of the beam coherence-polarization matrix for propagated speckle is now able to be derived.

3.3 Evolution of the polarization and coherence properties on propagation for polarization speckle generated by gentle rough-surfaced retardation plate

The propagation analysis of the polarization speckle generated by a given gentle rough-surfaced retardation plate is now able to be conducted within the frame work of complex ABCD theory under paraxial approximation. Although the conclusion in section 3.2 for plate modulation is applicable for general incident source and without specific restriction, we will implement the following investigation in virtue of a spatial coherent Gaussian beam with a polarization angle θ to x axis and $1/e$ amplitude radius r_s as an example. The corresponding beam coherence-polarization matrix for Gaussian beam just in front of the depolarizer is

$$\mathbf{W}^i(\mathbf{r}_1,\mathbf{r}_2) = I_o \exp\left\{-\frac{|\mathbf{r}_1|^2+|\mathbf{r}_2|^2}{r_s^{\,2}}\right\}\begin{pmatrix}\cos^2\theta & \cos\theta\sin\theta\\ \cos\theta\sin\theta & \sin^2\theta\end{pmatrix}. \tag{3.7}$$

Apply the $\mathbf{W}^i(\mathbf{r}_1,\mathbf{r}_2)$ in Eq. (3.7) and approximation in Eq. (3.5) to the definition of $\mathbf{W}^t(\mathbf{r}_1,\mathbf{r}_2)$ in Eq. (3.2), the beam coherence-polarization matrix of the random field after the plate that was modulated from the Gaussian beam could be written as

$$\mathbf{W}_{xx}^{t}(\mathbf{r}_1,\mathbf{r}_2) = I_o \cos^2\theta \exp\left\{-\frac{|\mathbf{r}_1|^2+|\mathbf{r}_2|^2}{r_s^{\,2}}\right\}\exp\left\{-k^2{\sigma_d}^2(n_x-1)^2\right\}$$
$$\left[1+\left(\exp\left\{k^2{\sigma_d}^2(n_x-1)^2\right\}-1\right)\exp\left\{-\frac{|\Delta\mathbf{r}|^2 c_{xx}}{r_d^{\,2}}\right\}\right],$$
$$\mathbf{W}_{yy}^{t}(\mathbf{r}_1,\mathbf{r}_2) = I_o \sin^2\theta \exp\left\{-\frac{|\mathbf{r}_1|^2+|\mathbf{r}_2|^2}{r_s^{\,2}}\right\}\exp\left\{-k^2{\sigma_d}^2(n_y-1)^2\right\}$$
$$\left[1+\left(\exp\left\{k^2{\sigma_d}^2(n_y-1)^2\right\}-1\right)\exp\left\{-\frac{|\Delta\mathbf{r}|^2 c_{yy}}{r_d^{\,2}}\right\}\right], \tag{3.8}$$
$$\mathbf{W}_{xy}^{t}(\mathbf{r}_1,\mathbf{r}_2) = \mathbf{W}_{yx}^{t}(\mathbf{r}_1,\mathbf{r}_2)$$
$$I_o \sin\theta\cos\theta \exp\left\{-\frac{|\mathbf{r}_1|^2+|\mathbf{r}_2|^2}{r_s^{\,2}}\right\}\exp\left\{-\frac{k^2{\sigma_d}^2\left[(n_x-1)^2+(n_y-1)^2\right]}{2}\right\}$$
$$\times\left[1+\left(\exp\left\{k^2{\sigma_d}^2(n_x-1)(n_y-1)\right\}-1\right)\exp\left\{-\frac{|\Delta\mathbf{r}|^2 c_{xy}}{r_d^{\,2}}\right\}\right].$$

The fact has to be emphasized is that: the non-zero residual values in the expression of the above matrix elements for large point distance $\Delta\mathbf{r}$ are the indication of the non-negligible specular components in the modulated field. This phenomenon is associated with the growth of rates of specular and scattered (diffused) components in respect to the decreasing σ_d for smoother surface model. It well coincides with our everyday experience and that is we mean by "partially developed" for the random electric field generated from the gentle rough-surfaced retardation plate. The fraction of the specular components in each $W_{lm}^{t}(\mathbf{r}_1,\mathbf{r}_2)$, $(l,m=x,y)$ is given by $\exp\{-k^2{\sigma_d}^2[(n_l-1)^2+(n_m-1)^2]/2\}$.

To assess the depolarization effect of the given depolarizer, we examine the degree of polarization for the modulated electric field first. By substituting matrix elements in Eq. (3.8) into Eq. (1.5), the $P^t(\mathbf{r})$ is obtained

$$P^t(\mathbf{r}) = \sqrt{1-\sin^2 2\theta\left[1-\exp\left\{-k^2{\sigma_d}^2(n_x-n_y)^2\right\}\right]}, \tag{3.9}$$

which is a spatially independent constant for the modulation field over the back surface of the depolarizer, and indicates the depolarization effect uniformly imposed on the linearly polarized incident field. The minimum degree of polarization is gained if the incident Gaussian beam is polarized by an angle $\theta = \pi / 4$. To adjust the depolarization depth of the gentle rough-surfaced retardation plate applied to incident source, one only needs to rotate the depolariser. By this, generated partially depolarized field with prescribed degree of polarization within 1~ $\exp\left\{-k^2\sigma_d{}^2(n_x - n_y)^2\right\}$ could be simply produced. The dependence of depolarization performance on the source polarization angle could also be considered as an illustration of the birefringence of the plate material. Compare with the depolarizer model with great roughness surface in Chapter 2, though the mathematical expressions of the degrees of polarization are the same for modulated fields by both depolarizers, the depolarization ability of the gentle rough-surfaced retardation plate is significantly weaker due to a smaller thickness fluctuation $\sigma_d{}^2$. It well coincides with our physical intuition.

Another statistical parameter of the randomly modulated field, the degree of coherence could be derived by Eq.(3.8) and the definition in Eq. (1.4), thus giving

$$\begin{aligned}&\eta^t(\mathbf{r_1},\mathbf{r_2})\\&=\cos^2\theta\exp\left\{-k^2\sigma_d{}^2(n_x-1)^2\right\}\left[1+\left(\exp\left\{k^2\sigma_d{}^2(n_x-1)^2\right\}-1\right)\exp\left\{-\frac{|\Delta\mathbf{r}|^2 c_{xx}}{r_d{}^2}\right\}\right]\\&+\sin^2\theta\exp\left\{-k^2\sigma_d{}^2(n_y-1)^2\right\}\left[1+\left(\exp\left\{k^2\sigma_d{}^2(n_y-1)^2\right\}-1\right)\exp\left\{-\frac{|\Delta\mathbf{r}|^2 c_{yy}}{r_d{}^2}\right\}\right].\end{aligned} \quad (3.10)$$

The decorrelation effect introduced to the transmitted fields has been demonstrated by this parameter. Compared with the depolarizer model with great roughness surface in Chapter 2, the weaker value of degrees of polarization Eq. (3.10) indicates that the rough-surfaced retardation plate will introduce weaker depolarization effect to incident the source.

In order to evaluate the propagated partially developed speckle on the observation plane, and to examine the polarization and coherence state undergoing change on propagation, we will continue our discussion and derive the beam coherence-polarization matrix of the modulated field discussed above after the propagated within a complex ABCD system. Recall the integral relation between the beam coherence-polarization matrix $\mathbf{W}^t(\mathbf{r}_1,\mathbf{r}_2)$ of the modulation field after plate and the beam coherence-polarization matrix $\mathbf{W}^o(\mathbf{p_1},\mathbf{p_2})$ for the propagated field on the observation plane indicated in Eq.(2.3), the analytical expression of $\mathbf{W}^o(\mathbf{p_1},\mathbf{p_2})$ could be calculated and given by

$$
\begin{aligned}
W_{xx}^o(\mathbf{p_1},\mathbf{p_2}) &= I_o \cos^2\theta \exp\left\{-k^2{\sigma_d}^2(n_x-1)^2\right\} \\
&\quad \left[W_b^{\ ABCD}(\mathbf{p}_1,\mathbf{p}_2)+\left(\exp\left\{k^2{\sigma_d}^2(n_x-1)^2\right\}-1\right)W_a^{\ ABCD}\left(\mathbf{p}_1,\mathbf{p}_2;\frac{{r_d}^2}{c_{xx}}\right)\right], \\
W_{yy}^o(\mathbf{p_1},\mathbf{p_2}) &= I_o \sin^2\theta \exp\left\{-k^2{\sigma_d}^2(n_y-1)^2\right\} \\
&\quad \left[W_b^{\ ABCD}(\mathbf{p}_1,\mathbf{p}_2)+\left(\exp\left\{k^2{\sigma_d}^2(n_y-1)^2\right\}-1\right)W_a^{\ ABCD}\left(\mathbf{p}_1,\mathbf{p}_2;\frac{{r_d}^2}{c_{yy}}\right)\right], \qquad (3.11) \\
W_{xy}^o(\mathbf{p_1},\mathbf{p_2}) &= \mathbf{W}_{yx}^o(\mathbf{p_1},\mathbf{p_2}) = I_o \sin\theta\cos\theta \exp\left\{-\frac{k^2{\sigma_d}^2\left[(n_x-1)^2+(n_y-1)^2\right]}{2}\right\} \\
&\quad \times\left[W_b^{\ ABCD}(\mathbf{p}_1,\mathbf{p}_2)+\left(\exp\left\{k^2{\sigma_d}^2(n_x-1)(n_y-1)\right\}-1\right)W_a^{\ ABCD}\left(\mathbf{p}_1,\mathbf{p}_2;\frac{{r_d}^2}{c_{xy}}\right)\right].
\end{aligned}
$$

where two integral functions $W_b^{\ ABCD}(\mathbf{p}_1,\mathbf{p}_2)$ and $W_a^{\ ABCD}(\mathbf{p}_1,\mathbf{p}_2;\beta)$ are evaluated analytically as

$$W_a^{ABCD}(\mathbf{p}_1,\mathbf{p}_2;\beta)=\int\int_{-\infty}^{\infty}\exp\left\{-\frac{|\mathbf{r}_1|^2+|\mathbf{r}_2|^2}{r_s^{\,2}}-\frac{|\Delta\mathbf{r}|^2}{\beta}\right\}G^*(\mathbf{r}_1,\mathbf{p}_1)G(\mathbf{r}_2,\mathbf{p}_2)\,d\mathbf{r}_1 d\mathbf{r}_2$$

$$=\frac{\beta}{4\,\mathrm{Im}\left[A^*B\right]/k+\beta|A|^2}\exp\left\{\frac{-|\mathbf{p}_1-\mathbf{p}_2|^2}{4\,\mathrm{Im}\left[A^*B\right]/k+\beta|A|^2}\right\}$$

$$\exp\left\{\frac{-j\left(|\mathbf{p}_1|^2-|\mathbf{p}_2|^2\right)\left\{\mathrm{Im}\left[B^2\right]-2\,\mathrm{Im}\left[A^*B\right]\mathrm{Re}\left[D^*B\right]+\frac{k\beta}{2}\left(\mathrm{Re}\left[AB\right]-\mathrm{Re}\left[D^*B\right]|A|^2\right)\right\}}{\left(4\,\mathrm{Im}\left[A^*B\right]/k+\beta|A|^2\right)|B|^2}\right\}$$

$$\exp\left\{\frac{-\left(|\mathbf{p}_1|^2+|\mathbf{p}_2|^2\right)\left\{-2\,\mathrm{Im}\left[B\right]^2+2\,\mathrm{Im}\left[A^*B\right]\mathrm{Im}\left[D^*B\right]+\frac{k\beta}{2}\left(|A|^2\,\mathrm{Im}\left[B^*D\right]-\mathrm{Im}\left[AB\right]\right)\right\}}{\left(4\,\mathrm{Im}\left[A^*B\right]/k+\beta|A|^2\right)|B|^2}\right\}. \tag{3.12}$$

and

$$W_b^{ABCD}(\mathbf{p}_1,\mathbf{p}_2)=\int\int_{-\infty}^{\infty}\exp\left\{-\frac{|\mathbf{r}_1|^2+|\mathbf{r}_2|^2}{r_s^{\,2}}\right\}G^*(\mathbf{r}_1,\mathbf{p}_1)G(\mathbf{r}_2,\mathbf{p}_2)\,d\mathbf{r}_1 d\mathbf{r}_2$$

$$=\frac{1}{|A|^2}\exp\left\{\frac{-jk\left(|\mathbf{p}_1|^2-|\mathbf{p}_2|^2\right)\left\{\left(\mathrm{Re}\left[AB\right]-\mathrm{Re}\left[D^*B\right]|A|^2\right)\right\}}{2|A|^2|B|^2}\right\} \tag{3.13}$$

$$\times\exp\left\{\frac{-k\left(|\mathbf{p}_1|^2+|\mathbf{p}_2|^2\right)\left\{\left(|A|^2\,\mathrm{Im}\left[B^*D\right]-\mathrm{Im}\left[AB\right]\right)\right\}}{2|A|^2|B|^2}\right\}.$$

One thing to point out here is the omitting of the illuminating beam size r_s in the Calculation of above integrals. As we have mentioned before in the introduction of complex ABCD theory: a Gaussian aperture lens is included as the first element while the ABCD matrix is calculated for the whole system. Thus, illumination beam shape is catered by this proper compensation, and it will also simplify the mathematical work significantly.

As a result, for field propagated through arbitrary complex ABCD optical system under paraxial approximation, the beam coherence-polarization matrix is expressed in an analytic form. It is now practicable to investigate the statistical properties of the random electric fields on the observation plane with a distance $z > 0$, especially the degree of polarization and the degree of coherence by definitions in Eq. (1.4) and Eq. (1.5), while the gentle rough-surfaced retardation plate is placed perpendicularly illuminated by a linearly polarized Gaussian incident beam.

To provide more natural perception of the relevant phenomena, the propagation in a classical space system over a distance $z > 0$ will be discussed as an example. The ABCD matrix of the whole propagation including a preceding aperture to compensate the spot size r_s is given by

$$\mathbf{M} = \begin{pmatrix} 1 - jz / z_R & z \\ -j / z_R & 1 \end{pmatrix}, \tag{3.14}$$

where z_R is the Rayleigh range $z_R = kr_s^2/2$. It is straightforward to obtain the corresponding expression of beam coherence-polarization matrix by substituting the ABCD parameters in Eq. (3.14) into the Eq. (3.11), and then reduce the degree of polarization and the degree of coherence for the free space propagation. To present the variation of statistical parameters on propagation more visually, and to provide an intuitive sense about the plate's modulation performance, we offer a numerical example here. The following system parameters are adopted: $r_s = 1\text{mm}$, $r_d = 0.1\text{mm}$, $\lambda = 0.633\mu\text{m}$, $\sigma_d = 0.982\mu\text{m}$, $n_x = 1.486$ and $n_y = 1.658$ for the birefringent material: Calcite[133]. In this case, the phase fluctuations $(n_m - 1)k\sigma_d$, $(m = x, y)$ introduced to the random electric field just behind the gentle rough-surfaced retardation plate are smaller than or comparable to 2π radians. For polarization speckle arising from this random modulated field after free-space propagation, the degree of polarization $P^o(\mathbf{p})$ plotted against the normalized propagation distance z/z_R and the normalized lateral distance measured in spot size p/r_s for some

selected values of the polarization angle $\pi/6$, $\pi/4$ and $\pi/3$ are shown below. At the same time, for the polarization speckle on observation plane with a distance away in free space system, the degree of coherence $\eta^o(\mathbf{p_1},\mathbf{p_2})$ for the generated speckle at two positions $\mathbf{p}_1$ and $\mathbf{p}_2$ symmetrically located with respect to the z axis are also provided. It is plotted against the normalized propagation distance z/z_R and the points distance $\Delta\mathbf{p}=\mathbf{p}_1-\mathbf{p}_2$ normalized by the incident spot size r_s. The figures show that, in general, the degree of coherence and degree of polarization will perform spatial variations in propagation. That is indicated by the non-uniformly distribution on the beam cross section changing along with the increasing propagation distance. The dependence of the depolarization effect on the polarization angle of incident source is also demonstrated by the differences between figures for degree of polarizations with $\theta=\pi/6$, $\pi/4$ and $\pi/3$. The variation trend of the degree of coherence is displayed obviously. The $\eta^o(\mathbf{p_1},\mathbf{p_2})$ approaching unity near the z axis shows the strong correlation between two points located very closely. Along with the increasing propagation distance, the lateral correlation length on the observation plane is increasing, which is well in accordance with the Van Cittert-Zernike theorem for the evolution of the field coherence increasing in propagation. Compared with the fully developed speckle discussed in Chapter 2, the lateral correlation length of the partially developed speckle on beam cross section seems narrower for observation plane with the same distance.

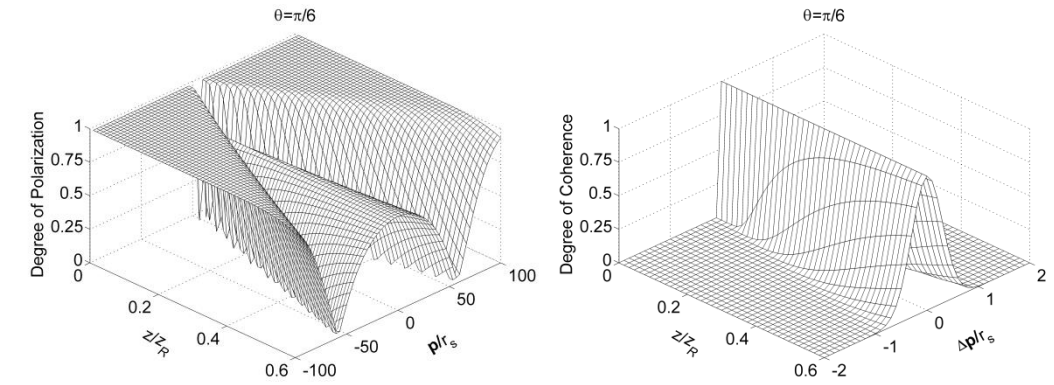

(a) (d)

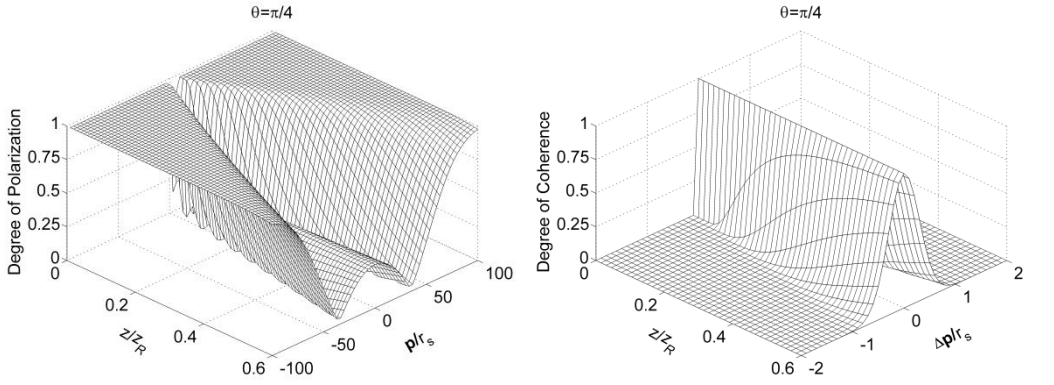

(b) (e)

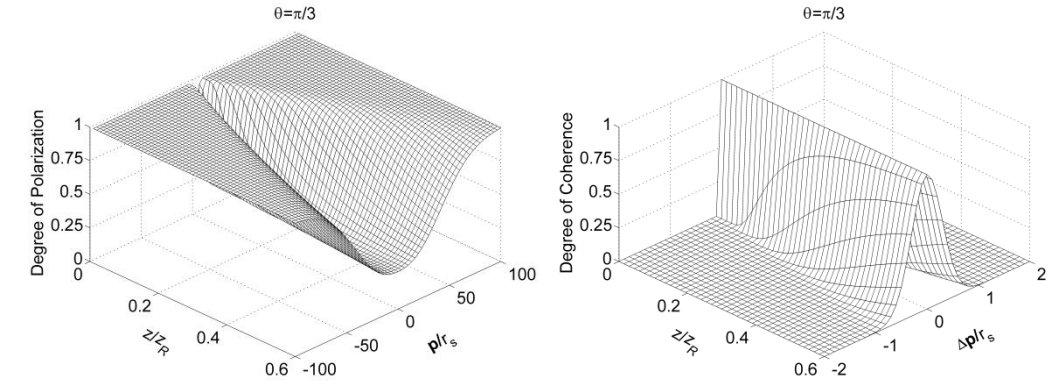

(c) (f)

Figure 3.1 Degree of polarization (left column) and coherence (right column) for free-space propagation. The angles of incidence of the polarized light are: $\pi/6$, $\pi/4$, and $\pi/3$.

3.4 Conclusion

Instead of the rough-surfaced retardation plate with large surface roughness and then causing large phase fluctuation to the modulated random field that has been analysed in Chapter 2, a gentle rough-surfaced or called as moderate rough-surfaced retardation plate is introduced as a depolarizer to generate partially developed polarization speckles. For this kind of thin plate with small thickness fluctuation causing a phase fluctuation smaller than 2π, the dependence of the modulated electric fields' coherence and polarization on the plate's surface roughness has been derived mathematically with the help of a Gaussian-Gaussian model and necessary numerical approximation.

The polarization-sensitivity of the birefringent plate's depolarization and decorrelation performance is illustrated by the analytical expressions of the degree of coherence and degree of polarization for the modulated field just behind the plate. By analysing the beam coherence-polarization matrix for the modulated field, the non-negligible specular components are indicated. That could be treated as the embodiment of a weaker ability of the plate with gentle roughness to scramble the polarization and coherence states of the incident source, while compared with the rougher model in Chapter 2. Within the complex ABCD matrix theory, the spatial variations of the degree of polarization and degree of coherence for the generated speckle in propagation are also examined. The significant dependence of depolarization and decorrelation effects on the polarization angle of the incident source and the propagation distance is shown clearly. As the natural extension of the work in chapter 2, the discussions and conclusions for a rough-surfaced retardation plate with a different extent of the surface roughness definitely enrich our understanding of this kind of depolarizer device. Such results will be helpful for modulating random vectorial magnetic field with specially prescribed statistical properties in theoretical studies. It is also essential for the efficient utilization of this kind of device in further applications.

Chapter 4

Statistics of Polarization Speckle Generated by Extremely Rough-surfaced Retardation Plate, and its Propagation as General Demonstration of Vectorial Van Cittert-Zernike Theorem

We analyse an extremely rough-surfaced retardation plate which realizes spatially independent phase modulation for generation of fully developed polarization speckle. The 2×2 field coherence and polarization matrix will be applied to examine the statistical properties of the generated random electromagnetic field behind the depolarizer plate including its coherence and polarization states, and the theoretical conclusion about their propagation in a general optical system under paraxial approximation will be studied within the framework of the complex ABCD-matrix theory.

A novel method to realize simultaneous depolarization and decorrelation effects is proposed by a compact single-device system with this kind of rough-surfaced retardation plate. Meanwhile, the analytical results of field propagation in a general system under the paraxial approximation have been derived within the framework of a complex ABCD-matrix system including inherent apertures, which is believed to a remarkable example to demonstrate the general version of the vectorial counterpart of the scalar Van Cittert-Zernike theorem for electromagnetic fields.

4.1 Introduction

Polarization and coherence states are usually considered as the most important statistical properties of an optical field and have been studied intensely in the past decades, especially after the invention of the ideal laser source [1, 2, 25, 29, 31][29]. In recent decades, more and more attention was paid to the analysis about the vectorial electromagnetic fields described in terms of 2×2 beam coherence-polarization matrix in space-temporal domain[76, 77] or cross-spectral density matrix in spatial-spectral domain [81, 34], especially after the setup of the unified theory of coherence and polarization [81].

Compared with the traditional scalar field description without polarization information, the vectorial form provides an approach to simultaneously investigate the evolution of polarization and coherence states that closely intercalate with each other. Related phenomena are studied and analysis about their change during propagation and nonuniform spatial distribution is conducted [8-14]. The random electromagnetic fields, and the resultant polarization speckle on propagation, could be applied to facilitate both theoretical and experimental research in optics, and have a great potential application prospect [17, 90, 91]. These kinds of modulated partially polarized and partially coherent electromagnetic fields with various prescribed statistical properties are usually applied as characterized secondary source to facilitate investigations. Especially, the requirement of the completely incoherent vectorial electromagnetic fields as the source is raised from some research on the vectorial extension of conventional Van Cittert-Zernike theorem [139][140]. Gori [76, 79, 141] might be the first rsearcher to provide its matrix form in the temporal domain, and Ostrovsly [85] achieved similar work in the spectral domain. Soon after, the research work about the variation of degree of coherence and degree of polarization within this topic was developed both theoretically [79, 88, 142] and experimentally [103] for various propagation systems including the free space system and Fourier system.

In previous chapters, a depolarizer device, the rough-surfaced retardation plate, was utilized to generate polarization speckle [15, 16]. The statistical properties including the variation of coherence and polarization states for the modulated field after the plate are assessed by the degree of coherence and polarization, and their strong dependence on the plate surface model was illustrated. Their evolution during propagation in general systems has been investigated too. Since we have proved the decorrelation and depolarization capability of the rough-surfaced retardation plate and derived their evolution phenomena in propagation, it is quite natural for us to consider the rough-surfaced retardation plate with extremely surface roughness to provide completely incoherent and partially depolarized field, and to analyse the corresponding field propagation for a demonstration of Van Cittert-Zernike theorem for electromagnetic field in this chapter.

The modulated field immediately behind the plate will be considered as a spatially incoherent and partially polarized secondary source, and this could be verified by the 2×2 beam coherence-polarization matrix and corresponding degree of coherence and degree of polarization. The coherence and polarization evolution and propagation of this secondary source within complex ABCD theory will be derived and expressed in an analytic form, which could be considered as a generalization of the vectorial Van Cittert-Zernike theorem for a general complex ABCD system under the paraxial approximation.

The analysis based on the spatially independent rough-surfaced retardation plate is perfectly consistent with earlier theoretical researches. One can gather physical intuition from this practical example which provides demonstration of the vectorial Van Cittert – Zernike theorem and the unified theory for coherence and polarization of a random beam generated by a compact single-device modulation method.

4.2 Generation of spatially incoherent and partially polarized random electromagnetic field by an extremely rough-surfaced retardation plate

Similar to the system used to examine the coherence and polarization properties of the electric field modulated by a rough-surfaced retardation plate [143], a speckle modulation and propagation forming the basis of this chapter is shown in Figure 2.1 of Chapter 2.

The extremely rough-surfaced retardation plate is a special kind of rough-surfaced retardation plate, whose lateral coherence length of its surface roughness is very small together with a great thickness fluctuation covariance. Because of this device manufactured from birefringent material causing divergent refractive indices for light with different polarization and propagation direction, a phase offset will be introduced between two orthogonally polarized components of incident field at a point. Since the polarization state of the field is depending on the phase shift proportional to the local thickness that is randomly fluctuating, this type of rough-surfaced retardation plate will not only achieve decorrelation effect to the incident field, in the meantime, it will also randomly scramble the polarization state of the field on the beam cross section. For the incident field vector $\mathbf{E}^i(\mathbf{r}) = \{E_x^i(\mathbf{r}), E_y^i(\mathbf{r})\}$ illuminating on a rough-surfaced retardation plate perpendicularly located to the propagation axis z, the plate provides a constant amplitude transmittance equal to unity and randomly varying phase retardance φ. And the phase retardance will be different for the orthogonal field components because of the different refractive indices depending on polarization of light components. And hence, the transmission field $\mathbf{E}^t$ after the depolarizer is determined by $\mathbf{E}^t = \mathbf{E}^i\mathbf{T}$, invoking the corresponding transmission matrix (Jones matrix) $\mathbf{T}$

$$\mathbf{T}(\mathbf{r}) = \begin{pmatrix} e^{-j\varphi_x(\mathbf{r})} & 0 \\ 0 & e^{-j\varphi_y(\mathbf{r})} \end{pmatrix} = \begin{pmatrix} e^{-jd(\mathbf{r})k(n_x-1)} & 0 \\ 0 & e^{-jd(\mathbf{r})k(n_y-1)} \end{pmatrix}, \tag{4.1}$$

where $\varphi_m(\mathbf{r}) = d(\mathbf{r})k(n_m - 1)$, $(m = x, y)$ is the effective phase delay for the x or y components of the electric fields, $k = |\vec{k}|$ is the wave number of light in vacuum, n_m $(m = x, y)$ denotes the refractive indices of the birefringent material, j is the imaginary unit, and $d(\mathbf{r})$ is the local thickness. For the modulated field $\mathbf{E}^t(\mathbf{r})$, the relative phase shift between the two orthogonally polarized wave components $k(n_y - n_x)d(\mathbf{r})$ proportional to the local thickness is randomly fluctuating along with the change of point $\mathbf{r}$'s location. As consequence, the polarization states of the field over the plate are randomly changed. For illustration of the statistical properties for the modulated fields, we will derive the beam coherence-polarization matrix $\mathbf{W}^t$ of the modulated fields just behind the depolarizer to demonstrate the relationship between incident and modulated fields. The modulation performance of the depolarizer will also be indicated clearly in this expression. The roughness statistics of the plate surface will be tacitly assumed as both space and time independent; i.e., stationarity and homogeneity are invoked. Therefore, the statistics of the surface roughness and the effective phase delay introduced will be statistically independent to the statistics of the incident field $\mathbf{E}^i(\mathbf{r})$. Thus, in the evaluation of ensemble average, these two parts could be separated, and we derive the $\mathbf{W}^t$

$$\begin{aligned}\mathbf{W}^t(\mathbf{r}_1, \mathbf{r}_2) &= \begin{pmatrix} \left\langle E^{t*}_x(\mathbf{r}_1) E^t_x(\mathbf{r}_2) \right\rangle & \left\langle E^{t*}_x(\mathbf{r}_1) E^t_y(\mathbf{r}_2) \right\rangle \\ \left\langle E^{t*}_y(\mathbf{r}_1) E^t_x(\mathbf{r}_2) \right\rangle & \left\langle E^{t*}_y(\mathbf{r}_1) E^t_y(\mathbf{r}_2) \right\rangle \end{pmatrix} \\ &= \begin{pmatrix} W^i_{xx}(\mathbf{r}_1, \mathbf{r}_2) \left\langle e^{j\Delta\varphi_{xx}(\mathbf{r}_1, \mathbf{r}_2)} \right\rangle & W^i_{xy}(\mathbf{r}_1, \mathbf{r}_2) \left\langle e^{j\Delta\varphi_{xy}(\mathbf{r}_1, \mathbf{r}_2)} \right\rangle \\ W^i_{yx}(\mathbf{r}_1, \mathbf{r}_2) \left\langle e^{j\Delta\varphi_{yx}(\mathbf{r}_1, \mathbf{r}_2)} \right\rangle & W^i_{yy}(\mathbf{r}_1, \mathbf{r}_2) \left\langle e^{j\Delta\varphi_{yy}(\mathbf{r}_1, \mathbf{r}_2)} \right\rangle \end{pmatrix}. \end{aligned} \tag{4.2}$$

where the asterisk * means complex conjugate, and angular brackets $\langle \ldots \rangle$ denote ensemble average as we defined. The random variable $\Delta\varphi_{lm}(\mathbf{r}_1, \mathbf{r}_2) = \varphi_l(\mathbf{r}_1) - \varphi_m(\mathbf{r}_2)$, $(l, m = x, y)$ in matrix elements of Eq. (4.2), is totally determined by the statistics of local thickness $d(\mathbf{r}_1)$, $d(\mathbf{r}_2)$. For the sake of simplicity in following derivation, it is reasonable to assume that the surface thickness fluctuation is in accordance with the most commonly adopted zero mean Gaussian distribution model. Under this

condition, random variable $\Delta\varphi_{lm}(\mathbf{r}_1,\mathbf{r}_2)$ is also a Gaussian variable, because both the $\varphi_l(\mathbf{r}_1)$ and $\varphi_m(\mathbf{r}_2)$ are proportional to Gaussian distributed d. Therefore, $\langle\exp\{j\Delta\varphi_{lm}(\mathbf{r}_1,\mathbf{r}_2)\}\rangle$, $(l,m=x,y)$ in matrix elements as the characteristic function of $\Delta\varphi_{lm}(\mathbf{r}_1,\mathbf{r}_2)$ is governed by the average and covariance of $\Delta\varphi_{lm}(\mathbf{r}_1,\mathbf{r}_2)$ or equivalently, the average and covariance of the random surface-thickness $d(\mathbf{r})$ which is conducted the same way in Chapter 2 and 3:

$$\begin{aligned}&\left\langle\exp\left\{j\Delta\varphi_{lm}(\mathbf{r}_1,\mathbf{r}_2)\right\}\right\rangle\\&=\exp\left\{-\frac{k^2\left[(n_l-1)^2+(n_m-1)^2\right]\left\langle d^2(\mathbf{r})\right\rangle}{2}+\frac{k^2 2(n_l-1)(n_m-1)\left\langle d(\mathbf{r}_1)d(\mathbf{r}_2)\right\rangle}{2}\right\}\end{aligned}\tag{4.3}$$

Furthermore, with the hypothesis of wide-sense stationarity, the lateral correlation of the plate thickness will be considered as isotropic and dependent on the spatial separation of points $\Delta\mathbf{r}=\mathbf{r}_1-\mathbf{r}_2$ by a Gaussian function with a lateral scale r_d, and a covariance $\sigma_d{}^2$, i.e.,

$$\left\langle d\left(\mathbf{r}_1\right)d\left(\mathbf{r}_2\right)\right\rangle=\sigma_d{}^2\exp\left\{-\frac{\left|\Delta\mathbf{r}\right|^2}{r_d{}^2}\right\}.\tag{4.4}$$

For the extremely rough-surfaced retardation plate in this Gaussian-Gaussian model, we could conduct the double exponential expression of $\langle\exp\{j\Delta\varphi_{lm}(\mathbf{r}_1,\mathbf{r}_2)\}\rangle$, same as the Eq. (2.14) of Chapter 2, which is the general conclusion for any rough-surfaced retardation plate with Gaussian-Gaussian roughness model. And considering the great phase fluctuation $(\mathrm{n}_l-1)(n_m-1)k^2\sigma_d^2\gg(2\pi)^2$,$(l,m=x,y)$, we will then conduct an approximation of spatial correlation properties of the phase modulation introduced by the plate, which regulate the random disturbance introduced to the incident source, and are mainly determined by the statistics of the plate roughness characters [143, 144] :

$$\begin{aligned}&\left\langle \exp\{j\Delta\varphi_{lm}(\mathbf{r}_1,\mathbf{r}_2)\}\right\rangle \\ &=\exp\left\{-\frac{k^2{\sigma_d}^2}{2}\left[(n_l-n_m)^2+2(n_l-1)(n_m-1)\frac{|\Delta\mathbf{r}|^2}{{r_d}^2}\right]\right.\end{aligned} \tag{4.5}$$

On the basis of the above conclusions for coherence matrix elements, we extract the expressions of the degree of coherence $\eta^t(\mathbf{r_1},\mathbf{r_2})$ and degree of polarization $P^t(\mathbf{r})$ [34] to assess the modulation effect on the polarization and coherence of the field.

$$\begin{aligned}\eta^t(\mathbf{r_1},\mathbf{r_2})=\left[W_{xx}(\mathbf{r}_1,\mathbf{r}_2)\exp\left\{-\frac{k^2{\sigma_d}^2(n_x-1)^2|\Delta\mathbf{r}|^2}{{r_d}^2}\right\}\right.\\ \left.+W_{yy}(\mathbf{r}_1,\mathbf{r}_2)\exp\left\{-\frac{k^2{\sigma_d}^2(n_y-1)^2|\Delta\mathbf{r}|^2}{{r_d}^2}\right\}\right]/\left[I(\mathbf{r}_1)I(\mathbf{r}_2)\right]^{1/2}\end{aligned} \tag{4.6}$$

and

$$\begin{aligned}P^t(\mathbf{r})&=\left\{1-\frac{4\det\mathbf{W}^t(\mathbf{r},\mathbf{r})}{\left[tr\mathbf{W}^t(\mathbf{r},\mathbf{r})\right]^2}\right\}^{1/2}\\ &=\left\{P^i(\mathbf{r})-\frac{4W_{xy}(\mathbf{r},\mathbf{r})W_{yx}(\mathbf{r},\mathbf{r})\left(1-\exp\left\{-s^2\left(1-\varepsilon\right)^2\right\}\right)}{\left[I(\mathbf{r})\right]^2}\right\}^{1/2}<P^t(\mathbf{r}).\end{aligned} \tag{4.7}$$

For the presented discussion about an extremely rough-surfaced retardation plate depolarizer, thickness varies rapidly with small lateral correlation length r_d and large fluctuation covariance ${\sigma_d}^2$. Under this condition, the exponential terms in η^t of Eq.(4.6) will quickly decrease to a value approaching zero for $\Delta\mathbf{r}\neq 0$, and are equal to 1 while $\Delta\mathbf{r}$ is zero. Thus, we have

$$\eta^t(\mathbf{r_1},\mathbf{r_2})\approx\begin{cases}0 & \mathbf{r_1}\neq\mathbf{r_2}\\ 1 & \mathbf{r_1}=\mathbf{r_2}\end{cases} \tag{4.8}$$

Hence it could be considered as the verification of a spatial incoherent field generated by this extremely rough-surfaced retardation plate, whatever the coherence state of the source is. At the same time, the depolarization is illustrating in the decrease of degree of polarization in the Eq. (4.7). Thus, as expected, a perfectly polarized coherent incident beam has become depolarized and spatial incoherent after passing through the extremely rough-surfaced retardation plate.

Earlier in this section, we patiently and intentionally repeated the derivation similar to the conclusion in Chapter 2, to elicit the following careful analysis about the incoherent electromagnetic field generated by the extremely rough-surfaced retardation plate. It is also important for the introduction of some deliberate amendment and special consideration in the description of the electromagnetic field propagation as a demonstration of Van Cittert-Zernike theorem for electromagnetic field.

However, preceding the evaluation of the Fresnel-integral to continuing the discussion on incoherent polarization speckle's propagation through a complex ABCD optical system, the beam coherence-polarization matrix elements of spatially incoherent partially depolarized random electromagnetic field will be approximately rewritten in terms of Dirac impulse delta function for further integral calculation:

$$\mathbf{W}^{t'}(\mathbf{r}_1, \mathbf{r}_2) = \delta(\Delta\mathbf{r})\mathbf{J}^{t'}(\mathbf{r}), \tag{4.9}$$

where $\mathbf{J}^{t'}(\mathbf{r})$ is a modified polarization matrix for general incoherent source, and is defined as

$$\mathbf{J}^{t'}(\mathbf{r}) = \frac{{r_d}^2\pi}{k^2{\sigma_d}^2(n_x-1)(n_y-1)} \begin{pmatrix} W_{xx}^i(\mathbf{r},\mathbf{r})\dfrac{(n_y-1)}{(n_x-1)} & W_{xy}^i(\mathbf{r},\mathbf{r})\exp\left\{-\dfrac{k^2{\sigma_d}^2(n_x-n_y)^2}{2}\right\} \\ W_{yx}^i(\mathbf{r},\mathbf{r})\exp\left\{-\dfrac{k^2{\sigma_d}^2(n_x-n_y)^2}{2}\right\} & W_{yy}^i(\mathbf{r},\mathbf{r})\dfrac{(n_x-1)}{(n_y-1)} \end{pmatrix}, \quad (4.10)$$

When the above equations were derived, we have made use of the fact that narrow Gaussian function in integral is legitimate to be approximately treated as Dirac delta function to facilitate further mathematical analysis, and in order later to arrive at analytical solutions for the propagation of the beam coherence-polarization matrix through a complex ABCD optical system. In distribution theory, the approximation is defined as:

$$\lim_{\vartheta\to 0}\exp\{-|\Delta\mathbf{r}|^2/\vartheta^2\} \approx \pi\vartheta^2\delta(\Delta\mathbf{r}), \quad (4.11)$$

We have to point out something special in the delta beam coherence-polarization matrix $\mathbf{W}^{t'}(\mathbf{r}_1,\mathbf{r}_2)$, and this is very important for the accuracy of propagation discussion. In previous works about the vectorial van Cittert-Zernike theorem [79] and van Cittert-Zernike theorem for electromagnetic fields [85, 142], the polarization matrix elements were assumed to be in accordance with the elements in intensity matrix $\mathbf{W}^t(\mathbf{r},\mathbf{r})$ for the incoherent field. Compared with Eq. (4.10), we find that, if we follow this treatment, numerical error about the polarization and coherence state for propagated field will be caused without the compensation factors introduced in each elements of (4.10). Simply speaking, the Gaussian correlation terms in all the element of $\mathbf{W}^t(\mathbf{r}_1,\mathbf{r}_2)$ are very narrow and can be approximately considered as Dirac function. However, they are in the same scale, and the difference of their widths will become very essential, especially while we consider the statistical properties involving relationships between themselves such as their polarization and coherence at propagation. For the same reason, we have to assess the modulated field's coherence and polarization by Eq. (4.6) and (4.7) instead of by the elements from Eq.

(4.10), because the compensation factors for Dirac function approximation are introduced to maintain the numerical accuracy only after integral calculation.

4.3 Changes in the degree of polarization and the degree of coherence on propagation

On the basis of the conclusion in the last section, we will calculate the propagation of the beam coherence-polarization matrix through an optical system. By the same time, the evolution of beam coherence-polarization matrix for the spatial incoherent field with polarization variety could be treated as a general demonstration to provide physical insight of the vectorial Van Cittert-Zernike theorem. Under the paraxial approximation, the beam coherence-polarization matrix $\mathbf{W}^o(\mathbf{p}_1,\mathbf{p}_2)$ for the field $\mathbf{E}^o$ arriving at the observation plane after passing through a complex ABCD optical system is connected to the beam coherence-polarization matrix of the integral formulation [14, 143]:

$$\mathbf{W}^o\left(\mathbf{p}_1,\mathbf{p}_2\right)=\iint_{\pm\infty}\mathbf{W}^{t'}(\mathbf{r}_1,\mathbf{r}_2)G^*\left(\mathbf{p}_1,\mathbf{r}_1\right)G\left(\mathbf{p}_2,\mathbf{r}_2\right)d\mathbf{r}_1 d\mathbf{r}_2, \tag{4.12}$$

By substituting Eq. (4.9) into (4.12), and rewiring Green function G by the corresponding ABCD matrix elements, we could get the beam coherence-polarization matrix for random field after travelling through the ABCD system:

$$\begin{aligned}\mathbf{W}^o\left(\mathbf{p}_1,\mathbf{p}_2\right)&=\frac{k^2}{4\pi^2|B|^2}\exp\left\{\frac{jk}{2}\left(\frac{D^*}{B^*}|\mathbf{p}_1|^2-\frac{D}{B}|\mathbf{p}_2|^2\right)\right\}\\&\iint\mathbf{J}^{t'}(\mathbf{r})\exp\left\{k\,\mathrm{Im}\left[\frac{A}{B}\right]|\mathbf{r}|^2+jk\mathbf{r}\left(\frac{\mathbf{p}_2}{B}-\frac{\mathbf{p}_1}{B^*}\right)\right\}d\mathbf{r},\end{aligned} \tag{4.13}$$

where we have taken the advantage of the sifting property of the Dirac delta function[145, 146].

Equation (4.13) could be treated as the generalized version of the vectorial counterpart of scalar Van Cittert-Zernike theorem for complex ABCD system under the paraxial approximation. It obviously shows that the mutual coherence of the resultant field is determined by the auto-coherence of the incoherent source field. This could be found consistent with the special cases of vectorial Van Cittert-Zernike theorem people discussed before, like the free space systems [88, 146] and the Fourier system [103], if we substitute the relevant ABCD parameters for given systems into Eq.(4.13).

Further deterministic analysis is impossible without the definition of the incident source. For demonstration purpose only, and without loss of generality, we will confine the following discussion for a specific incident Gaussian beam just in front of the depolarizer with the polarization angle θ and beam size radius r_s:

$$\mathbf{W}^{i}(\mathbf{r},\mathbf{r}) = I_o \exp\left\{-\frac{2|\mathbf{r}|^2}{r_s^{\,2}}\right\}\begin{pmatrix}\cos^2\theta & \cos\theta\sin\theta\\ \cos\theta\sin\theta & \sin^2\theta\end{pmatrix}, \tag{4.14}$$

Thus, we obtain the expressions of beam coherence-polarization matrix for the modulated field just behind the depolarizer:

$$\begin{aligned}\mathbf{W}^{t'}(\mathbf{r}_1,\mathbf{r}_2) = \exp\left\{-\frac{|\mathbf{r}_1|^2+|\mathbf{r}_2|^2}{r_s^{\,2}}\right\}&\frac{I_o r_d^{\,2}\sin\theta\cos\theta\pi\delta(\Delta\mathbf{r})}{k^2\sigma_d^{\,2}(n_x-1)(n_y-1)}\\ \times&\begin{pmatrix}\dfrac{\cot\theta(n_y-1)}{(n_x-1)} & \exp\left\{-\dfrac{k^2\sigma_d^{\,2}(n_x-n_y)^2}{2}\right\}\\ \exp\left\{-\dfrac{k^2\sigma_d^{\,2}(n_x-n_y)^2}{2}\right\} & \dfrac{\tan\theta(n_x-1)}{(n_y-1)}\end{pmatrix},\end{aligned} \tag{4.15}$$

whose degree of polarization is a constant calculated from Eq. (4.7)

$$P^{t}(\mathbf{r}) = \left\{1-\sin^2 2\theta\left[1-\exp\left\{-k^2\sigma_d^{\,2}(n_x-n_y)^2\right\}\right]\right\}^{1/2}. \tag{4.16}$$

Obviously, the $P^t(\mathbf{r})$ is spatial independent and mainly governed by the polarization angle θ of the incident source. The spatial degree of polarization attains its minimum value, i.e. $\exp\{-k^2\sigma_d^2(n_x-n_y)^2\}$ for $\theta=\pi/4$. For an extremely rough surface with the term $k^2{\sigma_d}^2(n_x-n_y)^2$ in Eq. (4.16) being very large, the $\exp\{-k^2\sigma_d^2(n_x-n_y)^2\}$ approximately equals zero. The depth of depolarizing modulation is principally depending on the polarization angle θ of the incident field, and thus a promising method for depolarization modulation with prescribed statistical properties is provide by a compact single device to cover a range of $P^t(\mathbf{r})$ from nearly zero to unity.

Furthermore, we considered the propagation of this random incoherent field. By the formula in Eq. (4.13), the analytical integral results for the propagated beam coherence-polarization matrix could be derived:

$$\mathbf{W}^o(\mathbf{p_1},\mathbf{p_2}) = \frac{I_o {r_d}^2 \sin\theta\cos\theta\pi}{k^2{\sigma_d}^2(n_x-1)(n_y-1)} W_c^{ABCD}(\mathbf{p}_1,\mathbf{p}_2) \begin{pmatrix} \dfrac{\cot\theta(n_y-1)}{(n_x-1)} & \exp\left\{-\dfrac{k^2{\sigma_d}^2(n_x-n_y)^2}{2}\right\} \\ \exp\left\{-\dfrac{k^2{\sigma_d}^2(n_x-n_y)^2}{2}\right\} & \dfrac{\tan\theta(n_x-1)}{(n_y-1)} \end{pmatrix}, \tag{4.17}$$

where $W_c^{ABCD}(\mathbf{p}_1,\mathbf{p}_2)$ is the integral evaluated as

$$\begin{aligned} & W_c^{ABCD}(\mathbf{p}_1,\mathbf{p}_2) \\ &= \int_{-\infty}^{\infty}\int \exp\left\{-\frac{2|\mathbf{r}|^2}{{r_s}^2}\right\} G^*(\mathbf{r},\mathbf{p_1}) G(\mathbf{r},\mathbf{p_2})\, d\mathbf{r} \\ &= \frac{k}{4\pi\,\mathrm{Im}(A^*B)} \exp\left\{-\frac{jk}{2}\left(\mathrm{Re}\left(\frac{D}{B}\right)-\frac{\mathrm{Re}(B)\,\mathrm{Im}(B)}{\mathrm{Im}(A^*B)|B|^2}\right)\left(|\mathbf{p}_1|^2-|\mathbf{p}_2|^2\right)\right\} \\ & \exp\left\{-\frac{k\left(|\mathbf{p}_1|^2+|\mathbf{p}_2|^2\right)\left[\mathrm{Im}(AB^*)\,\mathrm{Im}(DB^*)-[\mathrm{Im}(B)]^2\right]}{2\,\mathrm{Im}(A^*B)|B|^2} - \frac{k(\mathbf{p}_2-\mathbf{p}_1)^2}{4\,\mathrm{Im}(A^*B)}\right\}, \end{aligned} \tag{4.18}$$

One subtlety that needs to be mentioned is that we omitted the illuminating beam size r_s and compensated it in the same way as we did in the last chapter.

Equations (4.17) and (4.18) provide the analytic results for the propagation of the beam coherence-polarization matrix through a complex ABCD optical system for a spatially incoherent partially polarized field generated by the extremely rough-surfaced retardation plate from a Gaussian shape linearly polarized source. Using these results along with the definitions, the degree of spatial coherence and spatial degree of polarization for the stochastic electric fields in the observation plane with a distance $z > 0$ could be directly derived, and then the polarization and coherence state variations in propagtion could be examined.

We still cite the classical free space system as an example here. For a propagation distance z with a preceding aperture of size r_s to model the illuminating spot shape, the corresponding ABCD matrix can be written as

$$\mathbf{M} = \begin{pmatrix} 1 - jz / z_R & z \\ -j / z_R & 1 \end{pmatrix}, \tag{4.19}$$

where z_R is the Rayleigh range $z_R = kr_s^{\,2}/2$. By substituting these elements of the ABCD matrix into Eq. (4.18), on can get the propagated beam coherence-polarization matrix associated with the analytical expressions for the degree of polarization and degree of coherence for the resultant field:

$$P^o(\mathbf{p}) = \left\{ 1 - 4\tan^2\theta \frac{1 - \exp\left\{-k^2 {\sigma_d}^2 (n_x - n_y)^2\right\}}{\left[\dfrac{n_y - 1}{n_x - 1} + \tan^2\theta \dfrac{n_x - 1}{n_y - 1}\right]^2} \right\}^{1/2}, \tag{4.20}$$

$$\eta^o(\mathbf{p}_1,\mathbf{p}_2)=\exp\left\{-\frac{jk}{2z}\left(|\mathbf{p}_1|^2-|\mathbf{p}_2|^2\right)-\frac{(\mathbf{p}_2-\mathbf{p}_1)^2}{2z^2 r_s^{\,2}/z_R^{\,2}}\right\}. \tag{4.21}$$

The Eq. and Eq. (4.20) show that a partially coherent field is generated from an incoherent source after propagation. The lateral coherence length of the resultant field could be extracted from the width of the Gaussian terms of $\Delta\mathbf{p}=\mathbf{p}_2-\mathbf{p}_1$, i.e., $2\sqrt{2}z/(kr_s)$, in Eq. (4.21). Therefore, it is clearly illustrated that the coherent region will extend as the propagation distance increases, which conforms exactly to the Van Cittert-Zernike theorem. Figure 4.1 gives the values of the degree of coherence of the resultant polarization speckle at two positions located symmetrically with respect to the z, which is plotted against the normalized propagation distance z/z_R and normalized lateral distance measured in spot size $\Delta p/r_s$. The evolution of the degree of coherence is only determined by the shape of the incident source and the propagation distance, but will never change with the polarization angle of the source and roughness parameters of the plate.

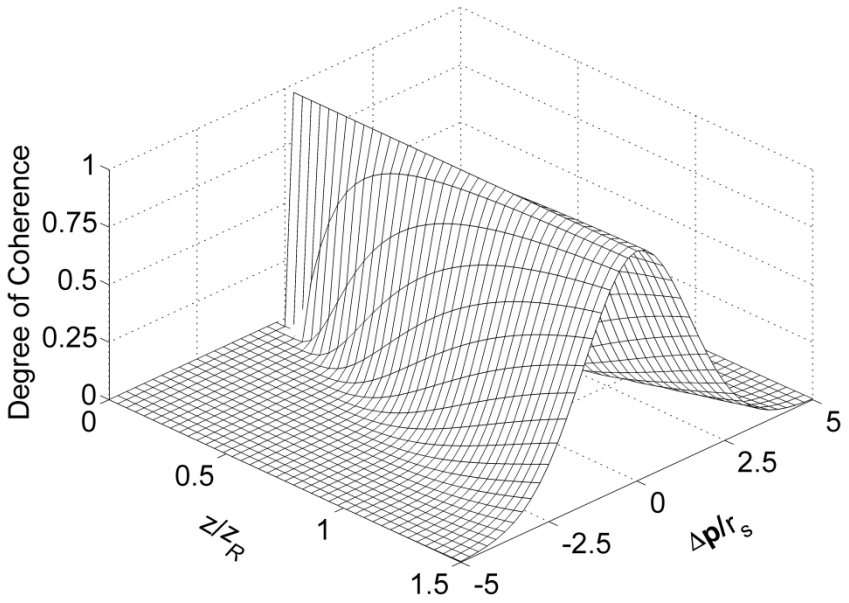

Figure 4.1 Degree of Coherence at two points located symmetrically for free-space propagation.

The other interesting phenomenon that has to be underlined is that, the degree of polarization as a constant is invariable through propagation and is distributed uniformly over the beam cross section. This degree of polarization as being independent to the location **p** and invariable through propagation is in accordance with the earlier conclusions for free space propagation [85, 88]. Furthermore, with the help of complex ABCD theory, it could be proved that the invariant polarization property will also hold for arbitrary general propagation systems. This novel invariant polarization property might be introduced as a general method to provide a partially polarized random field with a prescribed degree of polarization. This conclusion could be considered as an example of the theoretical analysis of E. Wolf about the polarization invariance in beam propagation [147].

4.4 Conclusions

We statistically analysed the statistical properties, especially the polarization and coherence of the field modulated by an extremely rough-surfaced retardation plate depolarizer as a novel optical modulation device to realize depolarization and decorrelation effects simultaneously by a compact single-device method. The beam coherence-polarization matrix associated with the degree of coherence and polarization of modulated field is derived and presented as the verification of the special incoherent polarization speckle. The propagation of the beam coherence-polarization matrix is investigated within the framework of complex ABCD theory, and analytical results for the propagated field are derived, thus revealing the evolution of the polarization and coherence properties of resulted polarization speckle as a general description of the vectorial Van Cittert-Zernike theorem.

The related conclusions in general form are proved to be well consistent with earlier researches for special cases like in the free space system or Fourier systems, and will facilitate our understanding of the related phenomena. Discussion about the necessary modification for the polarization matrix caused by the Dirac delta approximation is provided to improve the accuracy of the derivation for field propagation. We also reveal the invariant degree of polarization of the random field generated by this

extremely rough-surfaced retardation plate. We discover that the degree of polarization is hardly affected by the source and system parameters which determine the degree of coherence. Hence, this phenomenon reveals a potential field modulation method to provide various combinations of prescribed polarization and coherence properties in propagation.

Chapter 5

Statistical Analysis of the Dynamic Polarization Speckle

In order to better interpret the statistical properties of the polarization speckle generated by the rough-surfaced retardation plate, the observed dynamic polarization speckle generated by a moving rough-surfaced retardation plate will be examined to illustrate the dynamic properties. The investigation is based on a 2×2 time-lagged beam coherence-polarization matrix presenting its statistical coherence and polarization properties. The analysis about the propagation of the generated dynamic polarization speckle in general systems is conducted within the paraxial approximation as presented by complex ABCD matrix theory. Then, the sensitivities of spatial temporal characteristics of the observed dynamic polarization speckle to the plate surface structures, motion characters and the features of propagation system are discussed and interpreted in terms of the illuminating spot size, average speckle size, the temporal correlation length, the speckle boiling, and speckle translation. The differences of such dynamic polarization speckle to traditional dynamic speckle in scalar are considered carefully. Given space limitations, this chapter can't fully explore the dynamic properties for the three kinds of rough-surfaced retardation plates model with different extents of the surface roughness. The discussion will be confined to the model introduced in Chapter 2, but it is easy to extend the other two models in a similar way.

5.1 Introduction

While moving modulation object, for example, a rough-surfaced retardation plate, is illustrated by a coherent laser source, the generated laser speckle usually performs as a mass of small-scale twinkling particles on the observation screen. The dynamic speckle is predominately determined by the structural characteristics of the surface, the motion of the modulation plate, and the features of the beam propagation system. These relations stimulate the adoption of the speckle shape and dynamic features as a major measurement tool in non-destructive inspection of object motion [6] and surface roughness [4, 5]. It was then utilized to detect the vibration [148], displacement, velocity [149], and rotation [150]. Thus, the invention of equipment like Laser Doppler velocimeter [151] and laser time of flight velocimeter [152] were promoted at the same time.

The utilization of these relations as speckle generation methods or measurement methods primarily depends on the comprehensive understanding of the time-lagged statistical properties of the generated dynamic speckle. For fully developed speckle in free space, single lens, and double lens systems, the dynamic analysis has been achieved by Yoshimura [72]. Within the framework of the complex ABCD matrix theory [108][110], more general conclusions about dynamic speckle propagating through an arbitrary system with inherence apertures under the paraxial approximation were derived later [58, 119]. However, most of these works was accomplished in the scale form for either the polarized [4] or unpolarised field [153] [119, 150].

In recent years, especially on the basis of the unified theory of coherence and polarization [76, 81] as an effective analysis method, both theoretical and experimental analysis of the polarization speckle[16] with spatial variation of polarization states, was conducted in association with the study on its propagation [8, 13-15, 17, 18]. A few methods were proposed to generate this kind of polarization

speckle [16, 101, 123], and a compact single-device method by a rough-surfaced retardation was presented recently. The statistical properties of the corresponding polarization speckle in the propagation were also studied [143]. As a continuation and extension of the previous work, the speckle dynamics and shape features of the dynamic polarization speckle generated by this moving depolarizer will be researched in the form of the 2×2 time-lagged beam coherence-polarization matrix. The propagation analysis is also conducted invoking the general Fresnel integral in complex ABCD matrix theory under paraxial approximation. It is believed to be the first time for the dynamic research work of the polarization speckle to be achieved in a vector form, and it is expected to pave the road for the dissemination of the dynamic polarization speckle with spatial polarization variations into a wider field of application, both in laboratories and in industries.

5.2 Modulation behaviour of a moving rough-surfaced retardation plate to the incident beam

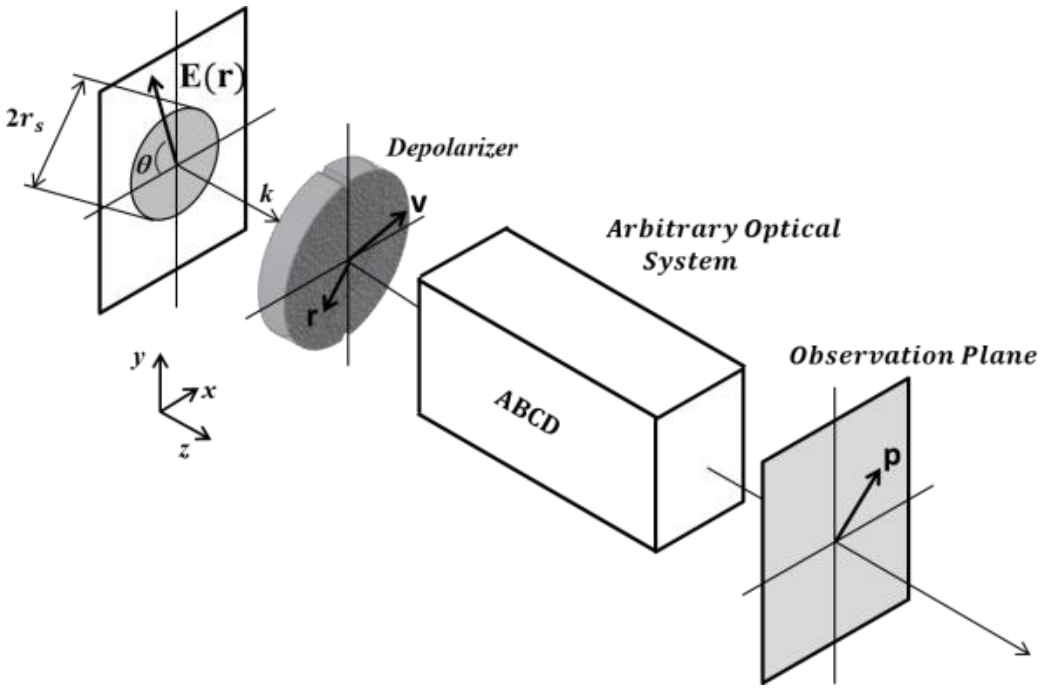

Figure 5.1. Schematic of the basic setup to examine the dynamic polarization speckle generated by a moving rough-surfaced retardation plate traveling through a complex ABCD optical system

Similar to the system used to examine the coherence and polarization properties of the electric field modulated by a rough-surfaced retardation plate [143] a speckle modulation and propagation system forms the basis of this chapter. The moving direction of the plate is indicated by velocity vector $\mathbf{v}$ in Figure 5.1.

As shown in Figure 5.1, an incident beam at instantaneous time t composed by two complex components of the electric vector $\mathbf{E}^i(\mathbf{r},t)=\{E_x^i(\mathbf{r},t),E_y^i(\mathbf{r},t)\}$ with its width r_s and wave vector $\vec{k}$ is incident on the rough-surfaced retardation plate employed as a depolarizer moving at a velocity vector $\mathbf{v}=\{v_x,v_y\}$ within the plane perpendicular to z axis. The optical axis of the rough-surfaced birefringent plate indicated by a line connecting the notches will be aligned along the y axis. Hence, for the incident field $\mathbf{E}^i$ before, and the transmission field $\mathbf{E}^t$ after the depolarizer presented by the superscripts i or t respectively, their relationship $\mathbf{E}^t=\mathbf{E}^i\mathbf{T}$ is governed by the transmission matrix $\mathbf{T}$ given by [129]

$$\mathbf{T}(\mathbf{r})=\begin{pmatrix} e^{-j\varphi_x(\mathbf{r})} & 0 \\ 0 & e^{-j\varphi_y(\mathbf{r})} \end{pmatrix}=\begin{pmatrix} e^{-j\left[d(\mathbf{r})k(n_x-1)\right]} & 0 \\ 0 & e^{-j\left[d(\mathbf{r})k(n_y-1)\right]} \end{pmatrix}, \tag{5.1}$$

where the effective phase delay $\varphi_m(\mathbf{r})=d(\mathbf{r})k(n_m-1)$, $(m=x,y)$, wave number in vacuum $k=|\vec{k}|$, the local thickness $d(\mathbf{r})$, and the refractive indices of the birefringent material n_m $(m=x,y)$ are denoted by the same symbols as in previous discussions. For the modulated field $\mathbf{E}^t(\mathbf{r})$, the random fluctuation of the local thickness $d(\mathbf{r})$ will lead to a random phase shift $k(n_y-n_x)d(\mathbf{r})$ between the two orthogonal components, which will be proportional to the local thickness $d(\mathbf{r})$ and will vary with the position $\mathbf{r}$. As we know, the phase shift determines the polarization state of the electric field. Thus, the rough-surfaced retardation plate randomly scrambles the polarization state of the field on the beam cross section, and realizes the depolarization effect. At the same time, the random rough surface also causes the decorrelation effect to the field. While the rough-surfaced retardation plate

is moving with a velocity vector $\mathbf{v}=\{v_x, v_y\}$, the instantaneous spatial distribution of random modulation within the beam spot applied to $\mathbf{E}^i$ will change. By this, the polarization speckle generated by the random modulated field on the observation plane will also change with the time, and this is what we call "dynamic".

We begin with the derivation of the second-order dynamic statistical properties of the modulated stochastic vector electric fields just behind the depolarizer, to comprehensively grasp the relationship between the speckle deformation and the plate motion. A 2×2 time-lagged beam coherence-polarization matrix [31, 34] is introduced to illustrate the relationship between field $\mathbf{E}^t(\mathbf{r}_1,t)$ of point $\mathbf{r}_1$ and field $\mathbf{E}^t(\mathbf{r}_2,t+\tau)$ of point $\mathbf{r}_2$ with time-lag τ conveniently: [13, 31].

$$\begin{aligned}\mathbf{W}^t(\mathbf{r}_1,\mathbf{r}_2;\tau)&=\begin{pmatrix}\left\langle \tilde{E}_x^{t*}(\mathbf{r}_1,t)\tilde{E}_x^{t}(\mathbf{r}_2,t+\tau)\right\rangle & \left\langle \tilde{E}_x^{t*}(\mathbf{r}_1,t)\tilde{E}_y^{t}(\mathbf{r}_2,t+\tau)\right\rangle \\ \left\langle \tilde{E}_y^{t*}(\mathbf{r}_1,t)\tilde{E}_x^{t}(\mathbf{r}_2,t+\tau)\right\rangle & \left\langle \tilde{E}_y^{t*}(\mathbf{r}_1,t)\tilde{E}_y^{t}(\mathbf{r}_2,t+\tau)\right\rangle \end{pmatrix}\\ &=\begin{pmatrix}W_{xx}^i(\mathbf{r}_1,\mathbf{r}_2)\left\langle e^{j[\varphi_x(\mathbf{r}_1,t)-\varphi_x(\mathbf{r}_2-\tau\mathbf{v},t)]}\right\rangle & W_{xy}^i(\mathbf{r}_1,\mathbf{r}_2)\left\langle e^{j[\varphi_x(\mathbf{r}_1,t)-\varphi_y(\mathbf{r}_2-\tau\mathbf{v},t)]}\right\rangle \\ W_{yx}^i(\mathbf{r}_1,\mathbf{r}_2)\left\langle e^{j[\varphi_y(\mathbf{r}_1,t)-\varphi_x(\mathbf{r}_2-\tau\mathbf{v},t)]}\right\rangle & W_{yy}^i(\mathbf{r}_1,\mathbf{r}_2)\left\langle e^{j[\varphi_y(\mathbf{r}_1,t)-\varphi_y(\mathbf{r}_2-\tau\mathbf{v},t)]}\right\rangle \end{pmatrix}.\end{aligned} \tag{5.2}$$

The statistical independent property between the field and polarizer surface roughness is cited again to derive Eq. (5.2). For an object moving with a constant velocity $\mathbf{v}$ normal to the incident direction of the illuminating source, we assume that the time evolution of the local thickness is

$$d(\mathbf{r},t+\tau)=d(\mathbf{r}-\tau\mathbf{v},t) \tag{5.3}$$

That is, the transmission matrix at any position in a coordinate system moving along with the object does not change in time (i.e., Taylor's hypothesis). Every element in the beam coherence-polarization matrix in Eq. (5.2) is closely related to the characteristic function of the corresponding random variable $\Delta\varphi_{lm}(\mathbf{r}_1,\mathbf{r}_2;\tau)=\varphi_l(\mathbf{r}_1,t)-\varphi_m(\mathbf{r}_2-\tau\mathbf{v},t)$. Since the phase retardance φ_m, $(m = x, y)$ is

proportional to the local thickness $d(\mathbf{r})$ which is conventionally assumed to be in accordance with a commonly accepted zero mean Gaussian distribution model, $\left\langle \exp\left\{ j\Delta\varphi_{lm}(\mathbf{r}_1,\mathbf{r}_2;\tau)\right\}\right\rangle$ as the characteristic function of a Gaussian random variable $\Delta\varphi_{lm}(\mathbf{r}_1,\mathbf{r}_2;\tau)$ could be expressed as

$$\begin{aligned}&\left\langle \exp\left\{ j\Delta\varphi_{lm}(\mathbf{r}_1,\mathbf{r}_2;\tau)\right\}\right\rangle \\ &= \exp\left\{ -\frac{k^2\left[(n_l-1)^2+(n_m-1)^2\right]\left\langle d^2(\mathbf{r})\right\rangle}{2}\right. \\ &\left. +\frac{k^2 2(n_l-1)(n_m-1)\left\langle d(\mathbf{r}_1)d(\mathbf{r}_2-\tau\mathbf{v})\right\rangle}{2}\right\}.\end{aligned} \tag{5.4}$$

Recall the Gaussian-Gaussian model we used for the surface roughness description of the rough-surfaced retardation plate before, the time-lagged lateral correlation function for the surface thickness is derived under the wide-sense stationarity assumption.

$$\left\langle d(\mathbf{r}_1)d(\mathbf{r}_2-\tau\mathbf{v})\right\rangle = {\sigma_d}^2 \exp\left\{ -\frac{\left|\Delta\mathbf{r}+\tau\mathbf{v}\right|^2}{{r_d}^2}\right\}. \tag{5.5}$$

where $\Delta\mathbf{r}=\mathbf{r}_1-\mathbf{r}_2$, r_d is the lateral correlation length of surface thickness and ${\sigma_d}^2$ is the variance of the local surface thickness. Therefore, the statistics of the time-lagged modulation due to random phase retardance in matrix elements of Eq. (5.2) are given by

$$\begin{aligned}&\left\langle \exp\left\{ j\Delta\varphi_{xx}(\mathbf{r}_1,\mathbf{r}_2;\tau)\right\}\right\rangle \\ &= \exp\left[-k^2{\sigma_d}^2(n_x-1)^2\left\{1-\exp\left\{-\left|\Delta\mathbf{r}+\tau\mathbf{v}\right|^2/{r_d}^2\right\}\right\}\right];\end{aligned} \tag{5.6}$$

$$\begin{aligned}&\left\langle \exp\left\{ j\Delta\varphi_{yy}(\mathbf{r}_1,\mathbf{r}_2;\tau)\right\}\right\rangle \\ &=\exp\left[-k^2{\sigma_d}^2(n_y-1)^2\left\{1-\exp\left\{-\left|\Delta\mathbf{r}+\tau\mathbf{v}\right|^2/{r_d}^2\right\}\right\}\right];\end{aligned} \tag{5.7}$$

$$\begin{aligned}&\left\langle \exp\left\{ j\Delta\varphi_{xy}(\mathbf{r}_1,\mathbf{r}_2;\tau)\right\}\right\rangle =\left\langle \exp\left\{ j\Delta\varphi_{yx}(\mathbf{r}_1,\mathbf{r}_2;\tau)\right\}\right\rangle \\ &=\exp\left\{-\frac{k^2{\sigma_d}^2}{2}\left[(n_x-1)^2+(n_y-1)^2\right.\right. \\ &\left.\left.-2(n_x-1)(n_y-1)\exp\left\{-\left|\Delta\mathbf{r}+\tau\mathbf{v}\right|^2/{r_d}^2\right\}\right]\right\}.\end{aligned} \tag{5.8}$$

Equations (5.6)-(5.8) can be considered as one of the prime results of this chapter to describe the correlation properties of the dynamic polarization speckle determined by the motion features of the moving plate and the surface thickness fluctuations of the birefringent material.

For the rough-surfaced retardation plate we considered here with a large surface roughness and large phase variance, the approximation once utilised in Chapter 2 by truncated Taylor's series will be applied to simplify those double exponential function in Equations (5.6)-(5.8) into Gaussian form:

$$\begin{aligned}&\left\langle \exp\left\{ j\Delta\varphi_{lm,\tau}\right\}\right\rangle \\ &=\exp\left\{-\frac{k^2{\sigma_d}^2}{2}\left[\left(n_l-n_m\right)^2+2\left(n_l-1\right)\left(n_m-1\right)\frac{\left|\Delta\mathbf{r}+\tau\mathbf{v}\right|^2}{{r_d}^2}\right]\right.\end{aligned} \tag{5.9}$$

In this way, it will become feasible to provide the analytical conclusions of the time-lagged beam coherence-polarization matrix for the dynamic polarization speckle after propagation within a complex ABCD theory, and elicit the elaborate investigation about the relationship between the spatial temporal characteristics of the observed dynamic polarization speckle and the plate surface structures, motion characters, together with the features of the propagation system.

5.3 Dynamic polarization speckle during propagation

Without giving specific definition of the incident field $\mathbf{E}^i$, any further progress with a deterministic analysis is impossible. The typical Gaussian laser beam will be considered as an example of proper source to facilitate the investigation of the propagation of the time-lagged beam coherence-polarization matrix for dynamic speckle. Consider an incident Gaussian beam with a polarization angle θ and beam radius r_s, the corresponding beam coherence-polarization matrix could be written as

$$\mathbf{W}^i(\mathbf{r}_1,\mathbf{r}_2) = I_o \exp\left\{-\frac{|\mathbf{r}_1|^2+|\mathbf{r}_2|^2}{r_s^{\,2}}\right\}\begin{pmatrix}\cos^2\theta & \cos\theta\sin\theta\\ \cos\theta\sin\theta & \sin^2\theta\end{pmatrix}. \tag{5.10}$$

According to the conclusions in Eq. (5.2), Eq. (5.9) and Eq. (5.10), the matrix elements of the time-lagged beam coherence-polarization matrix for modulated field after the moving plate are given by

$$\begin{aligned}\mathbf{W}_{xx}^t(\mathbf{r}_1,\mathbf{r}_2;\tau) = I_o\cos^2\theta\exp\left\{-\frac{(|\mathbf{r}_1|^2+|\mathbf{r}_2|^2)}{r_s^{\,2}}\right\}\\ \exp\left\{-k^2{\sigma_d}^2(n_x-1)^2\frac{|\Delta\mathbf{r}+\tau\mathbf{v}|^2}{r_d^2}\right\},\end{aligned} \tag{5.11}$$

$$\begin{aligned}\mathbf{W}_{yy}^t(\mathbf{r}_1,\mathbf{r}_2;\tau) = I_o\cos^2\theta\exp\left\{-\frac{(|\mathbf{r}_1|^2+|\mathbf{r}_2|^2)}{r_s^{\,2}}\right\}\\ \exp\left\{-k^2{\sigma_d}^2(n_y-1)^2\frac{|\Delta\mathbf{r}+\tau\mathbf{v}|^2}{r_d^2}\right\},\end{aligned} \tag{5.12}$$

$$\begin{aligned}\mathbf{W}_{xy}^t(\mathbf{r}_1,\mathbf{r}_2;\tau) = \mathbf{W}_{yx}^t(\mathbf{r}_1,\mathbf{r}_2;\tau) = I_o\sin\theta\cos\theta\exp\left\{-\frac{(|\mathbf{r}_1|^2+|\mathbf{r}_2|^2)}{r_s^{\,2}}\right\}\\ \times\exp\left\{-\frac{k^2{\sigma_d}^2}{2}\left[(n_y-n_x)^2+2(n_x-1)(n_y-1)\frac{|\Delta\mathbf{r}+\tau\mathbf{v}|^2}{r_d^2}\right]\right\}.\end{aligned} \tag{5.13}$$

We next consider the evolution of the statistical properties of the dynamic polarization speckle generated by the moving rough-surfaced retardation plate illustrated by the linearly polarized Gaussian beam during propagation.

Under the paraxial approximation, the time-lagged beam coherence-polarization matrix $\mathbf{W}^o(\mathbf{p}_1,\mathbf{p}_2;\tau)$ for the field $\mathbf{E}^o$ on the observation plane could be conducted by the Fresnel integral formula of $\mathbf{W}^t$ with Green functions within a Complex ABCD optical system.

$$\mathbf{W}^o\left(\mathbf{p}_1,\mathbf{p}_2,\tau\right)=\iint_{\pm\infty}\mathbf{W}^t(\mathbf{r}_1,\mathbf{r}_2;\tau)G^*\left(\mathbf{p_1},\mathbf{r_1}\right)G\left(\mathbf{p}_2,\mathbf{r}_2\right)d\mathbf{r_1}d\mathbf{r}_2, \tag{5.14}$$

Since the propagation system is assumed to be time independent, the Green function should be

$$G\left(\mathbf{p},\mathbf{r}\right)=-\frac{jk}{2\pi B}\exp\left\{-\frac{jk}{2B}\left(A|\mathbf{r}|^2-2\mathbf{r}\cdot\mathbf{p}+D|\mathbf{p}|^2\right)\right\}. \tag{5.15}$$

Usually, the amplitude of the time-lagged beam coherence-polarization matrix elements is of real interest. The phase term will be important if the ultimate goal is to calculate another field after further propagation, in which case the complete complex field is needed. In most cases, however, the intensity distribution on the observation plane will be the directly measured physical quantity, and the phase distribution is of no consequence. For example, the knowledge about the speckle's shape and dynamic features could be yielded from the amplitude of the beam coherence-polarization matrix elements by the relationship between the amplitude of the beam coherence matrix elements and the covariance of the intensity distribution [119, 154].

Hence, we derive the amplitude of the time-lagged beam coherence-polarization matrix after travelling the ABCD system by substituting $\mathbf{W}^t(\mathbf{r}_1,\mathbf{r}_2;\tau)$ into the integral defined in Eq. (5.14). And we get the analytical expressions shown below:

$$\left|W_{xx}^{o}\left(\mathbf{p}_1,\mathbf{p}_2,\tau\right)\right| = I_o\cos^2\left|W_{xx}(\mathbf{p_1},\mathbf{p_2};\tau,\frac{r_d^2}{k^2{\sigma_d}^2\left(n_x-1\right)^2})\right|; \tag{5.16}$$

$$\left|W_{yy}^{o}\left(\mathbf{p}_1,\mathbf{p}_2,\tau\right)\right| = I_o\cos^2\theta\left|W_{yy}\left(\mathbf{p_1},\mathbf{p_2};\tau,\frac{{r_d}^2}{k^2\sigma_d^2\left(n_y-1\right)^2}\right)\right|, \tag{5.17}$$

$$\begin{aligned}\left|W_{xy}^{o}\left(\mathbf{p}_1,\mathbf{p}_2,\tau\right)\right| &= \left|\mathbf{W}_{yx}^{o}\left(\mathbf{p}_1,\mathbf{p}_2,\tau\right)\right| \\ &= I_o\sin\theta\cos\theta\left|W_{xy}\left(\mathbf{p_1},\mathbf{p_2};\tau,\frac{{r_d}^2}{k^2\sigma_d^2\left(n_y-1\right)^2}\right)\right|.\end{aligned} \tag{5.18}$$

In each W_{lm}^{o} $(l,m=x,y)$, the corresponding $W_{lm}(\mathbf{p_1},\mathbf{p_2};\tau,\beta_{lm})$ is an integral function with parameter r_{lm}^{η} and r_{lm}^{w} evaluated analytically as

$$W_{lm}(\mathbf{p_1},\mathbf{p_2};\tau,\beta_{lm}) = \frac{\beta_{lm}}{\left(r_{lm}^{\eta}\right)^2}\exp\left\{\frac{-\left|\Delta\mathbf{p}+A\mathbf{v}\tau\right|^2}{\left(r_{lm}^{\eta}\right)^2}\right\}\exp\left\{\frac{-\left(\left|\mathbf{p}_1\right|^2+\left|\mathbf{p}_2\right|^2\right)}{\left(r_{lm}^{w}\right)^2}\right\}, \tag{5.19}$$

$$r_{lm}^{w} = \frac{\left|B\right|r_{lm}^{\eta}}{\left(-2\,\mathrm{Im}\left[B\right]^2+2\,\mathrm{Im}\left[A^*B\right]\mathrm{Im}\left[D^*B\right]+\frac{k\beta_{lm}}{2}\left(\left|A\right|^2\,\mathrm{Im}\left[B^*D\right]-\mathrm{Im}\left[AB\right]\right)\right)^{1/2}}. \tag{5.20}$$

and,

$$r_{lm}^{\eta} = \left(4\,\mathrm{Im}\left[A^*B\right]/k+\beta_{lm}\left|A\right|^2\right)^{1/2} \tag{5.21}$$

In derivation of the above propagation integral for $|W_{lm}^{o}\left(\mathbf{p_1},\mathbf{p_2},\tau\right)|$, the illuminating beam size r_s and possible radius of curvature are omitted and compensated by ABCD matrix elements as we did before, when the total ABCD matrix is calculated [108].

The above mathematical expressions in close-term provide the analytic results for the propagation of the dynamic beam coherence-polarization matrix through a complex ABCD optical system, and could be considered as key conclusions of the section. Using these results, one can analyse the evolution of the corresponding dynamic and shape features of the dynamic polarization speckle in any observation plane of general optical systems while the depolarizer is illuminated by a linearly polarized Gaussain electromagnetic beam. Thus, we achieve the extension of previous work for scalar speckle in particular propagation systems [6] into a vectorial form for polarization speckle. Thereby, some interesting phenomena which cannot be illustrated in the traditional scalar context will be revealed.

Consider the x wave component of the propagated field and the corresponding dynamic speckle generated. If the $\Delta\mathbf{p} = \mathbf{p_1} - \mathbf{p_2}$ and τ are set to zero, matrix element $|W^o{}_{xx}(\mathbf{p},\mathbf{p};0)|$ in Gaussian form will illustrate the beam's intensity distribution of x wave component. The $1/e^2$ radius r_{xx}^w defined in Eq. (5.20) will demonstrate the illuminated spot region size of the x wave component on the observation plane. At the same, the illuminated spot region size of y wave component, as distinct from the x one, is correspondingly indicated by the $1/e^2$ radius r_{yy}^w of matrix element $|W_{yy}^o(\mathbf{p},\mathbf{p};0)|$. The diversity of these two wave components' beam shapes is directly caused by the differences of β_{lm} $(l,m = x,y)$ in $|W^o{}_{xx}(\mathbf{p},\mathbf{p};0)|$ and $|W_{yy}^o(\mathbf{p},\mathbf{p};0)|$. As one of the significantly important conclusions of this chapter, it illustrates the birefringence effect of the depolarizer on field modulation which results from the orientation dependence. And thus it raises the requirement of vectorial field presentation instead of the traditional scalar form in related researches.

Moreover, as the denominator of Gaussian terms of $\Delta\mathbf{p}$ in $|W_{mm}^o(\Delta\mathbf{p},0)|$, $(m = x \text{ or } y)$ for x and y wave components respectively, in the absence of time lag $\tau = 0$, the r_{mm}^{η}, $(m = x \text{ or } y)$ measures the lateral correlation length of corresponding wave component's intensity and specifies the difference between average speckle sizes of x and y wave components. Similar to the disparities of speckle shape

features between x and y wave components, if non-zero time lag τ is introduced, differences in dynamic features of the polarization speckle embodied in the mathematical expression of matrix elements in Eq. (5.16)-(5.18) could also be investigated.

While points distance $\Delta\mathbf{p}$ is zero, the temporal correlation length τ_{lm}^{c}, $(l,m=x,y)$ between x and y wave components of the dynamic polarization speckle will be illustrated by the denominators $r_{lm}^{\eta}/(A\mathbf{v})$ in Gaussian functions about τ in corresponding $|W_{lm}^{o}(\Delta\mathbf{p},0)|$ $(l,m=x,y)$:

$$\tau_{xx}^{c}=\frac{\left(4k\,\mathrm{Im}\left[\frac{B}{A}\right]+\frac{r_d^2}{\sigma_d{}^2\left(n_x-1\right)^2}\right)^{1/2}}{k|\mathbf{v}|}; \tag{5.22}$$

$$\tau_{yy}^{c}=\frac{\left(4k\,\mathrm{Im}\left[\frac{B}{A}\right]+\frac{r_d^2}{\sigma_d{}^2\left(n_y-1\right)^2}\right)^{1/2}}{k|\mathbf{v}|}; \tag{5.23}$$

$$\tau_{xy}^{c}=\tau_{yx}^{c}=\frac{\left(4k\,\mathrm{Im}\left[\frac{B}{A}\right]+\frac{r_d^2}{\sigma_d{}^2\left(n_x-1\right)\left(n_y-1\right)}\right)^{1/2}}{k|\mathbf{v}|}; \tag{5.24}$$

Eq. (5.22)-(5.24) are the generalization of the transition times for speckle engendered by the $x-x$, $y-y$, and $x-y$ wave components respectively.

Different from the scalar speckle generated by the traditional depolarizer with identical temporal correlation length of x, y wave components and whole field in observation, the variety of temporal correlation length between different observed wave components is indicated clearly in the above discussion.

We normalize the matrix element, $|W_{lm}^{o}(\mathbf{p_1},\mathbf{p_2},\tau)|$, $(l,m=x,y)$ in Eq. (5.16)-(5.18) to their corresponding square roots at points $\mathbf{p_1}$ and $\mathbf{p_2}$ i.e., $|W_{lm}^{o}(\mathbf{p_1},\mathbf{p}_1,0)|$ and $|W_{lm}^{o}(\mathbf{p}_2,\mathbf{p}_2,0)|$, then yield the normalized coherence expression

$$\gamma_{lm}\left(\mathbf{p_1},\mathbf{p_2},\tau\right)=\exp\left\{\frac{-\left|\Delta\mathbf{p}+\mathrm{Re}\left[A\right]\mathbf{v}\tau\right|^2}{\left(r_{lm}^{\eta}\right)^2}\right\}\exp\left\{\frac{-\left|\mathrm{Im}\left[A\right]\mathbf{v}\tau\right|^2}{\left(r_{lm}^{\eta}\right)^2}\right\}. \tag{5.25}$$

by which more dynamic properties of the speckle could be extracted.

In a far field propagation distance or Fourier plane of the Fourier system $(\mathrm{Re[A]}\to 0)$, the Eq. (5.25) consists of two Gaussian functions for $\Delta\mathbf{p}$ and τ independently, as shown in Eq. (5.26):

$$\gamma_{lm}\left(\mathbf{p_1},\mathbf{p_2},\tau\right)=\exp\left\{\frac{-\left|\Delta\mathbf{p}\right|^2}{\left(r_{lm}^{\eta}\right)^2}\right\}\exp\left\{\frac{-\left|\mathrm{Im}\left[A\right]\mathbf{v}\tau\right|^2}{\left(r_{lm}^{\eta}\right)^2}\right\}. \tag{5.26}$$

This means that the fluctuation of the speckle in time is in isolation from the other speckles with a distance further than the speckle size. The shape of the individual speckles will change independently of one another. This is called speckle boiling [119], and the x and y speckle element could be involved in this boiling state together. Under this condition, the disparity between corresponding temporal correlation length given embodied in Eq. (5.22)-(5.24) for different wave components will be observed for boiling speckles.

On the other hand, when $\mathrm{Im[A]}\to 0$, (i.e. in the near field or in the image plane), Eq. (5.25) becomes

$$\gamma_{lm}\left(\mathbf{p_1},\mathbf{p_2},\tau\right)=\exp\left\{\frac{-\left|\Delta\mathbf{p}+\mathrm{Re}\left[A\right]\mathbf{v}\tau\right|^2}{\left(r_{lm}^{\eta}\right)^2}\right\}, \tag{5.27}$$

and the $\Delta\mathbf{p}$ and τ in the numerator of the same Gaussian function are closed related, illustrating the speckles' moving as a whole. This characteristic speckle pattern is usually called speckle translation [119]. As indicated in Eq.(5.27), the time required for each element of speckles to translate a fixed distance $\Delta\mathbf{p}$ equals $|\Delta\mathbf{p}/A\mathbf{v}|$, and hence the speed of the speckles translation, $\mathbf{v}_s$, is obtained in general as

$$\mathbf{v}_s=\mathrm{Re}[A]\mathbf{v} \tag{5.28}$$

That means, though beam size and mean speckle size are in disparity for speckles generated by different wave components, the translation of these speckles are in the same speed. While we observe the whole field, the speckle separation will not be observed.

5.4 Conclusion

In this chapter, we introduced a moving rough-surfaced retardation plate as a depolarizer to generate dynamic polarization speckle. Based the Gaussian-Gaussian surface roughness model, we derived the corresponding time-lagged beam coherence-polarization matrix for modulated field after the plate to reveal the dependence of the modulation performance of such moving depolarizer on its surface structure and motion features. Based on this conclusion, the time-lagged beam coherence-polarization matrix of propagated dynamic polarization speckle on the observation plane is analytically expressed within the frame work of complex ABCD theory, and thus, we reveal the variation of the shape feature for the propagated polarization speckle. Particularly, the disparities of speckle shape features, like the mean spot size, the mean speckle size and the temporal coherence length for speckle generated from both *x* and *y* wave components are investigated and demonstrated clearly. The diversity performances of the wave components could be considered as the

manifestation of the polarization-dependent modulation property of the rough-surfaced retardation plate. It is illustrated that identical performance for wave components in traditional scalar speckles will no longer be valid for the dynamic polarization speckle generated by the moving rough-surfaced retardation plate, though they are generated with the same propagation system. Additionally, the feasibility of generating both pure boiling and translation polarization speckle has been demonstrated with a general description of the system prerequisite. Further, a systematic analysis about the beam dynamic variety of different beam component of polarization speckle generated by moving the rough-surfaced retardation plate is important because it will facilitate our understanding of the evolution of polarization speckle motion. Hence, this chapter provides a practical insight into a wide class of dynamic phenomena of polarization speckles.

Chapter 6

Depolarizing and Decorrelating Modulation to Electromagnetic Fields by a Depolarizer of Random Polarizer Array

A random polarizer array consisting of multitude of contiguous square cells of polarizer with randomly distributed orientation angles is introduced as a depolarizer in this chapter. The incident fields will experience random polarization modulation after passing through this polarizer array. On the basis of the 2×2 beam coherence-polarization matrix, statistical properties of the modulated fields are investigated. The complex ABCD matrix theory is invoked to study the propagation of the modulated fields through any quadratic optical system to show how the degree of coherence and polarization changes during propagation.

6.1 Introduction

Optical systems are often sensitive to the polarization states of the incident light. In many applications, the polarization sensitivity may cause serious deviation in the system's output if some unwanted polarization of the inputs has been introduced. To reduce the undesirable effects of the polarization sensitivity, a depolarizer has been widely used to scramble the polarization state of the incident beam. An ideal depolarizer can convert a polarized beam into a light with temporally and/or spatially random polarization states. Unfortunately, all commercially available depolarizers can only provide the output light with pseudo-random polarization states, having spatially, temporally or spectrally periodic variations. To overcome this difficulty of pseudo-randomness, many different approaches have been proposed to minimize the unwanted effects of polarization sensitivity in optical systems [155-157]. Although they differ in the detailed patterned structure for crystalline chips of birefringent materials, all of the above-mentioned devices are fabricated from a large number of small polarizer cells with their optical axes randomly oriented [1, 2, 29, 73].

In this chapter, we present a model for the depolarizer composed of a multitude of contiguous small $l \times l$ square cells of linear polarizers with randomly orientated polarizing axes. An analytical description of its modulation behaviour is provided, and the statistical properties of random electric fields engendered by the depolarizer are discussed. Consequently, the evolution of the statistical properties of the modulated random electric fields is investigated within the framework of the complex ABCD method, and the special variation of degree of the coherence and the degree of polarization of such a beam during propagation is indicated.

6.2 Modulation behaviour of a random polarizer array as a depolarizer to the incident beam

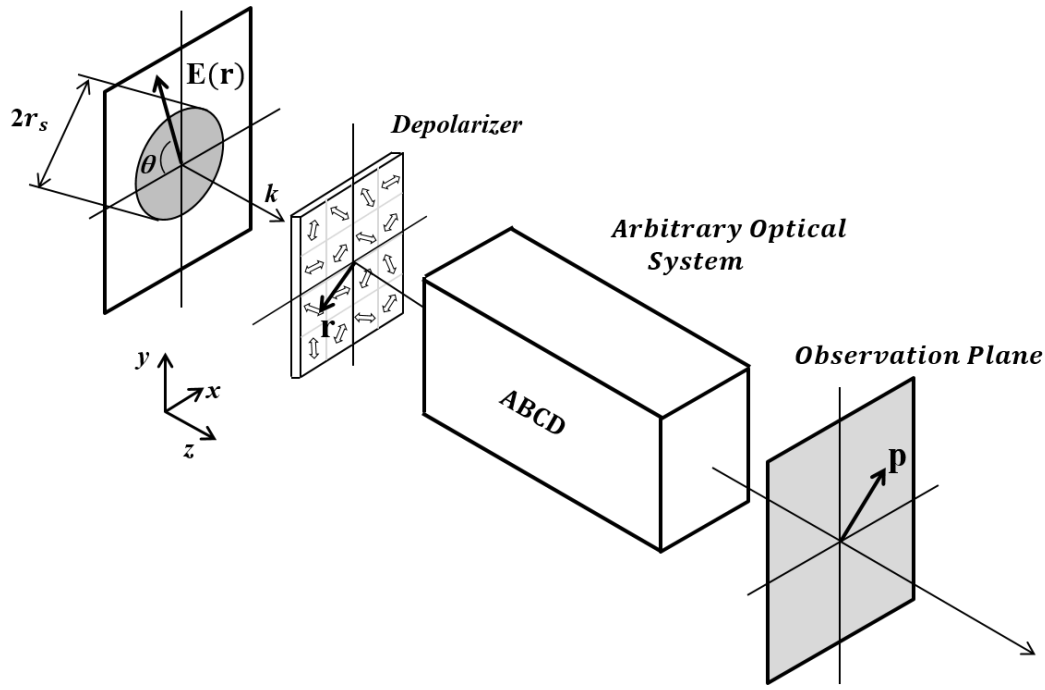

Figure 6.1 Schematic of the setup for obtaining the degree of polarization and coherence of the field propagating through random polarizer array and ABCD optical systems

As shown in Figure 6.1, an optical system is setup to examine the propagation of the electric field modulated by a random polarizer array. An incident electric field $\mathbf{E}^i(\mathbf{r}) = \{E_x^i(\mathbf{r}), E_y^i(\mathbf{r})\}$ with its beam radius r_s and wave vector $\vec{k}$ illustrates on and passes through a depolarizer perpendicularly settled to the z optic-axis. The modulated light $\mathbf{E}^t$ after the optical system will pass through the complex ABCD optical system [108, 110] under the paraxial approximation, and arrive at the observation plane.

In order to understand the modulation behaviour of random polarizer array as a depolarizer that is reliant on the plate structure, and to specify the statistical properties of the modulated light during its propagation, we begin with the derivation of the 2×2 beam coherence-polarization matrix $\mathbf{W}^t(\mathbf{r}_1, \mathbf{r}_2)$ of the modulated light just behind the depolarizer.

$$\mathbf{W}^t(\mathbf{r}_1,\mathbf{r}_2)=\begin{pmatrix}\left\langle E^{t*}_x(\mathbf{r}_1)E^t_x(\mathbf{r}_2)\right\rangle & \left\langle E^{t*}_x(\mathbf{r}_1)E^t_y(\mathbf{r}_2)\right\rangle\\ \left\langle E^{t*}_y(\mathbf{r}_1)E^t_x(\mathbf{r}_2)\right\rangle & \left\langle E^{t*}_y(\mathbf{r}_1)E^t_y(\mathbf{r}_2)\right\rangle\end{pmatrix}. \tag{6.1}$$

As shown in Figure 6.2, this random polarizer array consists of a multitude of contiguous small $l\times l$ squares in rows and columns. In this random polarizer array, the small polarizer cells will only transmit the vector field components polarized in parallel with the polarization angle γ of the local polarizer cell whose orientation is indicated by the small arrow. Although the random polarizer array is a regular spatial structure, the randomness of its modulation behavior is introduced by the randomly and independently distributed polarization angle γ of the cells. In this analysis, the size of the random polarizer array itself may be regarded as infinite in extent, and only a finite portion lies within the pupil of the optical system. Because of a lack of knowledge of the exact location of the depolarizer on the scale of a single cell, an assumption has been made that it is at least wide-sense stationary [29]. The location of the depolarizer with respect to the optical axis is chosen to be random with a uniform distribution of probability over any square cell.

When the rows and columns of the random polarizer array cells are aligned along the x and y axis respectively, with reference to the depolarizer pattern of Figure 6.2, for each square cell with its polarization angle γ to x axis, the transmission matrix (Jones matrix) delineating its modulation behaviour is given by

$$\mathbf{T}(\mathbf{r})=\begin{pmatrix}T_{xx}(\mathbf{r}) & T_{xy}(\mathbf{r})\\ T_{yx}(\mathbf{r}) & T_{yy}(\mathbf{r})\end{pmatrix}=\begin{pmatrix}\cos^2\gamma(\mathbf{r}) & \sin\gamma(\mathbf{r})\cos\gamma(\mathbf{r})\\ \cos\gamma(\mathbf{r})\sin\gamma(\mathbf{r}) & \sin^2\gamma(\mathbf{r})\end{pmatrix}. \tag{6.2}$$

It is indicated by the above expression that this device realizes the polarization modulation by the amplitude modulation to the incident field instead of the phase modulation as the rough-surfaced retardation plate.

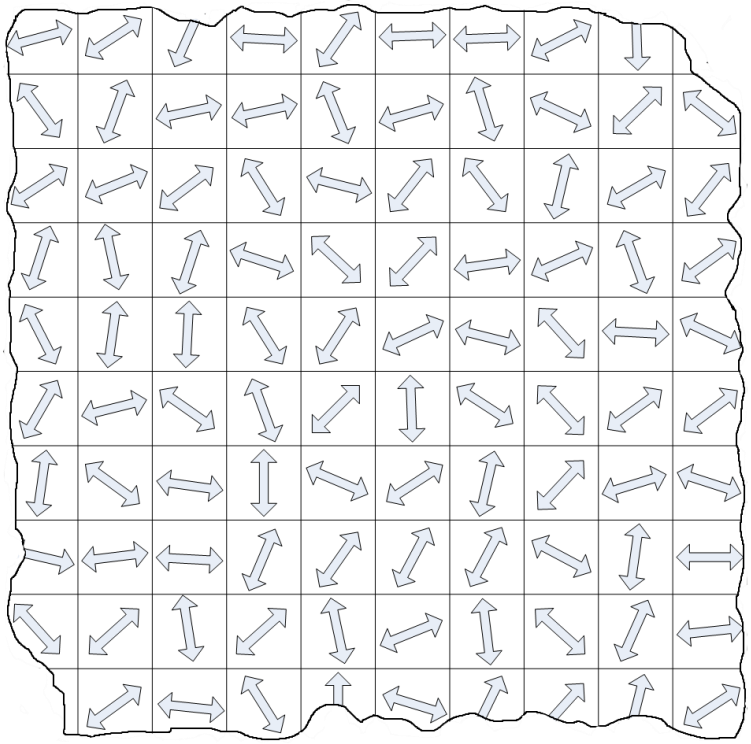

Figure 6.2 Diagram of depolarizer (0-180 deg): random polarizer array

When the incident electric field passes through the depolarizer, the polarization state is modified accordingly, i.e., $\mathbf{E}^t(\mathbf{r})=\mathbf{T}(\mathbf{r})\mathbf{E}^i(\mathbf{r})$ with the superscript *i* or *t* representing the incident or transmission field. Let $\mathbf{W}^i(\mathbf{r}_1,\mathbf{r}_2)$ be the beam coherence-polarization matrix of the incident beam, then the beam coherence-polarization matrix $\mathbf{W}^t(\mathbf{r}_1,\mathbf{r}_2)$ of the modulated field just behind the depolarizer is given by

$$\mathbf{W}^t(\mathbf{r}_1,\mathbf{r}_2)=\left\langle \mathbf{T}^\dagger(\mathbf{r}_1)\mathbf{W}^i(\mathbf{r}_1,\mathbf{r}_2)\mathbf{T}(\mathbf{r}_2)\right\rangle, \tag{6.3}$$

where the † denotes the Hermitian conjugate. Because of the statistical independence between the incident field and the depolarizer structure, we have the expression for matrix elements in Eq. (6.3).

$$W_{fg}^t(\mathbf{r}_1,\mathbf{r}_2)=\sum_{l,m=x,y}\left\langle T_{lf}(\mathbf{r}_1)T_{mg}(\mathbf{r}_2)\right\rangle W_{lm}^i(\mathbf{r}_1,\mathbf{r}_2). \tag{6.4}$$

Given that different cells have statistically independent polarization angles for each polarizer cell, polarizations angles are the same for points in the same polarizer cell, and totally independent for points in different cells. The beam coherence-polarization matrix $\mathbf{W}^t$ of the modulate fields can be written as a combination

$$\begin{aligned}\mathbf{W}^t(\mathbf{r_1},\mathbf{r_2}) = {}^S\mathbf{W}^t(\mathbf{r_1},\mathbf{r_2})\text{Prob}\left\{\begin{matrix}\mathbf{r_1}\text{ and }\mathbf{r_2}\text{ are}\\ \text{in the same cell}\end{matrix}\right\}\\ +{}^D\mathbf{W}^t(\mathbf{r_1},\mathbf{r_2})\text{Prob}\left\{\begin{matrix}\mathbf{r_1}\text{ and }\mathbf{r_2}\text{ are}\\ \text{in different cells}\end{matrix}\right\}.\end{aligned} \tag{6.5}$$

In the expression above, ${}^S\mathbf{W}^t$ and ${}^D\mathbf{W}^t$ have been introduced to denote the coherence matrices for the transmitted fields with points $\mathbf{r}_1$ and $\mathbf{r}_2$ in the same and different cells, respectively. Similar to the random checkerboard absorbing screen [29, 111], we are able to write down the desired probabilities for both conditions, because of the uniform distribution of the absolute location of the depolarizer. They are

$$\text{Prob}\left\{\mathbf{r_1},\mathbf{r_2}\text{ in the same cell}\right\} = \wedge\left(\Delta r_x/l\right)\wedge\left(\Delta r_y/l\right), \tag{6.6}$$

and

$$\text{Prob}\left\{\mathbf{r_1}\text{ and }\mathbf{r_2}\text{ are in different cells}\right\} = 1-\wedge\left(\Delta r_x/l\right)\wedge\left(\Delta r_y/l\right), \tag{6.7}$$

where Δr_x and Δr_y are the two components of the location vector $\Delta\mathbf{r} = \mathbf{r}_1 - \mathbf{r}_2$ along x and y directions, and unit triangle function $\wedge(x) = 1-|x|$ for $|x|\le 1$ and zero otherwise.

Notice that the polarization angle γ of the polarizer in each cell is assumed to be random and independent from cell to cell. We have

$$ {}^{S}\mathbf{W}^{t}(\mathbf{r}_1,\mathbf{r}_2)=\begin{pmatrix} \sum\limits_{lm=x,y}\langle T_{lx}T_{mx}\rangle W_{lm}^{i}(\mathbf{r}_1,\mathbf{r}_2) & \sum\limits_{lm=x,y}\langle T_{lx}T_{my}\rangle W_{lm}^{i}(\mathbf{r}_1,\mathbf{r}_2) \\ \sum\limits_{lm=x,y}\langle T_{ly}T_{mx}\rangle W_{lm}^{i}(\mathbf{r}_1,\mathbf{r}_2) & \sum\limits_{lm=x,y}\langle T_{ly}T_{my}\rangle W_{lm}^{i}(\mathbf{r}_1,\mathbf{r}_2) \end{pmatrix} \tag{6.8} $$

and

$$ {}^{D}\mathbf{W}^{t}(\mathbf{r}_1,\mathbf{r}_2)=\begin{pmatrix} \sum\limits_{lm=x,y}\langle T_{lx}\rangle\langle T_{mx}\rangle W_{lm}^{i}(\mathbf{r}_1,\mathbf{r}_2) & \sum\limits_{lm=x,y}\langle T_{lx}\rangle\langle T_{my}\rangle W_{lm}^{i}(\mathbf{r}_1,\mathbf{r}_2) \\ \sum\limits_{lm=x,y}\langle T_{ly}\rangle\langle T_{mx}\rangle W_{lm}^{i}(\mathbf{r}_1,\mathbf{r}_2) & \sum\limits_{lm=x,y}\langle T_{ly}\rangle\langle T_{my}\rangle W_{lm}^{i}(\mathbf{r}_1,\mathbf{r}_2) \end{pmatrix}. \tag{6.9} $$

When Eq. (6.8) and Eq. (6.9) have been derived, we have made use of the fact that the coherence property of the electric fields and correlation property of the random polarizer array are statistically independent, and that the ensemble average denoted by angular brackets has been taken over the depolarizer. The beam coherence-polarization matrix for the modulated field just behind the depolarizer can be assessed only if some specific assumptions are made regarding the statistics of the polarization angle γ for the random polarizer array. A case of the most interest is the depolarizer whose stochastic polarization angle has a uniform probability distribution function within $[0,\pi)$. Under the assumption of the probability distribution function (PDF) $p_{\gamma}(\gamma)=1/\pi$, the first-order and second-order moments of the elements in Jones Matrix in Eq. (6.2) have been evaluated and listed in Table 1.

Therefore, the expression beam coherence-polarization matrix $\mathbf{W}^{t}$ for the modulated field just behind the depolarizer could be easily calculated. Thus we have

$$ \begin{aligned} \mathbf{W}^{t}(\mathbf{r}_1,\mathbf{r}_2) &= \frac{1}{4}\begin{pmatrix} W_{xx}^{i} & W_{xy}^{i} \\ W_{yx}^{i} & W_{yy}^{i} \end{pmatrix} \\ &\quad + \frac{1}{8}\wedge\left(\frac{\Delta r_x}{l}\right)\wedge\left(\frac{\Delta r_y}{l}\right)\begin{pmatrix} W_{xx}^{i}+W_{yy}^{i} & -W_{xy}^{i}+W_{yx}^{i} \\ -W_{yx}^{i}+W_{xy}^{i} & W_{yy}^{i}+W_{xx}^{i} \end{pmatrix}. \end{aligned} \tag{6.10} $$

Table 1 First-order and Second-order Moments of the Elements in Jones Matrix for (0-180 deg) model

$$\langle T_{xx}\rangle = \langle \cos^2\gamma(\mathbf{r})\rangle = 1/2 \qquad \langle T_{yy}\rangle = \langle \sin^2\gamma(\mathbf{r})\rangle = 1/2$$

$$\langle T_{xy}\rangle = \langle \cos\gamma(\mathbf{r})\sin\gamma(\mathbf{r})\rangle = 0 \qquad \langle T_{yx}\rangle = \langle \cos\gamma(\mathbf{r})\sin\gamma(\mathbf{r})\rangle = 0$$

$$\langle T_{xx}^2\rangle = \langle \cos^4\gamma(\mathbf{r})\rangle = 3/8 \qquad \langle T_{yy}^2\rangle = \langle \sin^4\gamma(\mathbf{r})\rangle = 3/8$$

$$\langle T_{xy}^2\rangle = \langle T_{yx}^2\rangle = \langle \sin^2\gamma(\mathbf{r})\cos^2\gamma(\mathbf{r})\rangle = 1/8$$

$$\langle T_{xx}T_{xy}\rangle = \langle T_{xx}T_{yx}\rangle = \langle \sin\gamma(\mathbf{r})\cos^3\gamma(\mathbf{r})\rangle = 0$$

$$\langle T_{xy}T_{yy}\rangle = \langle T_{yx}T_{yy}\rangle = \langle \sin^3\gamma(\mathbf{r})\cos\gamma(\mathbf{r})\rangle = 0$$

$$\langle T_{xx}T_{yy}\rangle = \langle \sin^2\gamma(\mathbf{r})\cos^2\gamma(\mathbf{r})\rangle = 1/8$$

The desired correlation properties for the depolarizer of random polarizer array plate are presented in Eq. (6.10) and can be regarded as one of the key conclusions of this chapter to portray the statistics of the scattered electric field.

We now have the necessary tools for further progress to investigate the propagation of the beam coherence-polarization matrix through an optical system when the electric fields are modulated by the random polarizer array. For further progress with a deterministic analysis, and without loss of generality, one of the best examples we can cite in the following discussion is a spatially coherent Gaussian beam with the linearly polarized angle θ with respect to x axis. The beam coherence-polarization matrix for the field just in front of the depolarizer is given by

$$\mathbf{W}^i(\mathbf{r}_1,\mathbf{r}_2) = I_o \exp\left\{-\frac{|\mathbf{r}_1|^2+|\mathbf{r}_2|^2}{r_s^{\,2}}\right\}\begin{pmatrix}\cos^2\theta & \cos\theta\sin\theta\\ \cos\theta\sin\theta & \sin^2\theta\end{pmatrix}. \tag{6.11}$$

where I_0 is the on axis intensity of the incident field. By substituting Eq. (6.11) into (6.10), the expressions for the beam coherence-polarization matrix of the modulated beam just behind the depolarizer is obtained

$$\mathbf{W}^t(\mathbf{r}_1,\mathbf{r}_2)=\frac{I_o}{8}\exp\left\{-\frac{|\mathbf{r}_1|^2+|\mathbf{r}_2|^2}{r_s^{\,2}}\right\}$$
$$\times\left\{2\begin{pmatrix}\cos^2\theta & \sin\theta\cos\theta\\ \sin\theta\cos\theta & \sin^2\theta\end{pmatrix}+\wedge\left(\frac{\Delta r_x}{l}\right)\wedge\left(\frac{\Delta r_y}{l}\right)\begin{pmatrix}1 & 0\\ 0 & 1\end{pmatrix}\right\}. \tag{6.12}$$

Our interest here is the static random spatial distribution of the modulated electric fields' polarization state illustrated by the degree of polarization for the modulated fields. It is calculated from matrix elements of Eq. (6.12) :

$$P^t(\mathbf{r})=1/2, \tag{6.13}$$

which is constant no matter where the observation point is chosen. In a similar way, the degree of spatial coherence of the modulated electric fields behind the depolarizer is obtained

$$\eta^t(\mathbf{r}_1,\mathbf{r}_2)=\frac{1+\wedge(\Delta r_x/l)\wedge(\Delta r_y/l)}{2}, \tag{6.14}$$

indicating that a spatially partial coherence has been achieved for the transmitted fields regardless the incident polarization angle.

6.3 Evolution of the polarization and coherence properties on propagation for polarization speckle generated by random polarizer array

We next consider the propagation of this modulated field just behind the random polarizer illustrated by a linearly polarized Gaussian beam. Under the paraxial approximation, the beam coherence-polarization matrix $\mathbf{W}^o$ for the field $\mathbf{E}^o$ arriving at the observation plane after propagating through a complex ABCD optical system is given in general terms of the Huygens-Fresnel integral formulation

$$\mathbf{W}^o(\mathbf{p}_1,\mathbf{p}_2)=\iint \mathbf{W}^t(\mathbf{r_1},\mathbf{r_2})G^*(\mathbf{p_1},\mathbf{r_1})G(\mathbf{p}_2,\mathbf{r}_2)d\mathbf{r_1}d\mathbf{r}_2, \tag{6.15}$$

and can now be written as

$$\begin{aligned}&\mathbf{W}^o(\mathbf{p}_1,\mathbf{p}_2)\\&=\frac{I_o}{8}\left\{2\begin{pmatrix}\cos^2\theta & \sin\theta\cos\theta\\ \sin\theta\cos\theta & \sin^2\theta\end{pmatrix}W_b^{ABCD}(\mathbf{p}_1,\mathbf{p}_2)\right.\\&\left.+\begin{pmatrix}1 & 0\\ 0 & 1\end{pmatrix}W_d^{ABCD}(\mathbf{p}_1,\mathbf{p}_2)\right\}\end{aligned} \tag{6.16}$$

where W_b^{ABCD} is the integral functions that has been evaluated analytically in Eq. (3.13) of Chapter 3:

$$\begin{aligned}&W_b^{ABCD}(\mathbf{p}_1,\mathbf{p}_2)\\&=\int_{-\infty}^{\infty}\exp\left\{-\frac{|\mathbf{r}_1|^2+|\mathbf{r}_2|^2}{r_s^{\,2}}\right\}G^*(\mathbf{r_1},\mathbf{p_1})G(\mathbf{r_2},\mathbf{p_2})d\mathbf{r}_1d\mathbf{r}_2\\&=\frac{1}{|A|^2}\exp\left\{\frac{jk\left[AC^*|\mathbf{p_1}|^2-A^*C|\mathbf{p}_2|^2\right]}{2|A|^2}\right\}.\end{aligned} \tag{6.17}$$

At the same time, W_b^{ABCD} is the integral function

$$\begin{aligned}&W_d^{ABCD}(\mathbf{p}_1,\mathbf{p}_2)\\&=\int_{-\infty}^{\infty}\exp\left\{-\frac{|\mathbf{r}_1|^2+|\mathbf{r}_2|^2}{r_s^{\,2}}\right\}\wedge\left(\frac{\Delta r_x}{l}\right)\wedge\left(\frac{\Delta r_y}{l}\right)G^*(\mathbf{p_1},\mathbf{r_1})G(\mathbf{p}_2,\mathbf{r}_2)d\mathbf{r}_1d\mathbf{r}_2.\end{aligned} \tag{6.18}$$

Unfortunately, there is no analytical result for the integral of W_d^{ABCD}, thought it could be numerically calculated. However, a Dirac delta approximation of the triangular function $\wedge(\Delta r_x/l)\wedge(\Delta r_y/l)\approx l^2\delta(\Delta\mathbf{r})$ is valid to provide an acceptable accuracy, while the cell size is significantly smaller than the beam size r_s. Note that in general,

the width of the triangular function will be much smaller than the other terms of the integrand. While it drops significantly, the variation of the other parts still varies gently enough and thus could be considered as a constant within the region of the triangular function. And under that condition, we have:

$$W_d^{ABCD}(\mathbf{p}_1,\mathbf{p}_2) \approx \frac{kl^2}{4\pi \operatorname{Im}[A^*B]} \exp\left\{\frac{jk}{2|B|^2}\left[D^*B|\mathbf{p}_1|^2 - DB^*|\mathbf{p}_2|^2 + j\frac{\left(B\mathbf{p}_1 - B^*\mathbf{p}_2\right)^2}{2\operatorname{Im}[A^*B]}\right]\right\}. \tag{6.19}$$

The illuminating beam size r_s and possible radius of curvature are omitted on purpose in integral and is properly compensated by a Gaussian lens while calculating the ABCD matrix. And thus, on the basis of the above beam coherence-polarization matrix, for the resultant field propagated to any plane $z>0$, two parameters of primary interest, i.e., the degree of coherence η^o and degree of polarization P^o defined in Eq. (1.4) and (1.5) could be extracted from matrix elements of Eq. (6.16):

$$P^o(\mathbf{p}) = \left|\frac{W_b^{ABCD}(\mathbf{p},\mathbf{p})}{W_b^{ABCD}(\mathbf{p},\mathbf{p}) + W_d^{ABCD}(\mathbf{p},\mathbf{p})}\right|, \tag{6.20}$$

and,

$$\eta^o(\mathbf{p}_1,\mathbf{p}_2) = \frac{W_b^{ABCD}(\mathbf{p}_1,\mathbf{p}_2) + W_d^{ABCD}(\mathbf{p}_1,\mathbf{p}_2)}{\sqrt{\left[W_b^{ABCD}(\mathbf{p}_1,\mathbf{p}_1) + W_d^{ABCD}(\mathbf{p}_1,\mathbf{p}_1)\right]\left[W_b^{ABCD}(\mathbf{p}_2,\mathbf{p}_2) + W_d^{ABCD}(\mathbf{p}_2,\mathbf{p}_2)\right]}}. \tag{6.21}$$

Above derivation provides the general results for the propagated beam coherence-polarization matrix for the field on an observation plane with a distance away in an arbitrary complex ABCD optical system, under the condition of a Gaussian illuminating source modulated by the random polarizer array with the cells' polarization angle uniformly distributed within $[0,\pi)$. The corresponding degree of

coherence and degree of polarization now are also provided. The very interesting thing is that they are found to be invariant with the linearly polarization angle of the incident Gaussian source!

From these conclusions, the evolution of the polarization and coherence states in propagation could be examined. To provide the same practical insight, we take the typical free space propagation over distance z with a receding aperture r_s to model the illuminating source, and the corresponding ABCD matrix is

$$\mathbf{M} = \begin{pmatrix} 1 - jz / z_R & z \\ -j / z_R & 1 \end{pmatrix}. \tag{6.22}$$

To present some numerical example, we have taken the following parameters: $r_s = 1mm$, $l = 0.1mm$, $\theta = \pi / 4$ and $\lambda = 0.633\mu m$.

Figure 6.3 shows the degree of polarization $P^o(p_x, 0)$ of the polarization speckle located on p_x axis, i.e., the points $\mathbf{p}\{p_x, 0\}$, for free-space propagation. It is plotted against the normalized propagation distance z/z_R and normalized lateral distance measured in spot size $\mathbf{p}/r_s$. As expected, the degree of polarization changes with the increasing propagation distance z. Instead of a uniform distribution for the modulated electric fields just behind the depolarizer, the degree of polarization for the developed polarization speckle after propagation does not remain uniform.

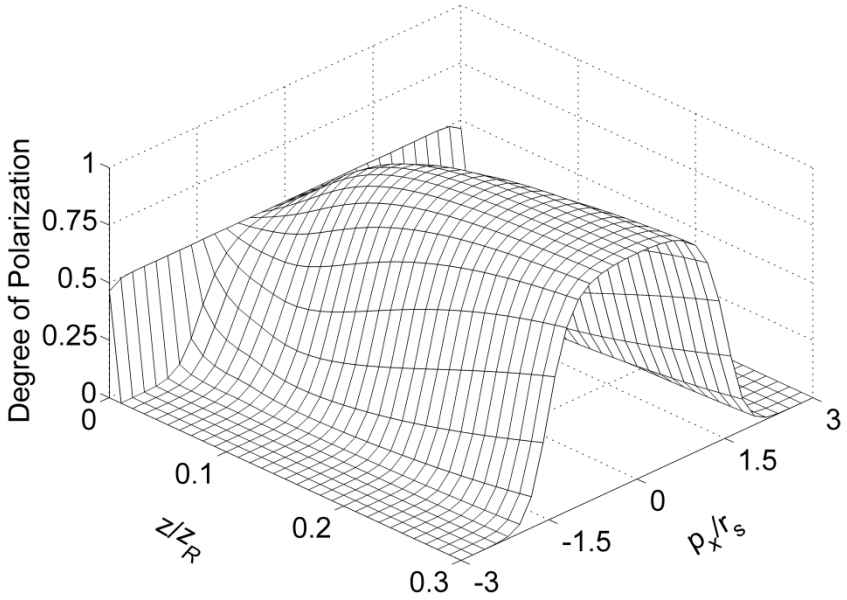

Figure 6.3. Degree of polarization (0-180 deg model)

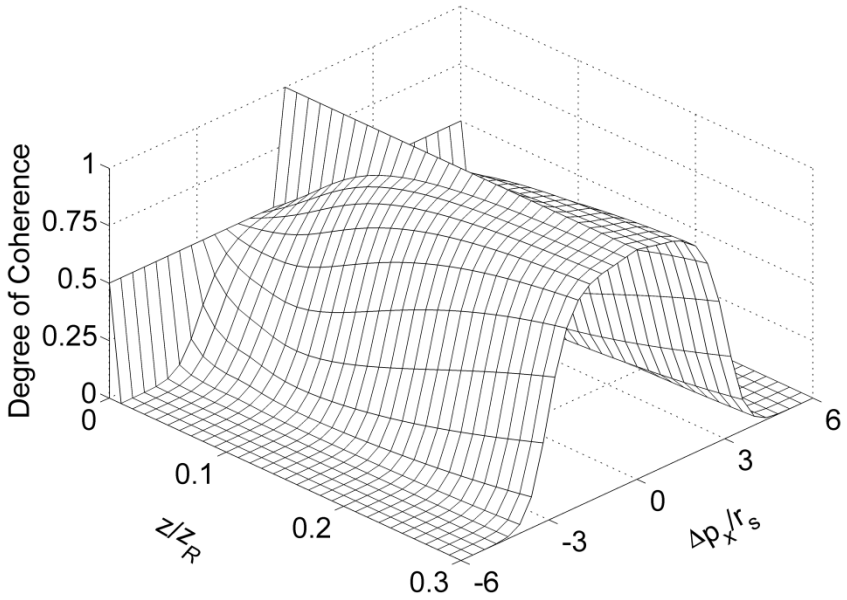

Figure 6.4. Degree of coherence (0-180 deg model)

Figure 6.4 gives the absolute values of the degree of coherence $\eta^o(p_x,0;-p_x,0)$ of the polarization speckle generated by the random polarizer array with the cells' polarization angle φ uniformly distributed between $0\sim 2\pi$. It is plotted against the normalized distance $\Delta\mathbf{p}/r_s$ for two positions $\mathbf{p}_1\{p_x,0\}$ and $\mathbf{p}_2\{-p_x,0\}$ located symmetrically and the normalized propagation distance z/z_R. It can readily be seen that the degree of coherence takes a large value close to unity for two points located near the optical axis. These figures indicate how the degree of coherence evolves for the selected polarization angle of the incident beam.

It has to be specifically pointed out that the depolarization and decorrelation performance of this kind of random polarizer array with the cells' polarization angle γ uniformly distributed between $0\sim 2\pi$ is totally independent to the incident beam's polarization angle. And this will make it harder for us to adjust the depolarization modulation depth.

6.4 Improvement of the random polarizer array by the statistics of the cells' polarization distribution

On the basis of the conclusion in the last section, some shortcomings of the random polarizer array (0-180 deg model) with uniformly distributed γ within $0\sim 2\pi$ are discovered. Firstly, its limited depolarization performance is indicated. The degree of polarization of the modulated field is 0.5, and for the resultant field around the optic-axis after propagation the degree of polarization will increase and approach unity. It seems impossible to generate a deeper depolarized field. The other disadvantage is the difficulty to manufacture cells with such uniformly distributed γ, which will be discussed later for the fabrication of the random polarizer array. To overcome these difficulties and facilitate the industrial and experimental application of this kind of device, an improved model for this kind of random polarizer array is proposed as shown in Figure 6.5.

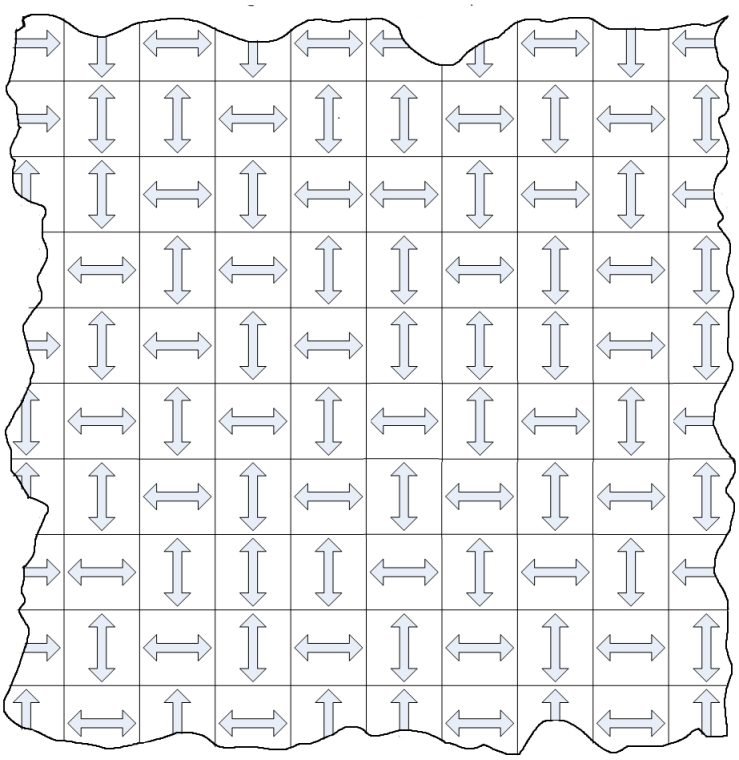

Figure 6.5 Diagram of depolarizer (0&90 deg): random polarizer array

Following similar analysis steps in the last section, we will assess the random modulation performance of the random polarizer array (0&90 deg model) by investigating the statistical properties of the modulated field and the propagated field in the ABCD system. We firstly employ the particular statistical distribution of the polarization angle γ which is confined to 0 and $\pi/2$ with the probability distribution function (PDF)

$$\begin{aligned} &p_{\varphi}(\varphi(\mathbf{r})=0)=1/2; \\ &p_{\varphi}\left(\varphi(\mathbf{r})=\pi/2\right)=1/2. \end{aligned} \tag{6.23}$$

Accordingly, first-order and second-order moments of corresponding Jones Matrix elements could be evaluated and are shown in Table 2.

Table 2 First-order and Second-order Moments of the Elements in Jones Matrix for (0&90 deg) model

$$\langle T_{xx}\rangle = \langle \cos^2\varphi(\mathbf{r})\rangle = 1/2 \qquad \langle T_{yy}\rangle = \langle \sin^2\varphi(\mathbf{r})\rangle = 1/2$$

$$\langle T_{xy}\rangle = \langle \cos\varphi(\mathbf{r})\sin\varphi(\mathbf{r})\rangle = 0 \qquad \langle T_{yx}\rangle = \langle \cos\varphi(\mathbf{r})\sin\varphi(\mathbf{r})\rangle = 0$$

$$\langle T_{xx}^2\rangle = \langle \cos^4\varphi(\mathbf{r})\rangle = 1/2 \qquad \langle T_{yy}^2\rangle = \langle \sin^4\varphi(\mathbf{r})\rangle = 1/2$$

$$\langle T_{xy}^2\rangle = \langle T_{yx}^2\rangle = \langle \sin^2\varphi(\mathbf{r})\cos^2\varphi(\mathbf{r})\rangle = 0$$

$$\langle T_{xx}T_{xy}\rangle = \langle T_{xx}T_{yx}\rangle = \langle \sin\varphi(\mathbf{r})\cos^3\varphi(\mathbf{r})\rangle = 0$$

$$\langle T_{xy}T_{yy}\rangle = \langle T_{yx}T_{yy}\rangle = \langle \sin^3\varphi(\mathbf{r})\cos\varphi(\mathbf{r})\rangle = 0$$

$$\langle T_{xx}T_{yy}\rangle = \langle \sin^2\varphi(\mathbf{r})\cos^2\varphi(\mathbf{r})\rangle = 0$$

We now will not repeat the analysis in the last section again, but directly cite the related conclusions. To illustrate the beam coherence-polarization matrix $\mathbf{W}^t$ of modulated field after this depolariser, we reuse classical Gaussian beam with the linearly polarized angle θ with respect to x axis, and get

$$\mathbf{W}^t(\mathbf{r}_1,\mathbf{r}_2) = \frac{I_o}{4}\exp\left\{-\frac{|\mathbf{r}_1|^2+|\mathbf{r}_2|^2}{r_s^{\,2}}\right\} \times\left\{\begin{pmatrix}\cos^2\theta & \sin\theta\cos\theta\\ \sin\theta\cos\theta & \sin^2\theta\end{pmatrix}+\wedge\left(\frac{\Delta r_x}{l}\right)\wedge\left(\frac{\Delta r_y}{l}\right)\begin{pmatrix}\cos^2\theta & -\sin\theta\cos\theta\\ -\sin\theta\cos\theta & \sin^2\theta\end{pmatrix}\right\} \tag{6.24}$$

and the corresponding degree of polarization is:

$$P^t(\mathbf{r}) = |\cos 2\theta|, \tag{6.25}$$

which is now polarization-dependent. It is easy to generate a random depolarized field with prescribed degree of polarization from zero to unity by rotating the plate. Its degree of coherence is exactly the same as the degree of coherence of the random polarizer array (0-180 deg model) shown in Eq. (6.14),

$$\eta^t(\mathbf{r}_1,\mathbf{r}_2)=\frac{1+\wedge\left(\frac{\Delta r_x}{l}\right)\wedge\left(\frac{\Delta r_y}{l}\right)}{2}, \tag{6.26}$$

By this, a random polarizer array with better polarization modulation performance is introduced. We next consider the propagation of the modulated electric field just behind the depolarizer in a complex ABCD system. To avoid the tedious mathematical description, we will not present the corresponding propagated beam coherence-polarization matrix, the degree of polarization or the degree of coherence, since they could be conducted through a straightforward discipline. However, we will take the typical free space propagation as an example to plot the degree of polarization and degree of coherence for systems with the same parameters defined in the last section to provide the same practical insight.

Figure 6.6 shows the degree of polarization of the polarization speckle for free-space propagation, plotted against the normalized propagation distance z/z_R and normalized lateral distance measured in spot size p/r_s. As expected, the degree of polarization changes appreciably depending both on the propagation distance z and on the polarization angle of the incident beam. Instead of a uniform distribution for the modulated electric fields just behind the depolarizer, the degree of polarization for the developed polarization speckle after propagation does not remain uniform.

Figure 6.7 gives the absolute values of the degree of coherence of the polarization speckle generated by the depolarizer at two positions $\Delta\mathbf{p}=\mathbf{p}_1-\mathbf{p}_2$ located symmetrically with respect to the z axis along the normalized propagation distance. It can readily be seen that the degree of coherence takes a large value close to unity for two points located near the optical axis. As discussed before, the degree of coherence will not change for different polarization angle of the incident beam. As an improvement, this model provide a better depolarization performance with a dependence on the polarization angle of the incident source, thus offering a regulation method to generate field with prescribed polarization state.

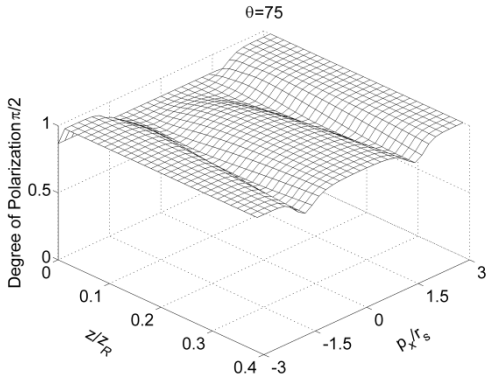

(a)

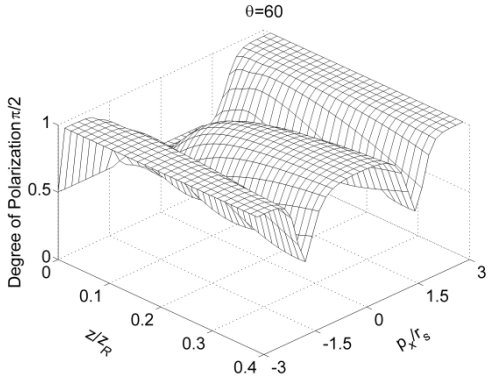

(b)

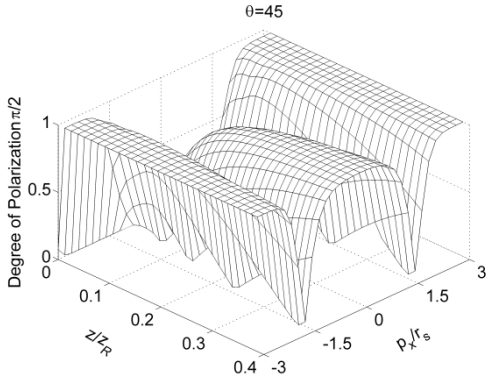

(c)

Figure 6.6. Degree of polarization (0&90 deg model)

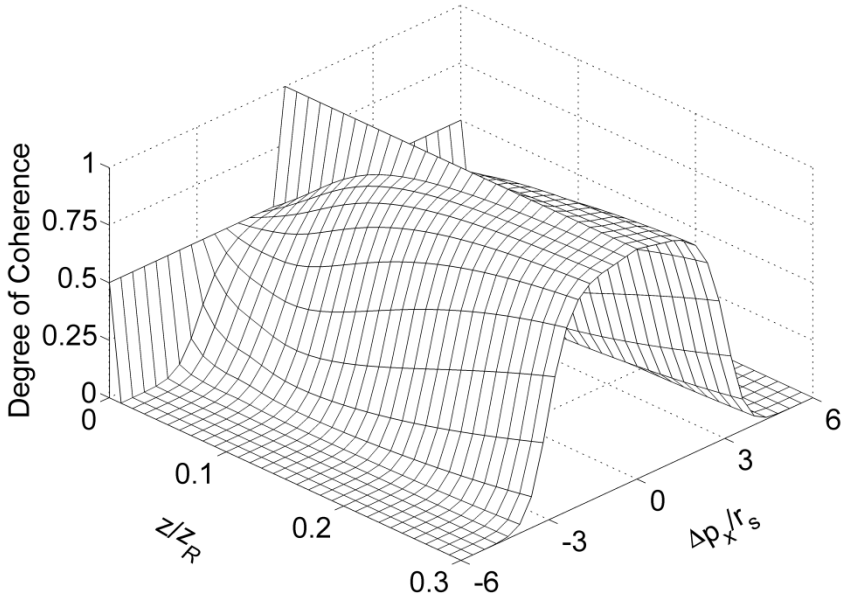

Figure 6.7. Degree of coherence (0&90 deg model)

6.5 Discussions on the cell size and diffraction effects in the random polarizer array depolarizer

The cell size of the random polarizer array is a very interesting structure parameter and deserves more discussion besides of that mentioned in the last section for its impact on the accuracy of the propagation integral calculation due to the Dirac approximation. For definiteness and without loss of generality, the discussion will be confined to the free space system, but similar arguments could apply to other systems with slight modifications.

Here, the diffraction effects in the random polarizer array will be discussed together with its relationship with the cell size. For both the x and y wave components of the incident beam, the random polarizer array imposes amplitude modulations determined by the orientation angles γ_i , $(i = 1, 2, 3....n)$ of each polarizer cell as $\cos^2 \gamma_i(\mathbf{r})$ and $\sin^2 \gamma_i(\mathbf{r})$ respectively (Figure 6.8).

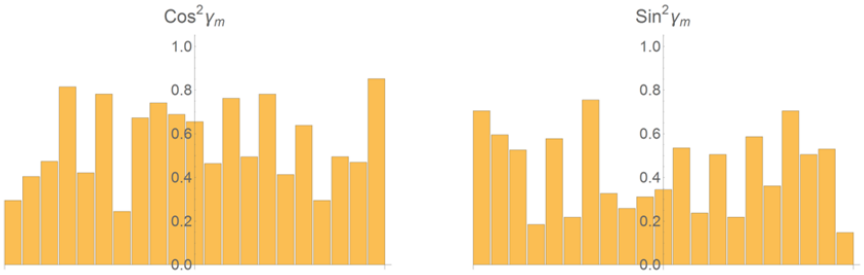

Figure 6.8. Random modulations in a series of cells (one bar for one cell)

Since the cell size l is smaller than the beam size r_s, the amplitude of the source in each cell is approximately considered as invariable (Figure 6.9). Thus, corresponding x and y wave components of the modulated field are discretely approximated as shown in Figure 6.10.

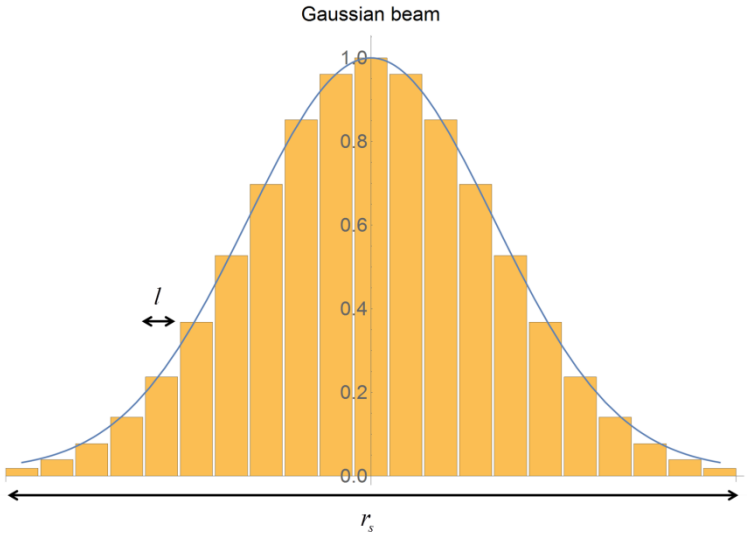

Figure 6.9. Gaussian source and its discrete approximation in cells

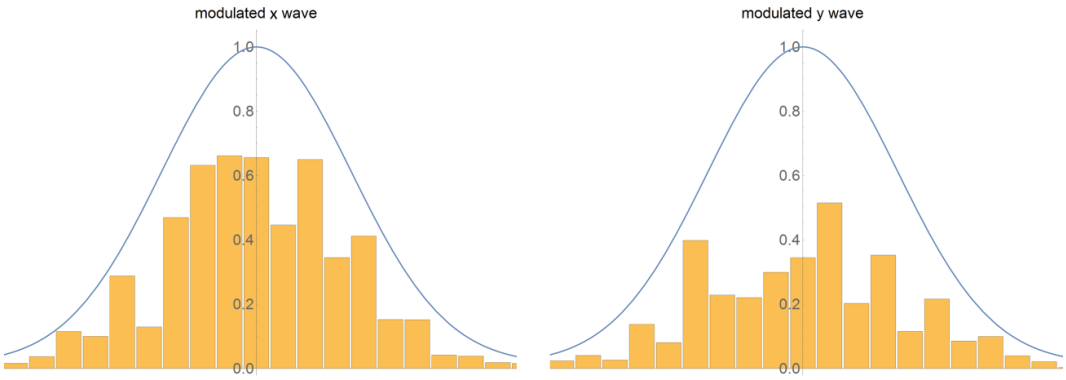

Figure 6.10. Modulated wave components

For the square truncated wave component in any cell with size l, the beam shape will change and then extend after propagation in a distance away. It is well known that, the beam shape is approximately a Sinc function with the width $\lambda z / l$ in the far field. The field from each cell will end up on the observation plane in a region centred at the geometrical projection of its original location (Figure 6.11). For the model that we are interested in, the field at a point on the observation screen is expected to be superimposition of propagated fields from the amount of different cells. Thus the amplitude of resultant field obeys the Gaussian distribution, and the high-order correlations could be expressed with the second-order correlation by Reeds theorem [158]. We assess it by the ratio between the Sinc width and the cell size, i.e., $\lambda z / l^2$, and will choose a cell size small enough or a propagation distance far enough in experiments.

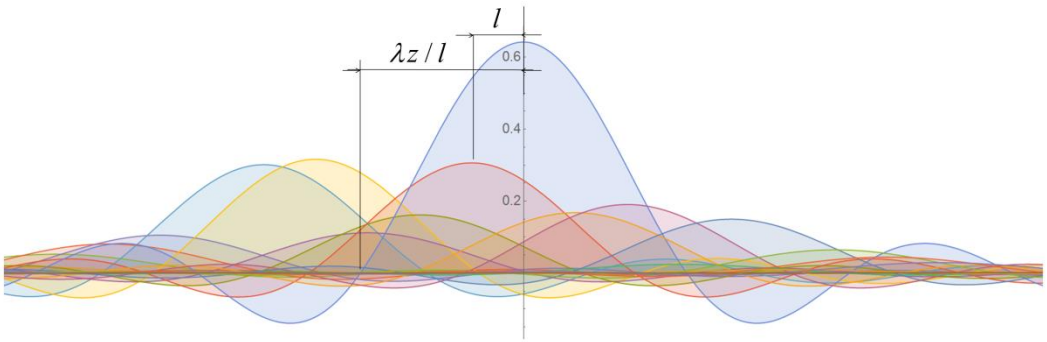

Figure 6.11. Superposition of modulated fields on observation plane

Notice that there is no specific restriction on the distribution of the polarization angle γ. Above discussion and conclusion are applicable for any random polarizer array with arbitrary statistics of φ.

6.6 Conclusion and discussion

We have examined the degree of coherence and degree of polarization of the polarization speckle generated by the depolarizer of random polarizer array plate. An analytic model for the modulation behaviour of the random polarizer array acting as a depolarizer was proposed and the dependence on the array structure has been established. Within the framework of complex ABCD method, we have also studied the changes in the degree of polarization and the degree of coherence for the generated polarization speckle on propagation, especially in free space system. In particular, we have shown their spatial non-uniformly distribution on beam cross section for the field after propagation and the variation with the propagation distance. This work provides a more comprehensive understanding of the modulation performance of the random polarizer array under the illustration of the evolution of modulated fields' coherence and polarization properties, and will help people choose proper system and structure parameters in application.

To facilitate the application of the random polarizer array, we review the relevant fabrication method here. This depolarizer device is not easy to fabricate due to the small cell size and the fine structure. For lab work, the straightforward method would be cutting and assembling the small polarizer cells manually. It might be feasible, but not proper for commercial and industrial applications because of the high cost and poor efficiency.

In industrial applications, polarizer arrays can be constructed using following effects: the high spatial frequency metal wires, high-resolution structures on dielectric surface, and dichromic molecular absorption in stretched polymer matrices [159-161]. Polarization filter arrays for the visible wavelength range were made by multilayer polyvinyl alcohol films with the resolution around 25 μm [159]. Some other thin-film

micropolarizer could provide smaller resolution at about 5 μm [162]. By reactive ion etching method, dual-tier thin film micropolarizer array is patterned [163]. However, most of the thin-film devices are not proper to work in the high temperature environment, and they consist of cells limited polarization states [159]. Thus, it is only proper to fabricate our second model. Metal wire grid cell might be another potential candidate for making a practical depolarizer based on our random polarizer array model [164, 165]. It consists of fine grid of parallel metal wires in cells. The interval space between wires is smaller than the wavelength. By nanofabrication, the period aluminium wire grids could be fabricated to create polarizer for UV to Infrared. The line and interval space could be small as around 100 nm [164, 166], and larger scale for infrared wavelength was also manufactured [165]. We cannot cover all the fabrication methods properly for creating a polarizer array here, and the researchers should choose the one most proper for their technical requirement and the working environment of this array. At least, considering these works about micro polarizer manufacture, it is proved that our model is possible to be realized.

Chapter 7

Conclusion and Perspectives

7.1 Conclusions and summary

In this thesis, the presented work was concerned with the statistical characteristics of random electromagnetic field generated by depolarizers, i.e., the rough-surfaced retardation plate and the random polarizer array. This work was achieved in a vector form invoking the 2×2 beam coherence-polarization matrix in space-temporal domain. The coherence and polarization properties of the modulated field are assessed by its degree of polarization and degree of coherence. By this, the depolarization and decorrelation modulation ability of the depolarizer was confirmed, and its relationship with the surface roughness/structure model was illustrated. Within the framework of the complex ABCD theory under the paraxial approximation, the propagation of the polarization speckle arising from this random modulated field was examined, and analytical results of the beam coherence-polarization matrix of the polarization speckle were also presented to reveal the evolution of the random polarization speckle's polarization and coherence properties on propagation. The dynamic analysis about this random modulated field generated from a moving rough-surfaced retardation plate is realized on the basis of the time-lagged beam coherence-polarization matrix. The shape characters and motion features of this dynamic polarization speckle are interpreted. These works provide analytical closed-form conclusions for the statistics of the resultant polarization speckle, which are very important and will facilitate both our understanding of the depolarizer itself and the resultant polarization speckle features. By this, both physical and mathematical

insights into a wide class of phenomena are provided within the unified theory of coherence and polarization.

The rough-surfaced retardation plate was proved to be able to realize simultaneous depolarization and decorrelation effects in our research. It is a compact single device modulation method compared with some other bulky modulation systems based on the Mach-Zehnder interferometer. It is novel to achieve whole field modulation, i.e., simultaneously but variously scrambling all four elements of beam coherence-polarization matrix. It is also economical and easy to access.

This analysis on the rough-surfaced retardation plate and the generated speckle brought conclusions in accordance with some researchers' theoretical or experimental works, thus could be treated as a demonstration or practical evidence by simple device and system. For example, the nonuniformly spatial distribution and variation in propagation of the degree of coherence and polarization once proposed by E Wolf was observed in this work. Chapter 4 provided a general demonstration of the vectorial Van Cittert-Zernike theorem.

This work also elicits some interesting considerations and discussions in related research fields. We discussed the necessity of the modification in the polarization matrix for demonstrating the vectorial Van Cittert-Zernike theorem by incoherent polarization speckle generated from the rough-surfaced retardation plate, which might have been treated inappropriately in some previous researches. Yet, as we know, the disparities of speckle shape features, correlation characters, and motion features for speckle generated from different wave elements of the polarization speckle were theoretically examined and revealed for the first time. They are expected to facilitate understanding of the relevant phenomena.

This work provided an elaborate and analytical description of the relationship between the polarization and coherence states of modulated random field and propagated speckle with the motion features, plate model, propagation system and the illuminating source. It is believed to be vital for making use of the depolarizer to

generate random electromagnetic field with prescribed statistical properties. It is also pivotal in the related speckle metrology.

7.2 Proposal of applications and further work

As we have stated before, in some optical researches and applications, systems might be polarization sensitive. Therefore, serious deviation in the system's output might be caused by this polarization sensitivity. The two kinds of depolarizers we introduced could be applied to scramble the polarization state of the incident field. Compared with some commercially available depolarizers with regular structures and thus providing pseudo-random polarization states, the depolarizer models introduced in this thesis have the ability to provide real random depolarized and decorrelated fields. The device related to the rough-surfaced retardation plate was proposed in the 1960s [125, 126], while several depolarizer models similar to the random polarizer array [155-157] were introduced from the 1980s. Both of these devices are applicable to the vast of commercial and industrial applications in optics, and it would be obviously beyond the ability of us to cover these broad subjects. However, in many of the applications, the detailed analysis and analytical conclusions established in this thesis might not be necessary. Since our work was mainly focusing on the comprehensively physical understanding of the depolarizer, and the theoretical interpretation within the statistical optics, a brief discussion about the relevant applications will be presented here. Firstly, these analytical results will promote the design and optimization of the related modulation method. Secondary source providing prescribed field with specific polarization and coherence state is very important in the research of statistical optics. The rough-surfaced retardation plate and random polarizer array are expected to create a secondary electromagnetic source with the desired coherence and polarization statistical properties for both theoretical and industrial research, and gain broader acceptance in this field. The rough-surfaced retardation plate could also be used in lab simulation work. Its generated fields are usually in anisotropic Gaussian correlation form. As we know, some phenomena will also cause similar random field, for example the turbulent atmosphere [22, 78, 99, 167]. The rough-surfaced retardation plate is able to generate an easily accessible random field with similar statistical characteristics for simulation. In some other field, these conclusions

presented in the thesis also have a great potential application prospect like the non-contact metrology, and the polarization-sensitive image.

Future works in some respects could be conducted to enhance the understanding of the depolarizer devices and related phenomena and to facilitate applications. The theoretical analysis in this thesis is almost totally focusing on the phenomena in spatial-temporal domain. While the ‘laser source’ is mentioned in discussion, it is implicitly assumed as a monochromatic source. However, the rough-surfaced retardation plate has no frequency restriction for applications. The incident field with a frequency band could introduce more interesting phenomena. Therefore, we think the device might be able to be applied in thermal light depolarization and decorrelation and spectrum modulation. The theoretical analysis could be conducted within the framework of spatial-spectral correlation analysis. Our discussions on the plate modulation and the speckle propagation in ABCD system are independent to each other. That means the results about the modulated field are applicable for further studies of more general propagation system beyond the paraxial restriction of ABCD theory. We could also extend current conclusions to various beam source shapes and surface models by similar way.

In recent years, more and more attention was paid to the analysis of the spatial polarization state distributions. To research and observe the phenomena, the pure polarization speckles are expected. The rough-surfaced retardation plate will be index matched to generate pure polarization speckles with minimum intensity fluctuations (or weakly developed intensity speckles). The statistical analysis for the generated field under this condition will be analysed to direct further experimental research.

For the disparities of shape features of the polarization speckle once discussed in Chapter 5, the analysis needs to be improved. The vectorial counterparts of many classical scalar concepts and definitions are required to describe related phenomena properly. This is not a straightforward work but needs much more care and delicate consideration. For example, the correlation area for scalar area now is different in each of the four coherence matrix elements, and there is still not vectorial counterpart

properly defined to describe the corresponding properties for the whole polarization speckle.

References

[1] J. C. Dainty, A. E. Ennos, M. Franqo, J. W. Goodman, T. S. McKechnie, and G. Parry, *Laser Speckle and related phenomena*, 1st ed. Berlin and New York: Springer-Verlag, 1975.

[2] J. W. Goodman, *Speckle Phenomena in Optics: Theory and Applications*. Roberts & Company, 2007.

[3] P. K. Rastogi, "Principles of Holographic Interferometry and Speckle Metrology," *Photomech. (Topics Appl. Physics)*, pp. 103–150, 1999.

[4] B. Ruffing, "Application of speckle-correlation methods to surface-roughness measurement: a theoretical study," *J. Opt. Soc. Am. A*, vol. 3, no. 8, 1986.

[5] R. S. Sirohi, *Speckle Metrology Optical Engineering*. Marcel Dekker, Inc, 1993.

[6] T. Asakura and N. Takai, "Dynamic laser speckles and their application to velocity measurements of the diffuse object," *Appl. Phys.*, vol. 25, no. 3, pp. 179–194, Jul. 1981.

[7] R. Martínez-Herrero, P. M. Mejías, and G. Piquero, *Characterization of Partially Polarized Light Fields*. Dordrecht Heidelberg London New York: Springer, 2009.

[8] D. F. V. James, "Change of polarization of light beams on propagation in free space," *J. Opt. Soc. Am. A*, vol. 11, no. 5, pp. 1641–1643, May 1994.

[9] G. P. Agrawal and E. Wolf, "Propagation-induced polarization changes in partially coherent optical beams," *J. Opt. Soc. Am. A*, vol. 17, no. 11, p. 2019, 2000.

[10] F. Gori, M. Santarsiero, G. Piquero, R. Borghi, A. Mondello, and R. Simon, "Partially polarized Gaussian Schell-model beams," *J. Opt. A Pure Appl. Opt.*, vol. 3, no. 1, pp. 1–9, Jan. 2001.

[11] E. Wolf, "Correlation-induced changes in the degree of polarization, the degree of coherence, and the spectrum of random electromagnetic beams on propagation.," *Opt. Lett.*, vol. 28, no. 13, pp. 1078–80, Jul. 2003.

[12] H. Roychowdhury and E. Wolf, "Determination of the electric cross-spectral density matrix of a random electromagnetic beam," *Opt. Commun.*, vol. 226, no. 1–6, pp. 57–60, Oct. 2003.

[13] T. Shirai and E. Wolf, “Coherence and polarization of electromagnetic beams modulated by random phase screens and their changes on propagation in free space,” *J. Opt. Soc. Am. A*, vol. 21, no. 10, pp. 1907–1916, 2004.

[14] S. G. Hanson, W. Wang, M. L. Jakobsen, and M. Takeda, “Coherence and polarization of electromagnetic beams modulated by random phase screens and their changes through complex ABCD optical systems,” *J. Opt. Soc. Am. A*, vol. 25, no. 9, pp. 2338–2346, 2008.

[15] M. Takeda, W. Wang, and S. G. Hanson, “Polarization speckles and generalized Stokes vector wave: a review,” in *Proceedings of SPIE*, 2010, vol. 7387, pp. 73870V–1–73870V–7.

[16] W. Wang, S. G. Hanson, and M. Takeda, “Statistics of polarization speckle: theory versus experiment,” in *Ninth International Conference on Correlation Optics, proceedings of SPIE*, 2009, vol. 7388, no. 0, pp. 738803–738803–9.

[17] O. V. Angelsky, P. V Polyanskii, and I. I. Mokhun, “Optical Measurements : Polarization and Coherence of Light Fields,” in *Modern Metrology Concerns*, 2012, pp. 263–317.

[18] R. K. Singh, D. N. Naik, H. Itou, Y. Miyamoto, and M. Takeda, “Characterization of spatial polarization fluctuations in scattered field,” *J. Opt.*, vol. 16, no. 10, p. 105010, Oct. 2014.

[19] O. Korotkova, M. Salem, and E. Wolf, “The far-zone behavior of the degree of polarization of electromagnetic beams propagating through atmospheric turbulence,” *Opt. Commun.*, vol. 233, no. 4–6, pp. 225–230, 2004.

[20] H. Roychowdhury, S. a. Ponomarenko, and E. Wolf, “Change in the polarization of partially coherent electromagnetic beams propagating through the turbulent atmosphere,” *J. Mod. Opt.*, vol. 52, no. 11, pp. 1611–1618, 2005.

[21] M. Yao, Y. Cai, H. T. Eyyuboğlu, Y. Baykal, and O. Korotkova, “Evolution of the degree of polarization of an electromagnetic Gaussian Schell-model beam in a Gaussian cavity,” *Opt. Lett.*, vol. 33, no. 19, pp. 2266–2268, 2008.

[22] L. Pan, M. Sun, C. Ding, Z. Zhao, and B. Lü, “Effects of astigmatism on spectra, coherence and polarization of stochastic electromagnetic beams passing through an astigmatic optical system,” *Opt. Express*, vol. 17, no. 9, pp. 7310–7321, 2009.

[23] O. Korotkova and E. Wolf, “Changes in the state of polarization of a random electromagnetic beam on propagation,” *Opt. Commun.*, vol. 246, no. 1–3, pp. 35–43, Feb. 2005.

[24] P. Hariharan, “Speckle Patterns: A Historical Retrospect,” *Opt. Acta Int. J. Opt.*, vol. 19, no. February 2015, pp. 791–793, 1972.

[25] M. Born and E. Wolf, *Principles of optics: Electromagnetic Theory of Propagation INterference and Diffraction of Light*, 7th ed. 1999.

[26] G. W. Stroke and D. Gabor, *An introduction to coherent optics and holography*. Academic Press, 1969.

[27] M. Takeda, “Spatial stationarity of statistical optical fields for coherence holography and photon correlation holography,” *Opt. Lett.*, vol. 38, no. 17, pp. 143–148, 2014.

[28] M. J. Beran and G. B. Parrent, *Theory of partial coherence*. Prentice-Hall, 1964.

[29] J. W. Goodman, *statistical optics*. New York: Wiley-Interscience, 2000.

[30] K. Blomstedt, “Electromagnetic Coherence Theory , Universality Results , and Effective Degree of Coherence,” Aalto University, 2013.

[31] L. Mandel and E. Wolf, *Optical Coherence and Quantum Optics*. 1995.

[32] G. B. Parrent, “Basic theory of partial coherence,” *Spring Jt. Comput. Conf. XX - AFIPS ’66*, no. 5, p. 17, 1966.

[33] D. Middleton, *An introduction to statistical communication theory*, vol. 960. McGraw-Hill New York, 1960.

[34] E. Wolf, *Introduction to the Theory of Coherence and Polarization of Light*. CAMBRIDGE UNIVERSITY, 2007.

[35] L. Wasserman, *All of Statistics: A Concise Course in Statistical Inference*. Springer Science & Business Media, 2004.

[36] R. G. Gallager, *Stochastic Processes: Theory for Applications*. CAMBRIDGE UNIVERSITY, 2013.

[37] J. C. Dainty, “an introduction to ‘gaussian’ speckle,” in *Proc. Soc. Photo-Opt. Instrum. Eng*, 1980, pp. 2–8.

[38] E. Jakeman and P. N. Pusey, “The statistics of light scattered by a random phase screen,” *J. Phys. A Math. Nucl. Gen.*, p. L88, 1973.

[39] H. M. Pedersen, “The roughness dependence of partially developed, monochromatic speckle patterns,” *Opt. Commun.*, vol. 12, no. 2, pp. 156–159, 1974.

[40] J. W. Goodman, “Some effects of target-induced scintillation on optical radar performance,” vol. 53, 1965.

[41] R. Barakat, “First-order Probability Densities of Laser Speckle Patterns Observed through Finite-size Scanning Apertures,” *Opt. Acta (Lond).*, vol. 20, pp. 729–740, 1973.

[42] C. T. Stansberg, “On the First-order Probability Density Function of Integrated Laser Speckle,” *Optica Acta: International Journal of Optics*, vol. 28. pp. 917–932, 1981.

[43] J. C. Dainty, “The statistics of speckle patterns,” *Prog. Opt.*, pp. 1–44, 1976.

[44] M. ROUSSEAU, “Statistical Properties of Optical Fields Scattered by Random Media. Application to Rotating Ground Glass,” *J. Opt. Soc. Am.*, vol. 61, no. 10, pp. 1307–1316, Oct. 1971.

[45] E. Jakeman, “The effect of wavefront curvature on the coherence properties of

laser light scattered by target centres in uniform motion," *J. Phys. A. Math. Gen.*, vol. 23, 1975.

[46] P. N. Pusey, "Photon correlation study of laser speckle produced by a moving rough surface," *J. Phys. D. Appl. Phys.*, vol. 9, pp. 1139–1409, 1976.

[47] E. Jakeman and J. McWhirter, "Fluctuations in radiation scattered into the Fresnel region by a random-phase screen in uniform motion," *J. Phys. A. Math. Gen.*, vol. 785, 1976.

[48] I. Yamaguchi and S.-I. Komatsu, "Theory and Applications of Dynamic Laser Speckles Due to In-plane Object Motion," *Optica Acta: International Journal of Optics*, vol. 24. pp. 705–724, 1977.

[49] J. Ohtsubo, "The second-order statistics of speckle patterns," *J. Opt.*, vol. 12, pp. 129–142, 1981.

[50] T. Yoshimura and S. Iwamoto, "Dynamic properties of three-dimensional speckles," *J. Opt. Soc. Am. A*, vol. 10, no. 2, p. 324, Feb. 1993.

[51] R. S. Hansen, H. T. Yura, S. G. Hanson, and B. Rose, "Three-Dimensional Speckles : Static and Dynamic Properties," in *Proceedings of SPIE*, 1999, vol. 3904, pp. 140–149.

[52] H. T. Yura, S. G. Hanson, R. S. Hansen, and B. Rose, "Three-dimensional speckle dynamics in paraxial optical systems," *J. Opt. Soc. Am. A*, vol. 16, no. 6, p. 1402, 1999.

[53] R. K. Erf, *Speckle metrology*, vol. 1. Elsevier Science, 1978.

[54] H. T. Yura, S. G. Hanson, and L. Lading, "Laser Doppler velocimetry analytical solution to the optical system including the effects of partial coherence of the target," *J. Opt. Soc. Am. A*, vol. 12, no. 9, pp. 2040–2047, Sep. 1995.

[55] I. Yamaguchi and T. Fujita, "Laser speckle rotary encoder.," *Appl. Opt.*, vol. 28, no. 20, pp. 4401–6, Oct. 1989.

[56] H. T. Yura and S. G. Hanson, "Laser-time-of-flight velocimetry: analytical solution to the optical system based on ABCD matrices," *J. Opt. Soc. Am. A*, vol. 10, no. 9, pp. 1918–1924, 1993.

[57] X. Dai, O. Sasaki, J. E. Greivenkamp, and T. Suzuki, "Measurement of small rotation angles by using a parallel interference pattern.," *Appl. Opt.*, vol. 34, no. 28, pp. 6380–8, Oct. 1995.

[58] H. T. Yura, B. Rose, and S. G. Hanson, "Speckle dynamics from in-plane rotating diffuse objects in complex ABCD optical systems," *J. Opt. Soc. Am. A*, vol. 15, no. 5, p. 1167, 1998.

[59] M. L. Jakobsen, M. J. Bækbo, and S. G. Hanson, "Dual-Laser vibrometry: Elimination or extraction of pseudo vibration," *Proc. SPIE*, vol. 9141, p. 91411G, May 2014.

[60] A. S. Olesen, A. T. Pedersen, S. G. Hanson, and K. Rottwitt, "Analytic model utilizing the complex ABCD method for range dependency of a monostatic

coherent lidar," *Appl. Opt.*, vol. 53, no. 26, pp. 5977–84, Sep. 2014.

[61] I. Yamaguchi, "Speckle Displacement and Decorrelation in the Diffraction and Image Fields for Small Object Deformation," *Opt. Acta Int. J. Opt.*, vol. 28, no. 10, pp. 1359–1376, Oct. 1981.

[62] H. J. H. J. Tiziani, "A study of the use of laser speckle to measure small tilts of optically rough surfaces accurately," *Opt. Commun.*, vol. 5, no. 4, pp. 271–276, Jul. 1972.

[63] E. Archbold, J. M. Burch, and A. E. Ennos, "Recording of In-plane Surface Displacement by Double-exposure Speckle Photography," *Opt. Acta Int. J. Opt.*, vol. 17, no. 12, pp. 883–898, Dec. 1970.

[64] J. W. Goodman, "Statistical properties of laser speckle patterns," in *Laser Speckle and Related Phenomena*, vol. 6, Springer-Verlag Berlin Heidelberg, 1975, pp. 9–75.

[65] J. W. Goodman, "Some fundamental properties of speckle," *J. Opt. Soc. Am.*, vol. 94305, no. May, pp. 1145–1150, 1976.

[66] J. C. Dainty, "Some statistical properties of random speckle patterns in coherent and partially coherent illumination," *Opt. Acta (Lond).*, vol. 17, no. 10, pp. 37–41, 1970.

[67] H. Fujii and T. Asakura, "Effect of surface roughness on the statistical distribution of image speckle intensity," *Opt. Commun.*, vol. 11, no. 1, pp. 35–38, May 1974.

[68] H. Fujii and T. Asakura, "A contrast variation of image speckle intensity under illumination of partially coherent light," *Opt. Commun.*, vol. 12, no. 1, pp. 32–38, Sep. 1974.

[69] H. Fujii and T. Asakura, "Statistical properties of image speckle patterns in partially coherent light," *Nouv. Rev. d'Optique*, vol. 6, no. 1, pp. 5–14, Jan. 2002.

[70] G. Parry, "Speckle patterns in partially coherent light," in *Laser Speckle and Related Phenomena*, vol. 9, Berlin, Heidelberg: Springer Berlin Heidelberg, 1975.

[71] M. Francon, *Laser Speckle and Applications in Optics*. Elsevier Science, 2012.

[72] T. Yoshimura, "Statistical properties of dynamic speckles," *J. Opt. Soc. Am. A*, vol. 3, no. 7, pp. 1032–1054, 1986.

[73] *Advances in Speckle Metrology and Related Techniques*. John Wiley & Sons, 2011.

[74] A. Yariv and P. Yeh, *Optical waves in crystals: propagation and control of laser radiation*, vol. 12. 1984.

[75] I. Vidal, E. J. S. Fonseca, and J. M. Hickmann, "Light polarization control during free-space propagation using coherence," *Phys. Rev. A*, vol. 84, no. 3, p. 033836, Sep. 2011.

[76] F. Gori, M. Santarsiero, S. Vicalvi, R. Borghi, G. Guattari, and F. G. and M. S. and S. V. and R. B. and G. Guattari, "Beam coherence-polarization matrix," *Pure Appl. Opt. J. Eur. Opt. Soc. Part A*, vol. 7, p. 941, 1998.

[77] F. Gori, "Matrix treatment for partially polarized, partially coherent beams," *Opt. Lett.*, vol. 23, no. 4, pp. 241–243, 1998.

[78] O. Korotkova, *Random Light Beams: Theory and Applications*. CRC Press, 2013.

[79] F. Gori, M. Santarsiero, R. Borghi, and G. Piquero, "Use of the van Cittert-Zernike theorem for partially polarized sources," *Opt. Lett.*, vol. 25, no. 17, pp. 1291–3, Sep. 2000.

[80] O. Korotkova, T. D. Visser, and E. Wolf, "Polarization properties of stochastic electromagnetic beams," *Opt. Commun.*, vol. 281, no. 4, pp. 515–520, Feb. 2008.

[81] E. Wolf, "Unified theory of coherence and polarization of random electromagnetic beams," *Phys. Lett. A*, vol. 312, pp. 263–267, 2003.

[82] J. Tervo, T. Setälä, and A. T. Friberg, "Theory of partially coherent electromagnetic fields in the space-frequency domain," *J. Opt. Soc. Am. A*, vol. 21, no. 11, p. 2205, Nov. 2004.

[83] P. Réfrégier and F. Goudail, "Invariant degrees of coherence of partially polarized light," *Opt. Express*, vol. 13, no. 16, p. 6051, Aug. 2005.

[84] J. W. Goodman, *Introduction to Fourier Optics*, vol. 35. 1988.

[85] A. S. Ostrovsky, G. Martínez-Niconoff, P. Martínez-Vara, and M. Á. Olvera-Santamaría, "The van Cittert-Zernike theorem for electromagnetic fields," *Opt. Express*, vol. 17, no. 3, pp. 1746–1752, Jan. 2009.

[86] E. Vélez-Juárez, G. Martínez-Niconoff, J. Muñoz-López, and A. S. Ostrovsky, "Experimental determining the coherent-mode structure of vector electromagnetic field through its decomposition in reference basis," *Opt. Express*, vol. 22, no. 21, pp. 26232–26239, Oct. 2014.

[87] Y. Ohtsuka, "Is the Van Cittert-Zernike Theorem Applicable to Spatially Incoherent Broadband Spectral Source?," *Optical Review*, vol. 5, no. I. pp. 27–29, 1998.

[88] T. Shirai, "Some consequences of the van Cittert – Zernike electromagnetic fields," *Opt. Lett.*, vol. 34, no. 23, pp. 3761–3763, 2009.

[89] M. Lahiri, "Contributions to the Theories of Coherence and Polarization of Light," University of Rochester, 2012.

[90] V. N. Bringi and A. Hendry, "Technology of polarization diversity radars for meteorology," in *Radar in Meteorology*, vol. -1, 1990, pp. 153–190.

[91] D. N. Naik, R. K. Singh, H. Itou, M. M. Brundavanam, Y. Miyamoto, and M. Takeda, "Single-shot full-field interferometric polarimeter with an integrated calibration scheme.," *Opt. Lett.*, vol. 37, no. 15, pp. 3282–4, 2012.

[92] L. C. Andrews and R. L. Phillips, *Laser beam propagation through random media*. SPIE press, 2005.

[93] A. S. Ostrovsky, G. Rodríguez-Zurita, C. Meneses-Fabián, M. Á. Olvera-Santamaría, and C. Rickenstorff-Parrao, "Experimental generating the partially coherent and partially polarized electromagnetic source," *Opt. Express*, vol. 18, no. 12, pp. 12864–12871, 2010.

[94] A. S. Ostrovsky, M. Á. Olvera, C. Rickenstorff, G. Martínez-Niconoff, and V. Arrizón, "Generation of a secondary electromagnetic source with desired statistical properties," *Opt. Commun.*, vol. 283, no. 22, pp. 4490–4493, Nov. 2010.

[95] T. Shirai, O. Korotkova, and E. Wolf, "A method of generating electromagnetic Gaussian Schell-model beams," *J. Opt. A Pure Appl. Opt.*, vol. 7, no. 5, pp. 232–237, May 2005.

[96] F. De Zela, "Secondary source of quantum or classical partially polarized states," *J. Opt. Soc. Am. A*, vol. 30, no. 8, pp. 1544–1547, Aug. 2013.

[97] C. Zhao, Y. Dong, G. Wu, F. Wang, Y. Cai, and O. Korotkova, "Experimental demonstration of coupling of an electromagnetic Gaussian Schell-model beam into a single-mode optical fiber," *Appl. Phys. B*, vol. 108, no. 4, pp. 891–895, 2012.

[98] S. Avramov-Zamurovic, C. Nelson, R. Malek-Madani, and O. Korotkova, "Polarization-induced reduction in scintillation of optical beams propagating in simulated turbulent atmospheric channels," *Waves in Random and Complex Media*, vol. 24, no. 4, pp. 452–462, Oct. 2014.

[99] M. Salem, O. Korotkova, A. Dogariu, and E. Wolf, "Polarization changes in partially coherent electromagnetic beams propagating through turbulent atmosphere," *Waves in Random Media*, vol. 14, no. 4, pp. 513–523, Oct. 2004.

[100] A. S. Ostrovsky, M. Á. Olvera-Santamaría, and P. C. Romero-Soría, "Effect of coherence and polarization on resolution of optical imaging system," *Opt. Lett.*, vol. 36, no. 9, pp. 1677–1679, 2011.

[101] F. Scudieri, M. Bertolotti, and R. Bartolino, "Light scattered by a liquid crystal: a new quasi-thermal source," *Appl. Opt.*, vol. 13, pp. 181–185, 1974.

[102] C. Rickenstorff, E. Flores, M. Á. Olvera-Santamaría, and A. S. Ostrovsky, "Modulation of coherence and polarization using nematic 90◦-twist liquid-crystal spatial light modulators," *Rev. Mex. Fis*, vol. 58, pp. 270–273, 2012.

[103] R. K. Singh, D. N. Naik, H. Itou, M. M. Brundavanam, Y. Miyamoto, and M. Takeda, "Vectorial van Cittert-Zernike theorem based on spatial averaging: experimental demonstrations," *Opt. Lett.*, vol. 38, no. 22, pp. 4809–12, Nov. 2013.

[104] K. Oka and Y. Ohtsuka, "Polarimetry for spatiotemporal photoelastic analysis," *Exp. Mech.*, vol. 33, no. 1, pp. 44–48, Mar. 1993.

[105] Y. Ohtsuka and K. Oka, "Contour mapping of the spatiotemporal state of polarization of light.," *Appl. Opt.*, vol. 33, no. 13, pp. 2633–6, May 1994.

[106] F. Gori, “Why is the Fresnel transform so little known?,” in *Current Trends in Optics*, Academic, New York, 1994, pp. 139–148.

[107] O. K. Ersoy, *Diffraction, Fourier Optics and Imaging*. Wiley, 2006.

[108] H. T. Yura and S. G. Hanson, “Optical beam wave propagation through complex optical systems,” *J. Opt. Soc. Am. A*, vol. 4, no. 10, pp. 1931–1948, 1987.

[109] S. Hanson, M. Jakobsen, and H. Yura, “Complex-Valued ABCD Matrices and Speckle Metrology,” in *Linear Canonical Transforms*, J. J. Healy, M. Alper Kutay, H. M. Ozaktas, and J. T. Sheridan, Eds. Springer New York, 2016, pp. 397–428.

[110] A. E. Siegman, *Lasers*. University Science Books, 1986.

[111] E. O’Neill, *Introduction to statistical optics*. Reading Mass.: Addison-Wesley Pub. Co., 1963.

[112] A. Gerrard and J. M. Burch, *Introduction to matrix methods in optics*. London;;New York: Wiley, 1975.

[113] C. Palma and V. Bagini, “Extension of the Fresnel transform to ABCD systems,” *J. Opt. Soc. Am. A*, vol. 14, no. 8, p. 1774, 1997.

[114] S. a. COLLINS, JR., “Lens-System Diffraction Integral Written in Terms of Matrix Optics,” *J. Opt. Soc. Am.*, vol. 60, no. 9, p. 1168, Sep. 1970.

[115] J. J. Healy, M. A. Kutay, H. M. Ozaktas, and J. T. Sheridan, *Linear Canonical Transforms: Theory and Applications*. Springer New York, 2015.

[116] A. Stern, “Why is the linear canonical transform so little known?,” in *AIP Conference Proceedings Series*, 2006, vol. 860, pp. 225–234.

[117] J. Alda, “Laser and Gaussian Beam Propagation and Transformation,” *Opt. Eng.*, vol. 110, no. 10 Pt 1, pp. 999–1013, 2003.

[118] G. Kloos, *Matrix methods for optical layout*. Bellingham Wash.: SPIE Press, 2007.

[119] H. T. Yura, B. Rose, and S. G. Hanson, “Dynamic laser speckle in complex ABCD optical systems,” *J. Opt. Soc. Am. A*, vol. 15, no. 5, pp. 1160–1165, 1998.

[120] B. Rose, S. G. Hanson, and H. T. Yura, “Complex ABCD-matrices: a general tool for analyzing arbitrary optical systems,” in *Optical Sensors and Microsystems*, Springer, 2000, pp. 97–114.

[121] S. G. Hanson and H. T. Yura, “Complex ABCD matrices: an analytical tool for analyzing light propagation involving stochastic processes,” in *19th Congress of the International Commission for Optics: Optics for the Quality of Life*, 2003, vol. 4829, pp. 592–593.

[122] O. V. Angelsky, *Optical Correlation: Techniques and Applications*. SPIE Press, 2007.

[123] A. F. Fercher and P. F. Steeger, “First-order Statistics of Stokes Parameters in

Speckle Fields," *Opt. Acta Int. J. Opt.*, vol. 28, no. 4, pp. 443–448, Nov. 1981.

[124] W. A. Shurcliff, *Polarized Light*. Harvard University Press, 1962.

[125] C. J. Peters, "Light Depolarizer," *Appl. Opt.*, vol. 3, no. 12, p. 1502, Dec. 1964.

[126] C. J. Peters, "Light depolarizer," US3433553 A, 18-Mar-1969.

[127] N. J. Diorio, M. R. Fisch, and J. L. West, "Filled liquid crystal depolarizers," *J. Appl. Phys.*, vol. 90, no. 8, p. 3675, Oct. 2001.

[128] S. Maurice and G. S. M. Anthony, "Depolariser with random orientated regions of polarisation state modulating material," 06-Aug-2003.

[129] R. C. Jones, "A New Calculus for the Treatment of Optical Systems. I. description and discussion of the calculus," *J. Opt. Soc. Am.*, vol. 31, no. 7, pp. 488–93, Jul. 1941.

[130] R. Paschotta, "Polarization beat length," *http://www.rp-photonics.com /polarization_beat_length.html*. .

[131] P. Beckmann and A. Spizzichino, *The scattering of electromagnetic waves from rough surfaces*. Norwood, MA, Artech House, Inc., 1987.

[132] M. Takeda, W. Wang, D. N. Naik, and R. K. Singh, "Spatial statistical optics and spatial correlation holography: A review," *Opt. Rev.*, vol. 21, no. 6, pp. 849–861, Nov. 2014.

[133] E. Hecht, *Optics 4th edition*. 2001.

[134] F. Ticconi, L. Pulvirenti, and N. Pierdicca, "Models for scattering from rough surfaces," in *Electromagnetic Waves*, V. Zhurbenko, Ed. InTech, 2011.

[135] J. W. Goodman, P. K. Rastogi, and E. Hack, "Some Properties of Speckle from 'Smooth' Surfaces," vol. 3, pp. 3–11, 2010.

[136] J. W. Goodman, "Some properties of speckle from smooth objects," *Opt. Eng.*, vol. 49, no. 6, p. 068001, Jun. 2010.

[137] M. W. Hyde, S. Basu, M. F. Spencer, S. J. Cusumano, and S. T. Fiorino, "Physical optics solution for the scattering of a partially-coherent wave from a statistically rough material surface.," *Opt. Express*, vol. 21, no. 6, pp. 6807–25, Mar. 2013.

[138] B. Rose, H. Imam, S. G. Hanson, and H. T. Yura, "Effects of target structure on the performance of laser time-of-flight velocimeter systems," *Appl. Opt.*, vol. 36, no. 2, pp. 518–33, Jan. 1997.

[139] P. H. van Cittert, "Die Wahrscheinliche Schwingungsverteilung in Einer von Einer Lichtquelle Direkt Oder Mittels Einer Linse Beleuchteten Ebene," *Physica*, vol. 1. pp. 201–210, 1934.

[140] F. Zernike, "The concept of degree of coherence and its application to optical problems," *Physica*, vol. 5. pp. 785–795, 1938.

[141] C. Roychoudhuri and K. R. Lefebvre, "Van Cittert-Zernike theorem for introductory optics course using the concept of fringe visibility," *Proc. SPIE*,

vol. 2525, pp. 148–160, 1995.

[142] J. Tervo, T. Setälä, J. Turunen, and A. T. Friberg, “Van Cittert-Zernike theorem with Stokes parameters,” *Opt. Lett.*, vol. 38, no. 13, pp. 2301–3, Jul. 2013.

[143] N. Ma, S. G. Hanson, M. Takeda, and W. Wang, “Coherence and polarization of polarization speckle generated by a rough-surfaced retardation plate depolarizer,” *J. Opt. Soc. Am. A*, vol. 32, no. 12, pp. 2346–2352, Nov. 2015.

[144] N. Ma, S. G. Hanson, T. K. Lee, M. Takeda, and W. Wang, “Coherence and polarization of polarization speckle generated by depolarizers and their changes through complex ABCD matrix,” in *Proc. SPIE: SPECKLE 2015: VI International Conference on Speckle Metrology*, 2015, vol. 9660, p. 96601D.

[145] F. Farassat, “Introduction to Generalized Functions with Applications in Aerodynamics and Aeroacoustics,” May 1994.

[146] M. A. Alonso, O. Korotkova, and E. Wolf, “Propagation of the electric correlation matrix and the van Cittert–Zernike theorem for random electromagnetic fields,” *J. Mod. Opt.*, vol. 53, no. 7, pp. 969–978, May 2006.

[147] E. Wolf, “Polarization invariance in beam propagation,” *Opt. Lett.*, vol. 32, no. 23, pp. 3400–3401, 2007.

[148] R. J. Dewhurst and Q. Shan, “Optical remote measurement of ultrasound,” *Meas. Sci. Technol.*, vol. 10, no. 11, pp. R139–R168, Nov. 1999.

[149] L. E. Drain, “The laser Doppler techniques,” *Chichester, Sussex, Engl. New York, Wiley-Interscience, 1980. 250 p.*, vol. -1, 1980.

[150] B. Rose, H. Imam, S. G. Hanson, H. T. Yura, and R. S. Hansen, “Laser-speckle angular-displacement sensor: theoretical and experimental study,” *Appl. Opt.*, vol. 37, no. 11, pp. 2119–2129, 1998.

[151] L. Lading, “Principles of laser anemometry,” in *Optical Diagnostics for Flow Processes*, Springer, 1994, pp. 85–125.

[152] L. H. Tanner, “A particle timing laser velocity meter,” *Opt. Laser Technol.*, vol. 5, no. 3, pp. 108–110, Jun. 1973.

[153] W. Wang, S. G. Hanson, and M. Takeda, “Complex amplitude correlations of dynamic laser speckle in complex ABCD optical systems.,” *J. Opt. Soc. Am. A*, vol. 23, no. 9, pp. 2198–207, Sep. 2006.

[154] H. T. Yura, S. G. Hanson, and T. P. Grum, “Speckle: statistics and interferometric decorrelation effects in complex ABCD optical systems,” *J. Opt. Soc. Am. A*, vol. 10, no. 2, pp. 316–323, 1993.

[155] S. Mceldowney, J. Zieba, and M. Newell, “Passive depolariser,” EP1892544, 27-Feb-2008.

[156] J. Begner, “depolariser,” GB2088078 (A), 24-Sep-1980.

[157] S. ATSUSHI and H. KOYANAGI, “depolarization element,” JP2008226405, 25-Sep-2008.

[158] I. Reed, “On a moment theorem for complex Gaussian processes,” *IEEE Trans. Inf. Theory*, vol. 8, no. 3, pp. 194–195, Apr. 1962.

[159] J. Guo and D. J. Brady, “Fabrication of high-resolution micropolarizer arrays,” *Opt. Eng.*, vol. 36, no. 8, pp. 2268–2271, 1997.

[160] A. G. Andreou and Z. K. Kalayjian, “Polarization imaging: principles and integrated polarimeters,” *IEEE Sens. J.*, vol. 2, no. 6, pp. 566–576, Dec. 2002.

[161] V. Gruev, R. Perkins, and T. York, “CCD polarization imaging sensor with aluminum nanowire optical filters.,” *Opt. Express*, vol. 18, no. 18, pp. 19087–94, Aug. 2010.

[162] J. Guo and D. Brady, “Fabrication of thin-film micropolarizer arrays for visible imaging polarimetry.,” *Appl. Opt.*, vol. 39, no. 10, pp. 1486–1492, Apr. 2000.

[163] V. Gruev, A. Ortu, N. Lazarus, J. Van der Spiegel, and N. Engheta, “Fabrication of a dual-tier thin film micropolarization array,” *Opt. Express*, vol. 15, no. 8, p. 4994, Apr. 2007.

[164] J. J. Wang, F. Walters, X. Liu, P. Sciortino, and X. Deng, “High-performance, large area, deep ultraviolet to infrared polarizers based on 40 nm line/78 nm space nanowire grids,” *Appl. Phys. Lett.*, vol. 90, no. 6, p. 061104, 2007.

[165] G. P. Nordin, J. T. Meier, P. C. Deguzman, and M. W. Jones, “Micropolarizer array for infrared imaging polarimetry,” *J. Opt. Soc. Am. A*, vol. 16, no. 5, p. 1168, May 1999.

[166] V. Gruev, R. Perkins, and T. York, “Integrated high resolution division of focal plane image sensor with aluminum nanowire polarization filters,” in *Proc. of SPIE*, 2010, vol. 7672, p. 76720G–76720G–9.

[167] H. T. Yura, “Mutual coherence function of a finite cross section optical beam propagating in a turbulent medium,” *Appl. Opt.*, vol. 11, no. 6, pp. 1399–1406, 1972.